От организации хроматина к пониманию функционирования геномов эукариот

Алексей Константинович Шайтан

д.ф.-м.н., профессор, чл.-корр. РАН

кафедра биоинженерии

биологический факультет

МГУ имени М.В.Ломоносова

Лекция 7.
Мир РНК. Практические аспекты эпигеномики.

Апрель 2024

Некодирующие РНК

До 90% генома человека транскрибируется – транскрипционный шум или функциональные элементы?

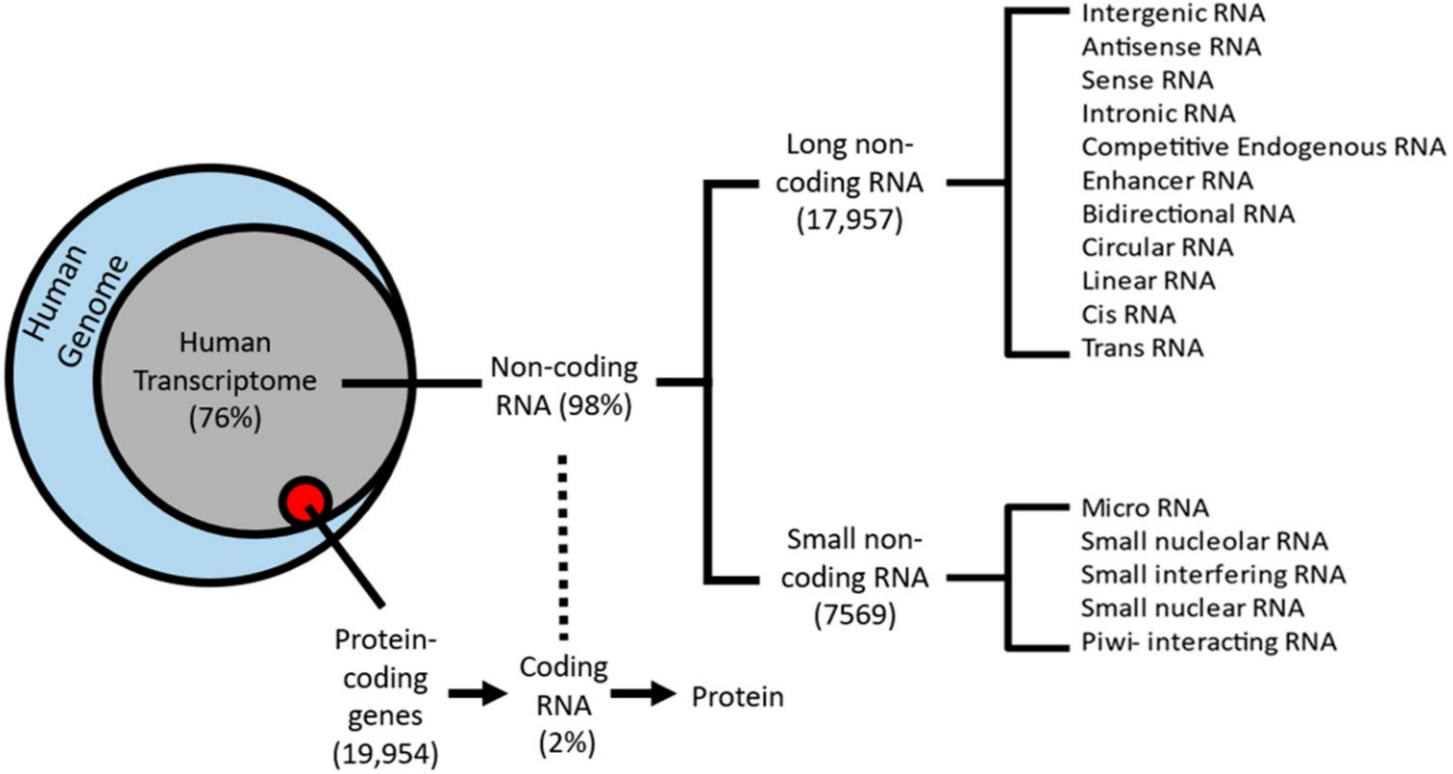

10.3390/ncrna8040059

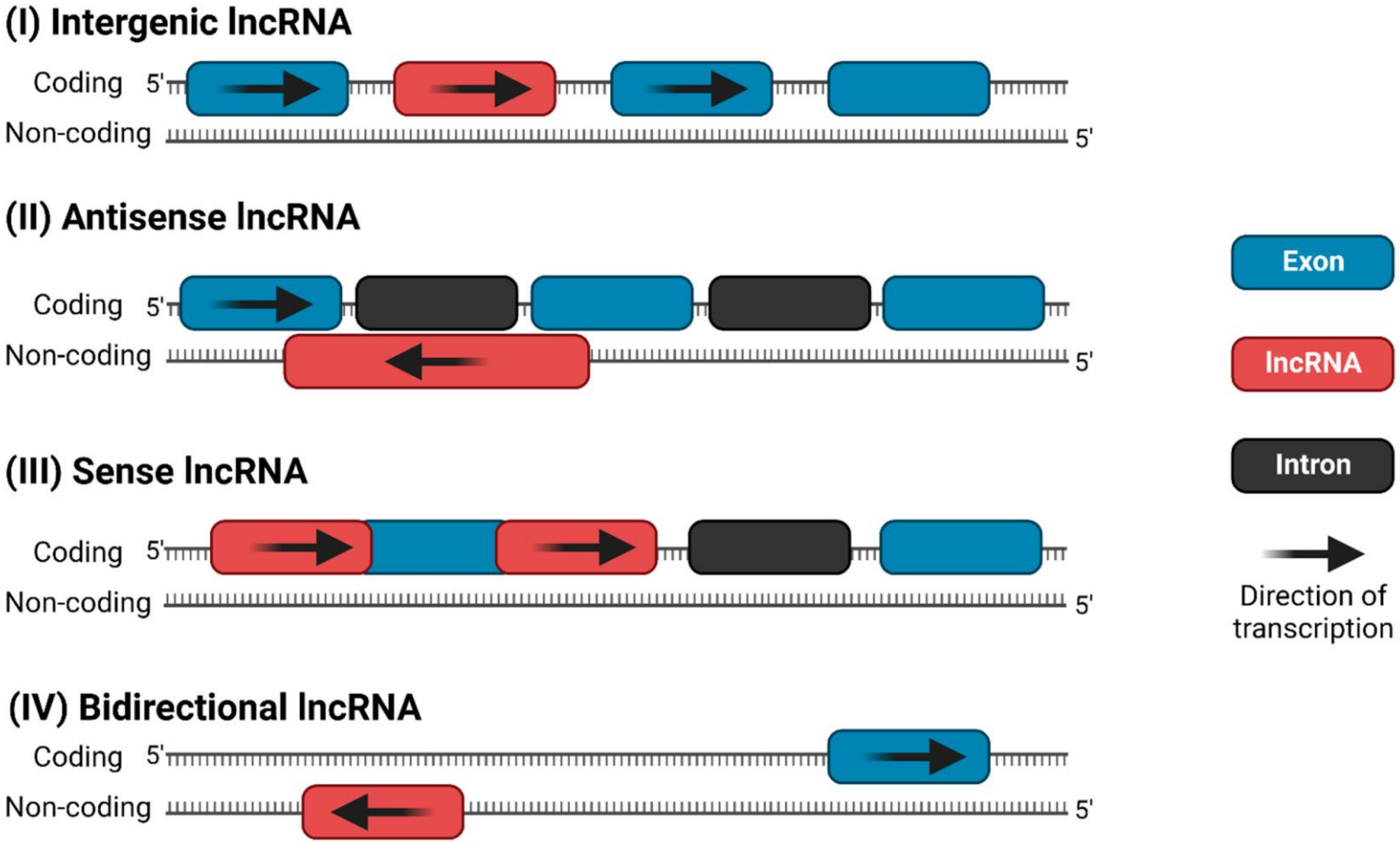

10.3390/ncrna8040059

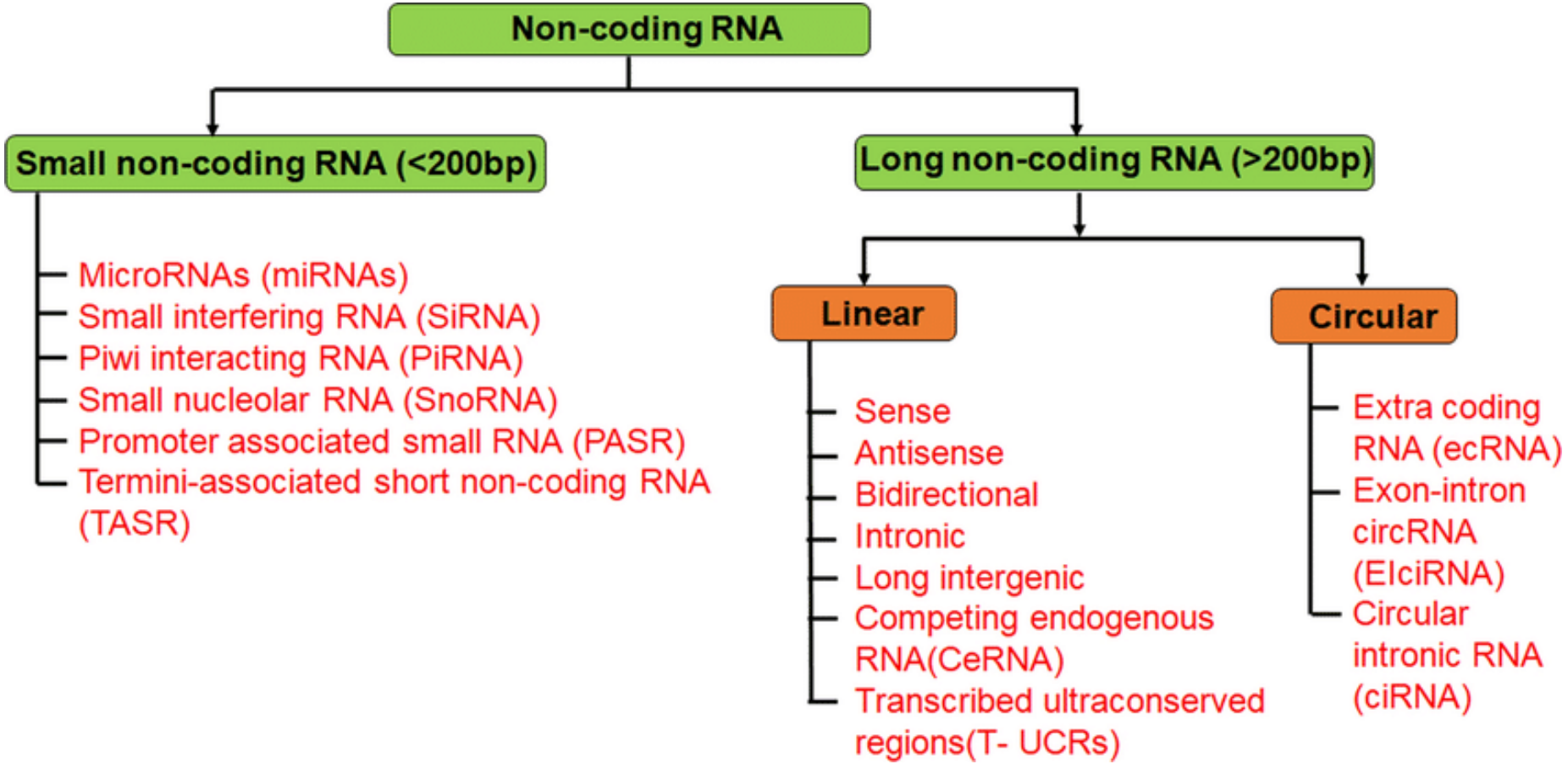
Non-coding RNA
Small non-coding RNA (<200bp)
MicroRNAs (miRNAs)
Small interfering RNA (SiRNA)
Piwi interacting RNA (PiRNA)
Small nucleolar RNA (SnoRNA)
Promoter associated small RNA (PASR)
Termini-associated short non-coding RNA (TASR)
Long non-coding RNA (>200bp)
Linear
Sense
Antisense
Bidirectional
Intronic
Long intergenic
Competing endogenous RNA(CeRNA)
Transcribed ultraconserved regions(T- UCRs)
Circular
Extra coding RNA (ecRNA)
Exon-intron circRNA (EIciRNA)
Circular intronic RNA (ciRNA)

Nobel price 2006

"for their discovery of RNA interference - gene silencing by double-stranded RNA"

Andrew Z. Fire

USA

Stanford University
School of Medicine
Stanford, CA, USA

Craig C. Mello

USA

University of Massachusetts
Medical School
Worcester, MA, USA

Discovered in 1998

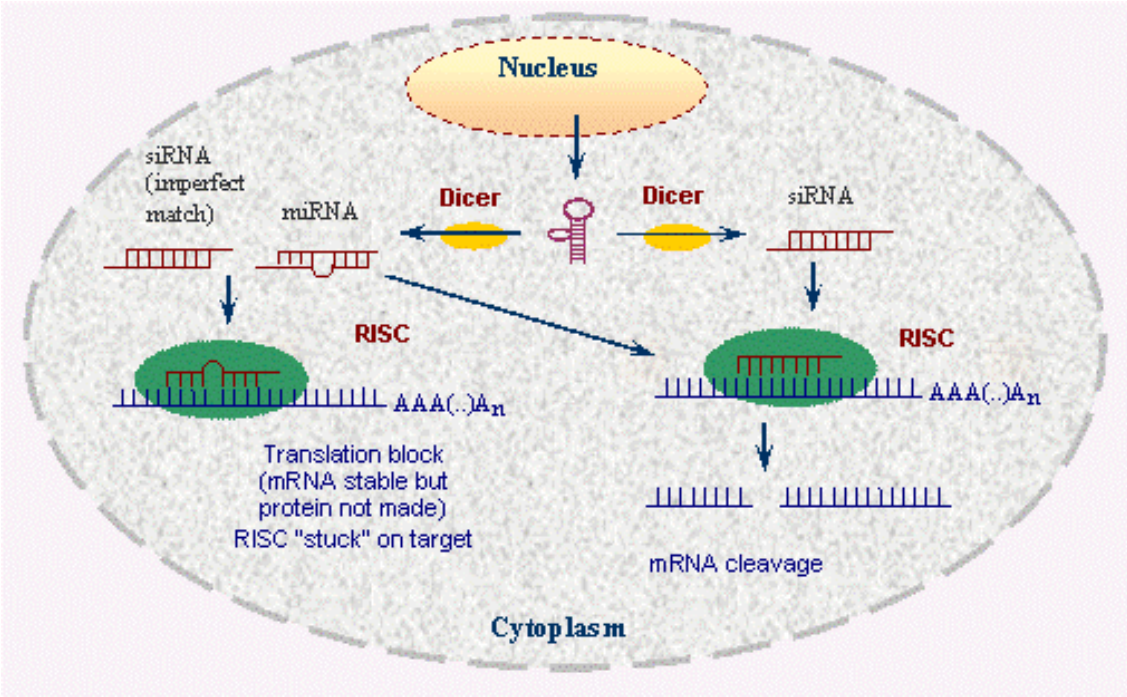

Малые некодирующие РНК

PMC9231384

Class	Symbol	Characteristics	Biological Functions Associations
MicroRNAs	miRNAs	18–26 nt; comprises 2% of human genome and regulate up to 50% of protein-coding genes.	Control of proliferation, apoptosis, and differentiation.
Small interfering RNAs	siRNA	19–23 nt; processed by Dicer, and guide sequence-specific degradation of target mRNA.	Post-transcriptional regulation of gene expression.
Piwi-interacting RNAs	piRNAs	24–31 nt; made by single-stranded RNA (ssRNA) precursors and it is Dicer-independent.	Embryonic development, germline DNA integrity, transposon transcription silencing, translation suppression, heterochromatin creation, and sex determination epigenetic control.
Small nucleolar RNAs	snoRNAs	60–300 nt; divided into two classes: C/D box snoRNAs and H/ACA box snoRNAs. It is primarily accumulated in the nucleoli.	Responsible for post-transcriptional modification and maturation of ribosomal RNAs (rRNAs), small nuclear RNAs (snRNAs), and other RNAs (snRNAs).
Centromere repeat-associated small interacting RNAs	crasiRNAs	34–42 nt; processed from long dsRNAs.	Activation of heterochromatin and centromeric proteins.
Telomere-specific small RNAs	tel-sRNAs	~24 nt; pi-like small RNA and independent of Dicer processing.	Epigenetic regulation.
Pyknons		>16 nt long; observed in groups in intergenic and intronic domains.	Primarily engaged in cell communication, transcriptional regulation, signalling, and transport.
tRNA fragments	tRFs	14–30 nt; dependent on angiogenin and Dicer processing.	Diverse molecular and physiological processes, including gene suppression, RNA processing, protein translation, stress responses, cell proliferation, and differentiation.
tRNA-derived stress-induced RNAs	tiRNAs (tRNA halves)	29–50 nt; the most abundant right downstream of transcriptional end sites. It exhibits spatial preservation patterns and predominantly resides in GC-rich promoters.	Control of protein-coding gene transcription by targeting epigenetic silencing complexes.

Некодирующие РНК вблизи промотера и 3’UTR

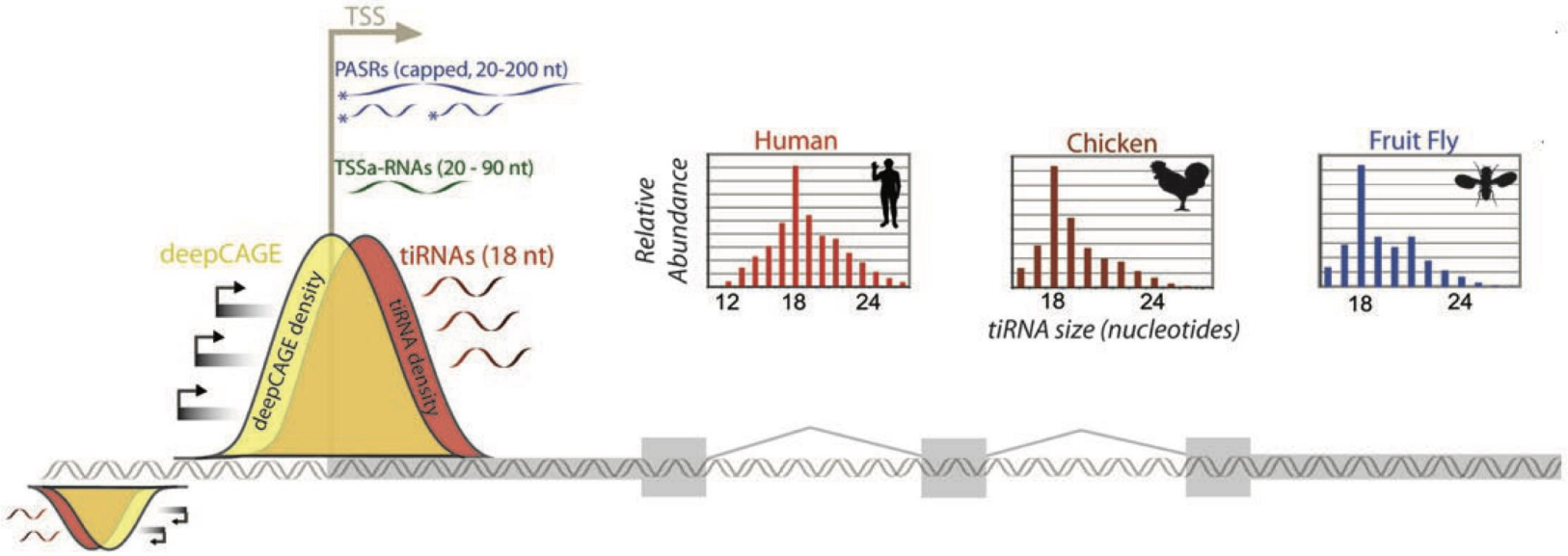

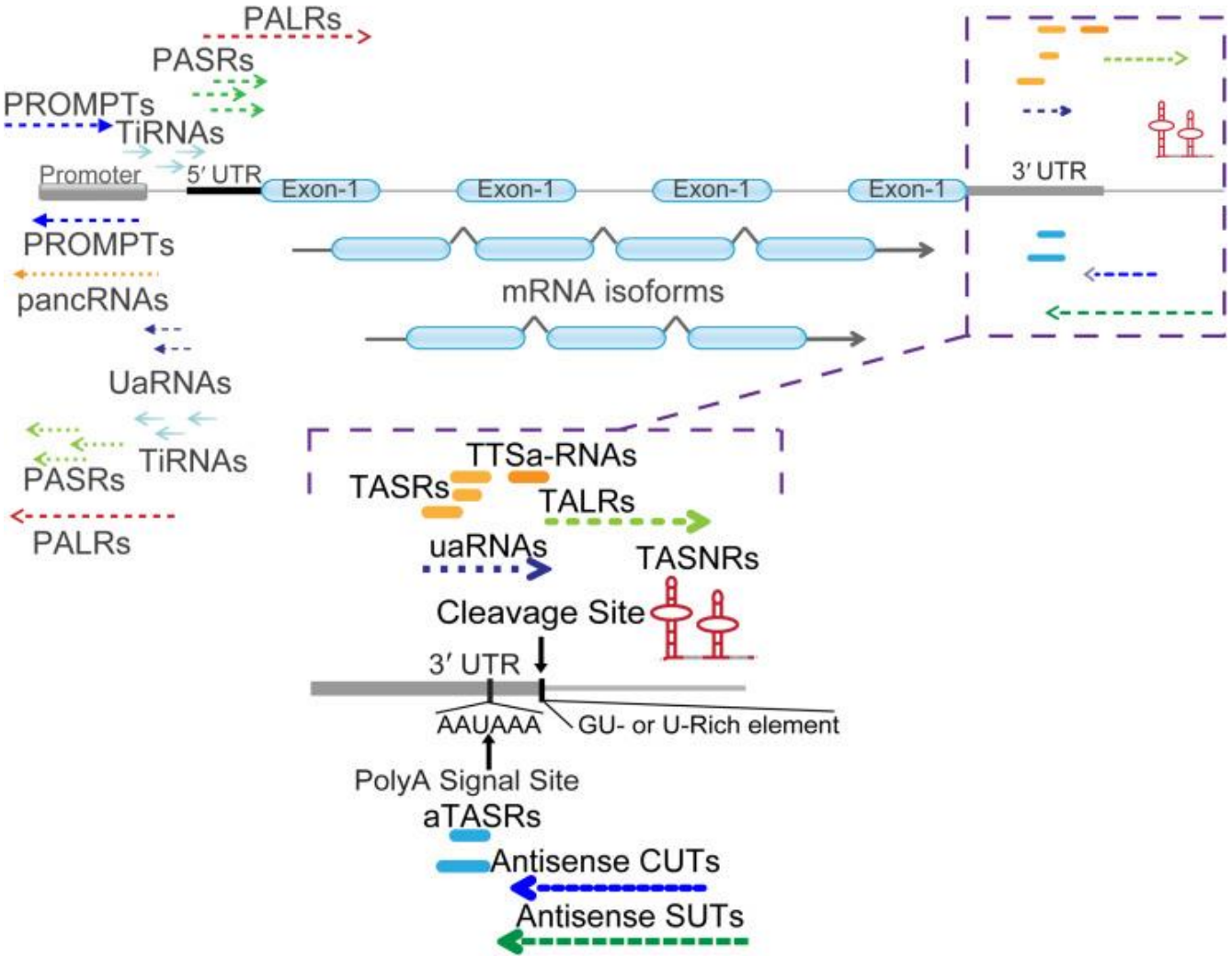
PALRs
PASRs
PROMPTs
TiRNAs
Promoter
5′ UTR
Exon-1
Exon-1
Exon-1
Exon-1
3′ UTR
PROMPTs
pancRNAs
mRNA isoforms
UaRNAs
TiRNAs
PASRs
PALRs
TTSa-RNAs
TASRs
TALRs
uaRNAs
TASNRs
Cleavage Site
3′ UTR
AAUAAA
GU- or U-Rich element
PolyA Signal Site
aTASRs
Antisense CUTs
Antisense SUTs

Длинные некодирующие РНК

Роль длинных некодирующих РНК

Длинные некодирующие РНК (днкРНК, lncRNAs) — некодирующие РНК, которые как правило имеют длину более 200 нуклеотидов, и расположены в ядре или в цитоплазме.

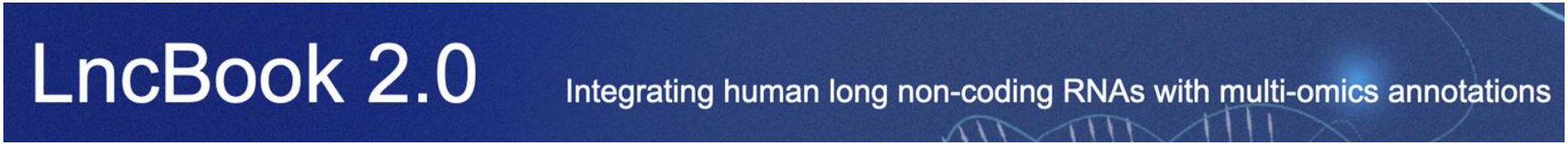

LncBook accommodates a high-quality collection of 95,243 human lncRNA genes and 323,950 lncRNA transcripts, and incorporates their abundant annotations at different omics levels, thereby enabling users to decipher functional signatures of lncRNAs in human diseases and different biological contexts.

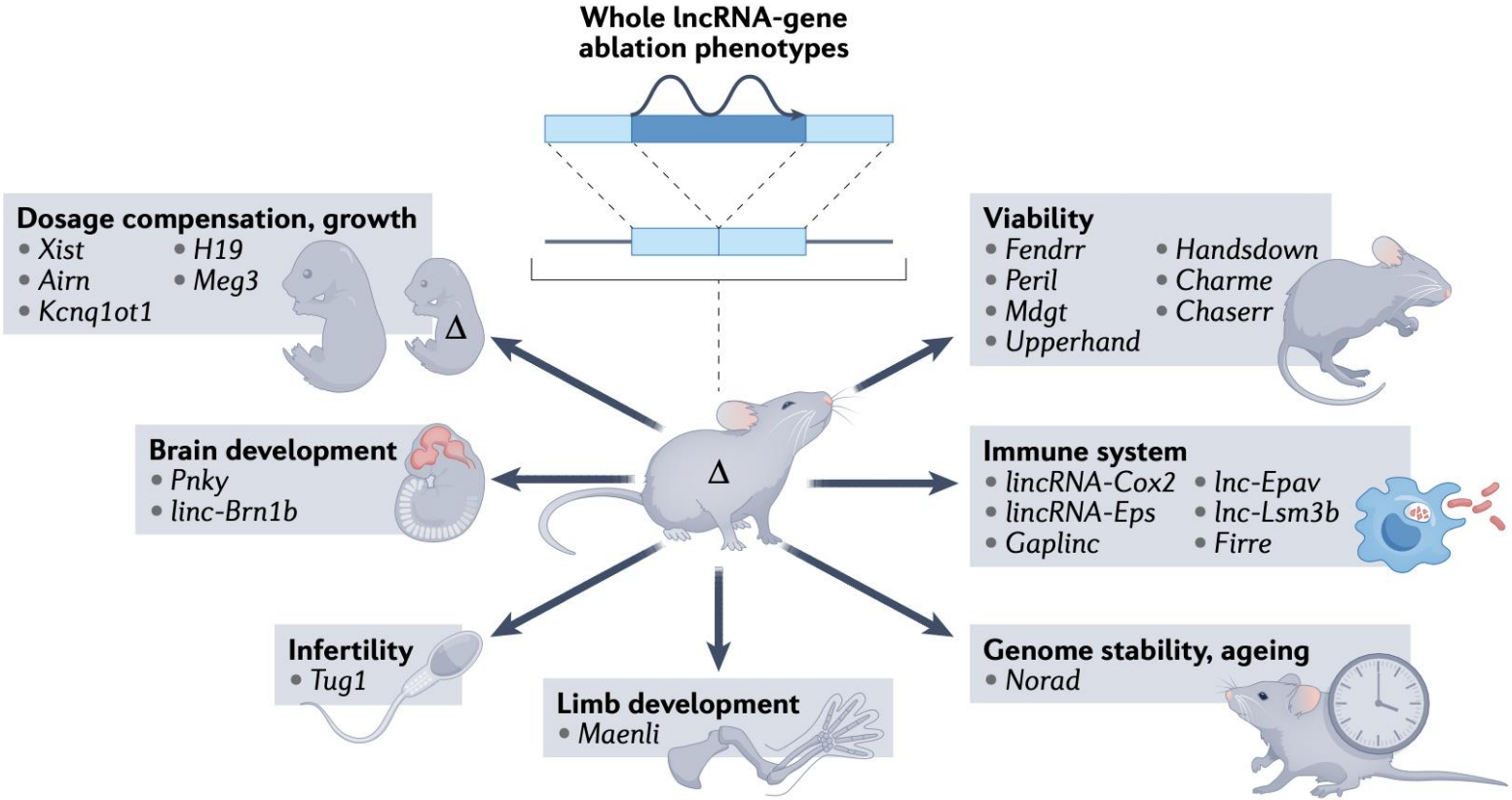

https://doi.org/10.1038/s41580-022-00566-8

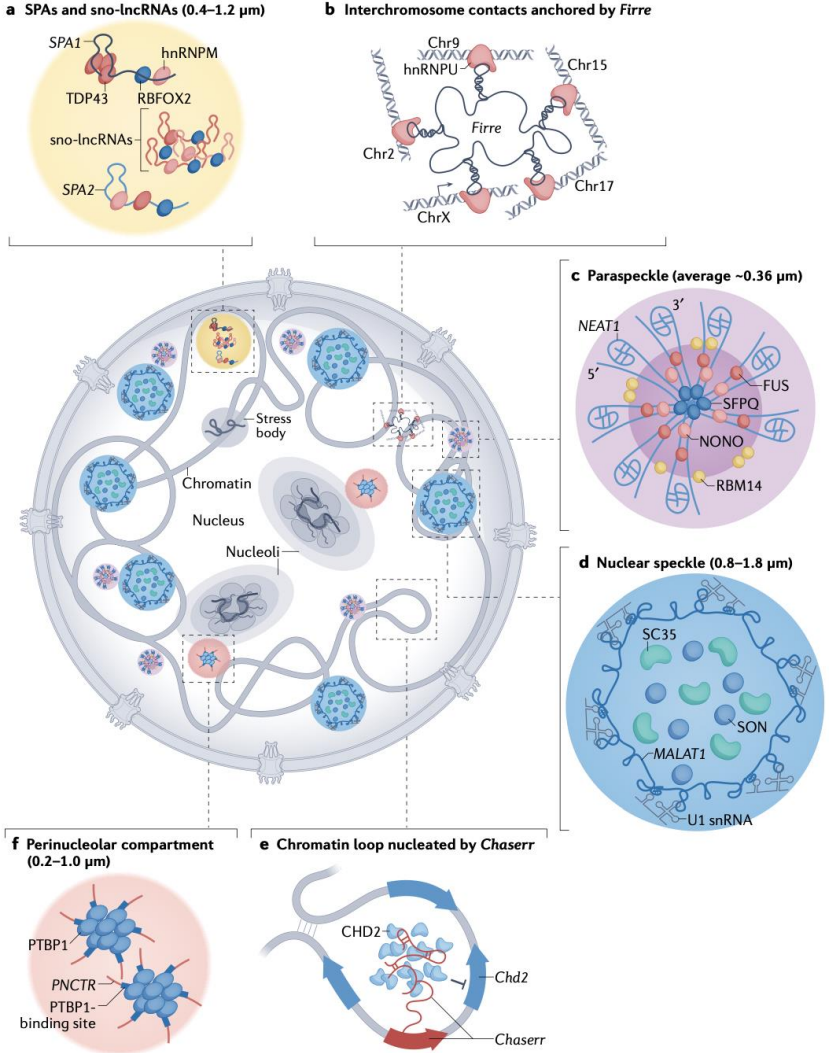
a SPAs and sno-lncRNAs (0.4–1.2 μm)
SPA1
hnRNPM
TDP43
RBFOX2
sno-lncRNAs
SPA2
b Interchromosome contacts anchored by Firre
Chr9
hnRNPU
Chr15
Firre
Chr2
Chr17
ChrX
Stress body
Chromatin
Nucleus
Nucleoli
c Paraspeckle (average ~0.36 μm)
NEAT1
3′
5′
FUS
SFPQ
NONO
RBM14
d Nuclear speckle (0.8–1.8 μm)
SC35
SON
MALAT1
U1 snRNA
f Perinucleolar compartment (0.2–1.0 μm)
PTBP1
PNCTR
PTBP1-binding site
e Chromatin loop nucleated by Chaserr
CHD2
Chd2
Chaserr

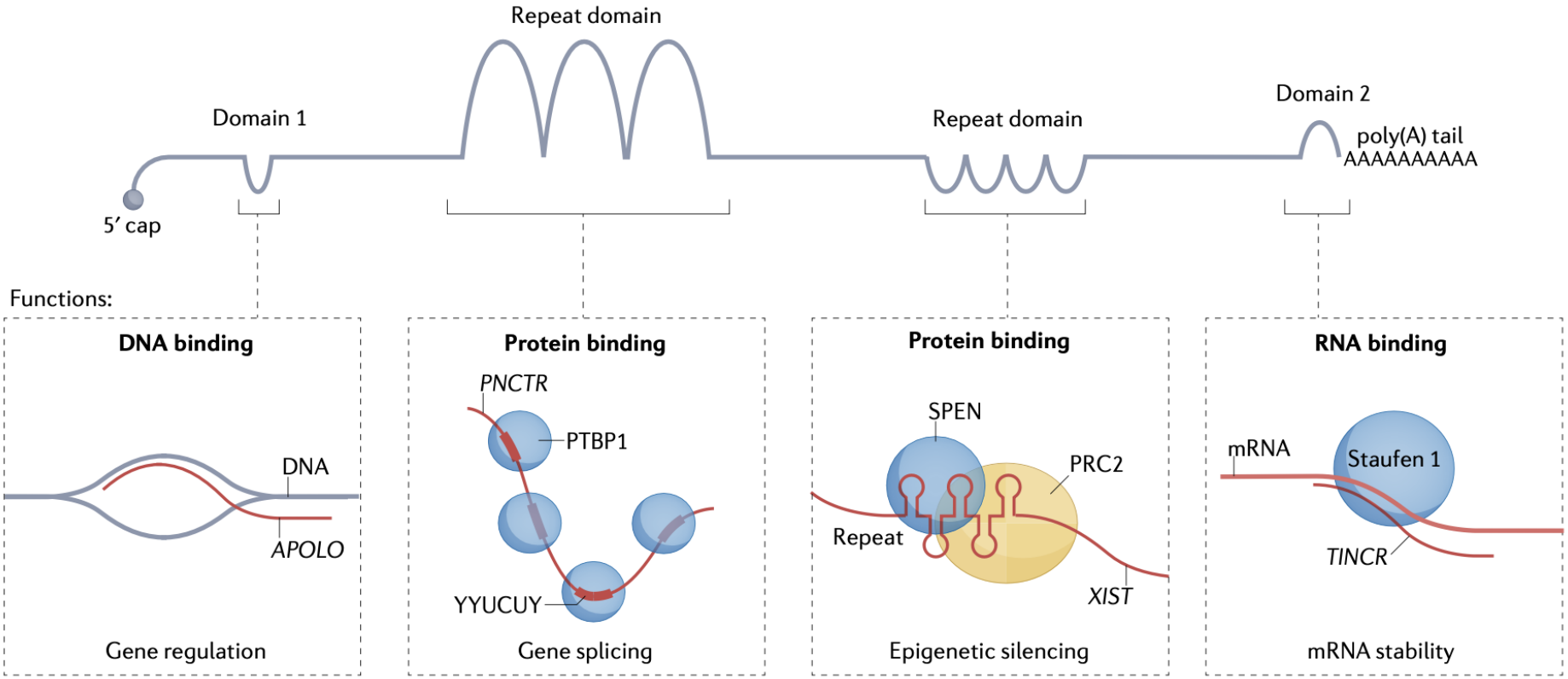
Repeat domain
Domain 1
Repeat domain
Domain 2
poly(A) tail
AAAAAAAAAA
5′ cap
Functions:
DNA binding
DNA
APOLO
Gene regulation
Protein binding
PNCTR
PTBP1
YYUCUY
Gene splicing
Protein binding
SPEN
PRC2
Repeat
XIST
Epigenetic silencing
RNA binding
mRNA
Staufen 1
TINCR
mRNA stability

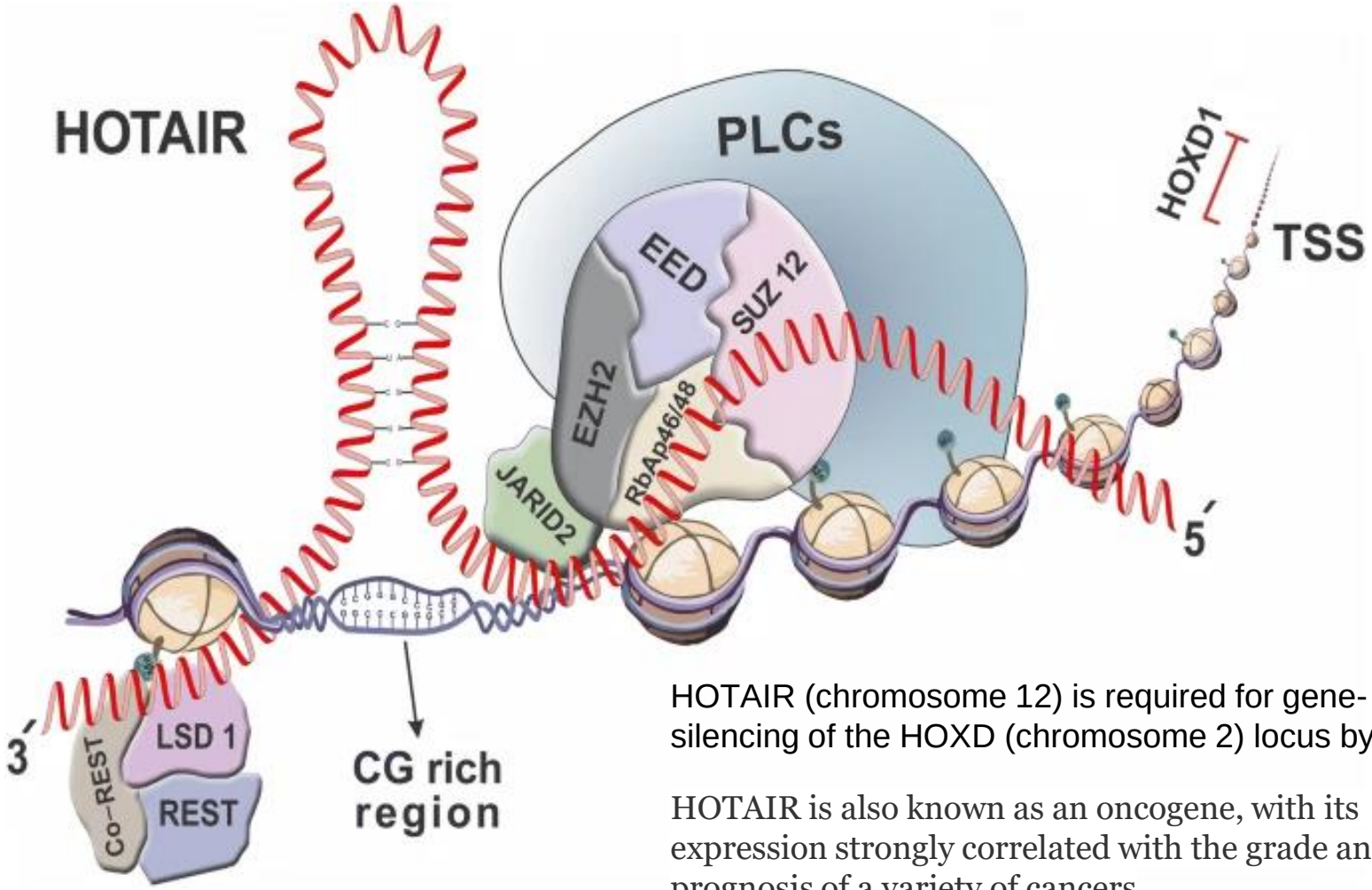

HOTAIR (chromosome 12) is required for gene-silencing of the HOXD (chromosome 2) locus by PRC2

HOTAIR is also known as an oncogene, with its expression strongly correlated with the grade and prognosis of a variety of cancers

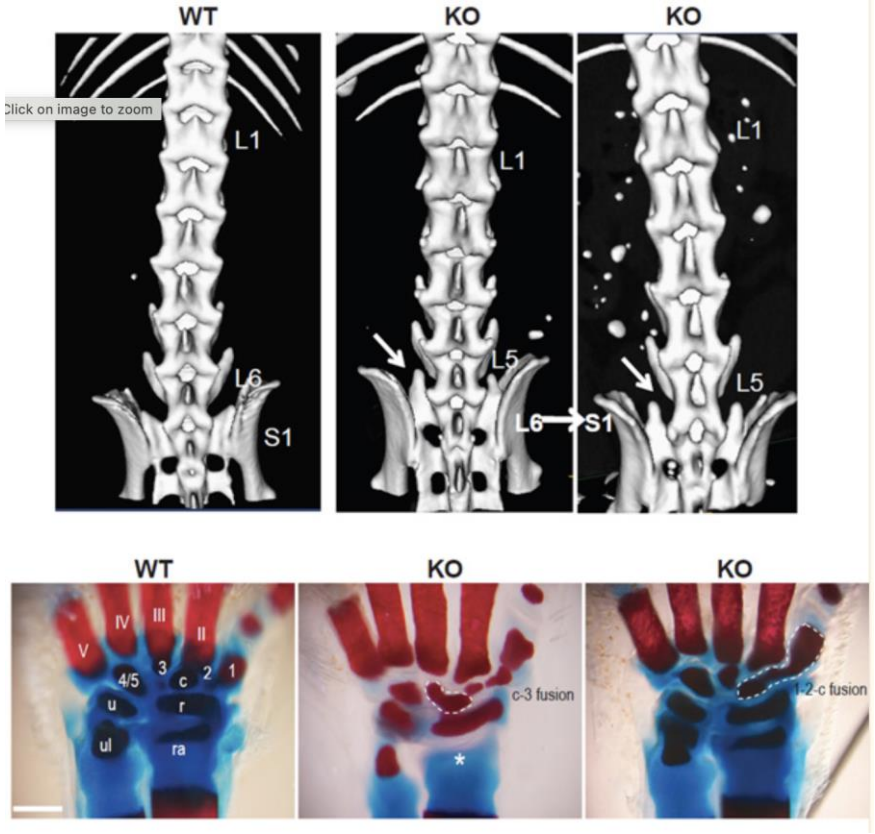

- Targeted disruption of *Hotair* leads to homeotic transformation and gene de-repression

targeted deletion of mouse Hotair lncRNA leads to de-repression of hundreds of genes, resulting in homeotic transformation of the spine and malformation of metacarpal-carpal bones

10.1016/j.celrep.2013.09.003

Xist (X-inactive specific transcript)

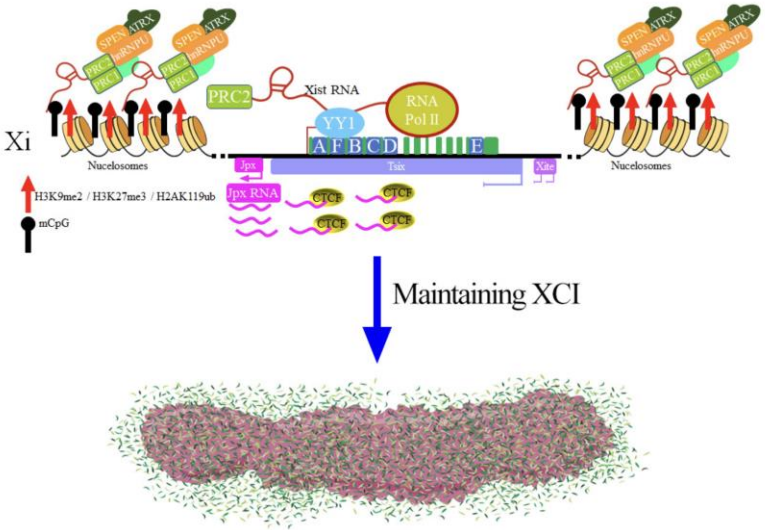

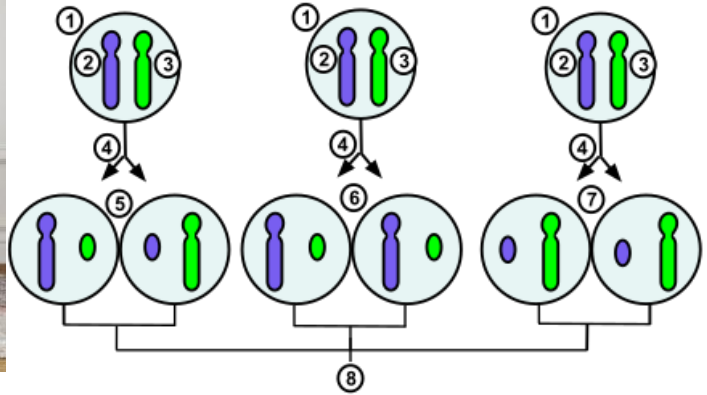

X inactivation centre (XIC)

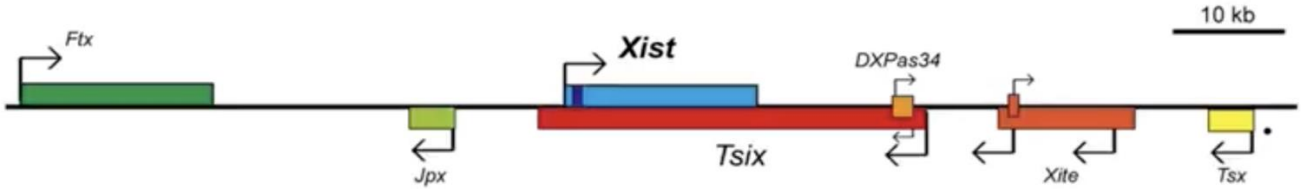

https://www.youtube.com/watch?v=4SN2Sh6W_L0 – см. подробнее о механизмах и стадиях инактивации

Dosage compensation

- X-chromosome inactivation (XCI) is the form of dosage compensation in mammalian female cells to balance X-linked gene expression levels of the two sexes

If there is but one X chromosome in a diploid cell (1X:2A), the fly is male. If there are two X chromosomes in a diploid cell (2X:2A), the fly is female

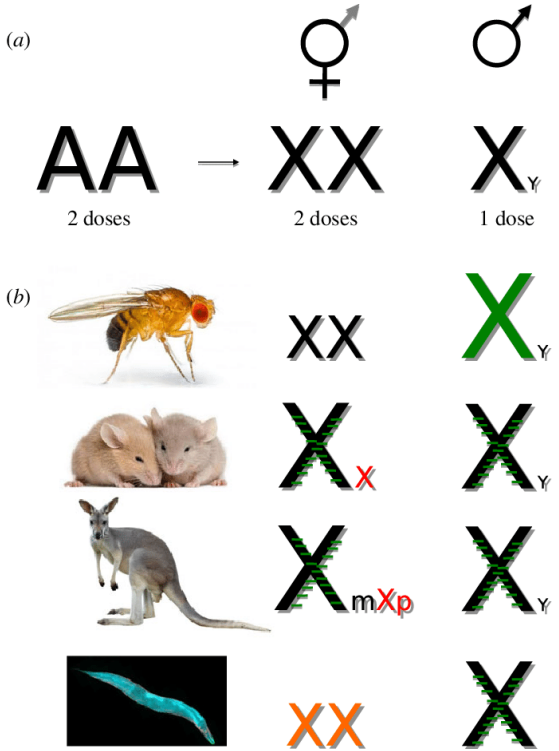

a Dosage Compensation in Drosophila

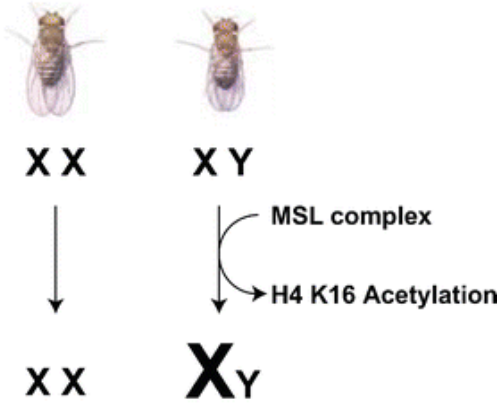

b The MSL Complex

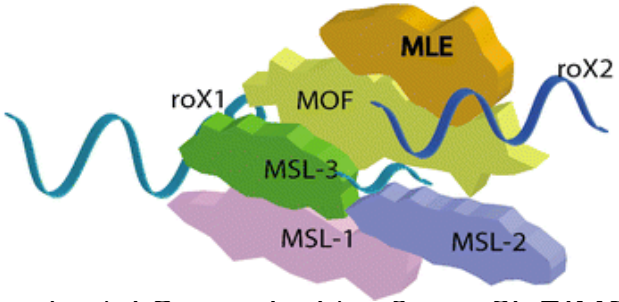

https://www.youtube.com/watch?app=desktop&v=wr0IcBIMGAs

Sex Determination In Humans

Dad XY	Mom XX	
	X	X
X	XX	XX
Y	XY	XY

Offspring

Sex Determination In Chickens

Dad ZZ	Mom ZW	
	Z	W
Z	ZZ	ZW
Z	ZZ	ZW

Offspring

Enhancer RNA

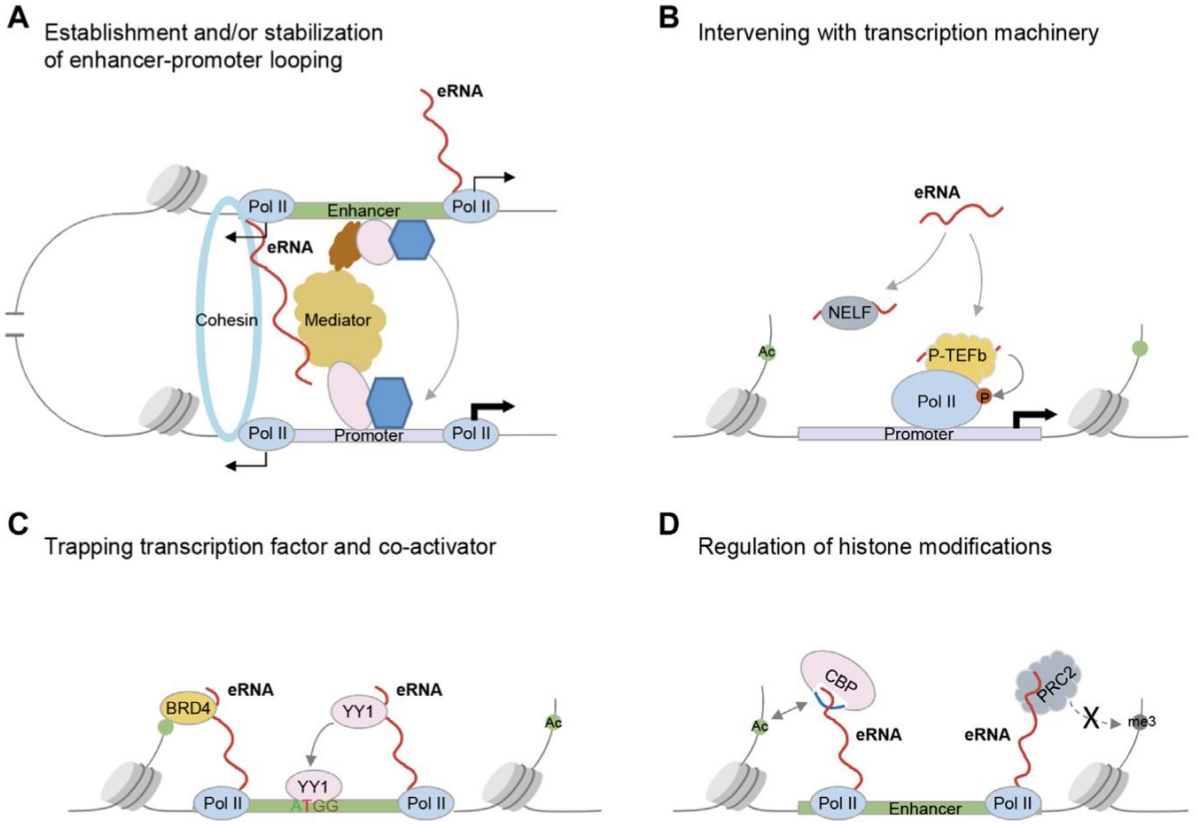

eRNAs are short, bidirectional ones, which are generally non-polyadenylated and unstable, whereas elncRNAs are usually polyadenylated and have higher stability

10.3389/fcell.2023.1205540

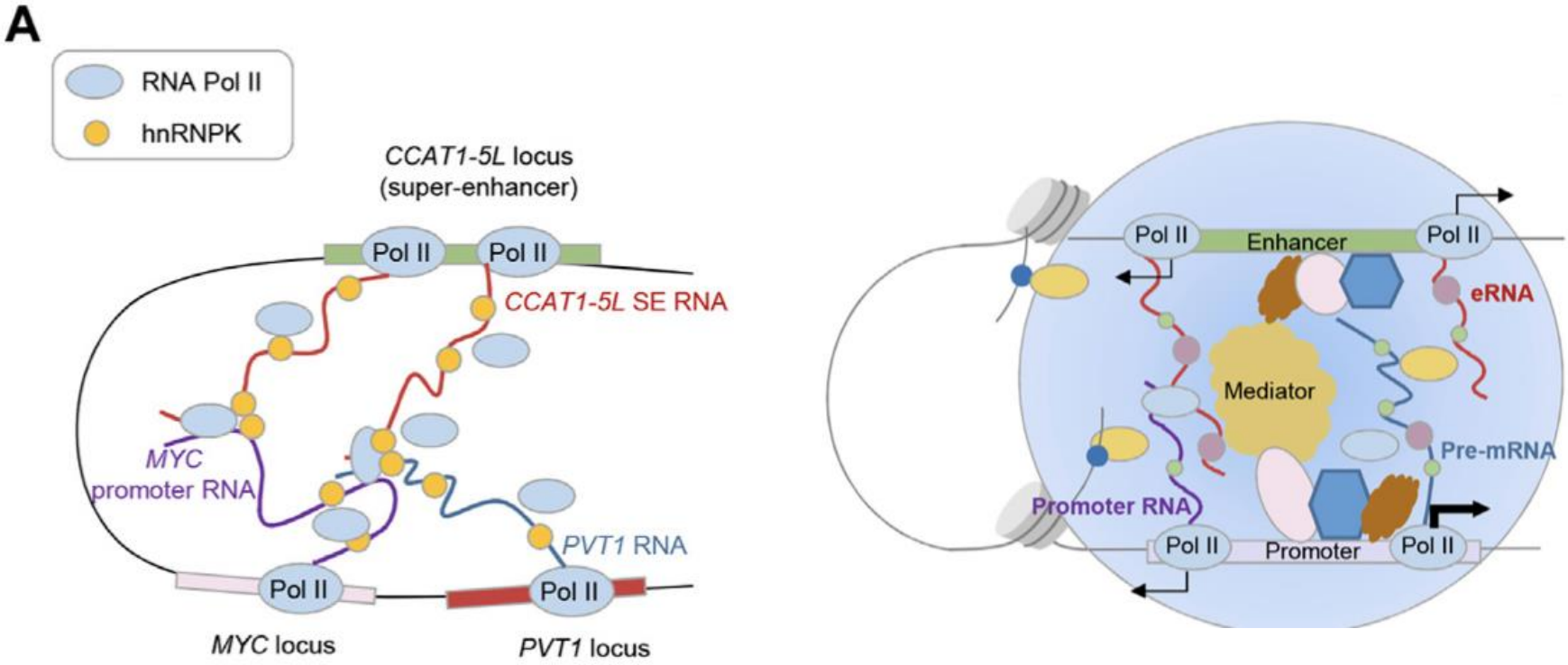
A
RNA Pol II
hnRNPK
CCAT1-5L locus
(super-enhancer)
Pol II
Pol II
CCAT1-5L SE RNA
MYC
promoter RNA
PVT1 RNA
Pol II
Pol II
MYC locus
PVT1 locus
Pol II
Enhancer
Pol II
eRNA
Mediator
Pre-mRNA
Promoter RNA
Pol II
Promoter
Pol II

Circular RNA

The biological function of most circular RNA is unclear

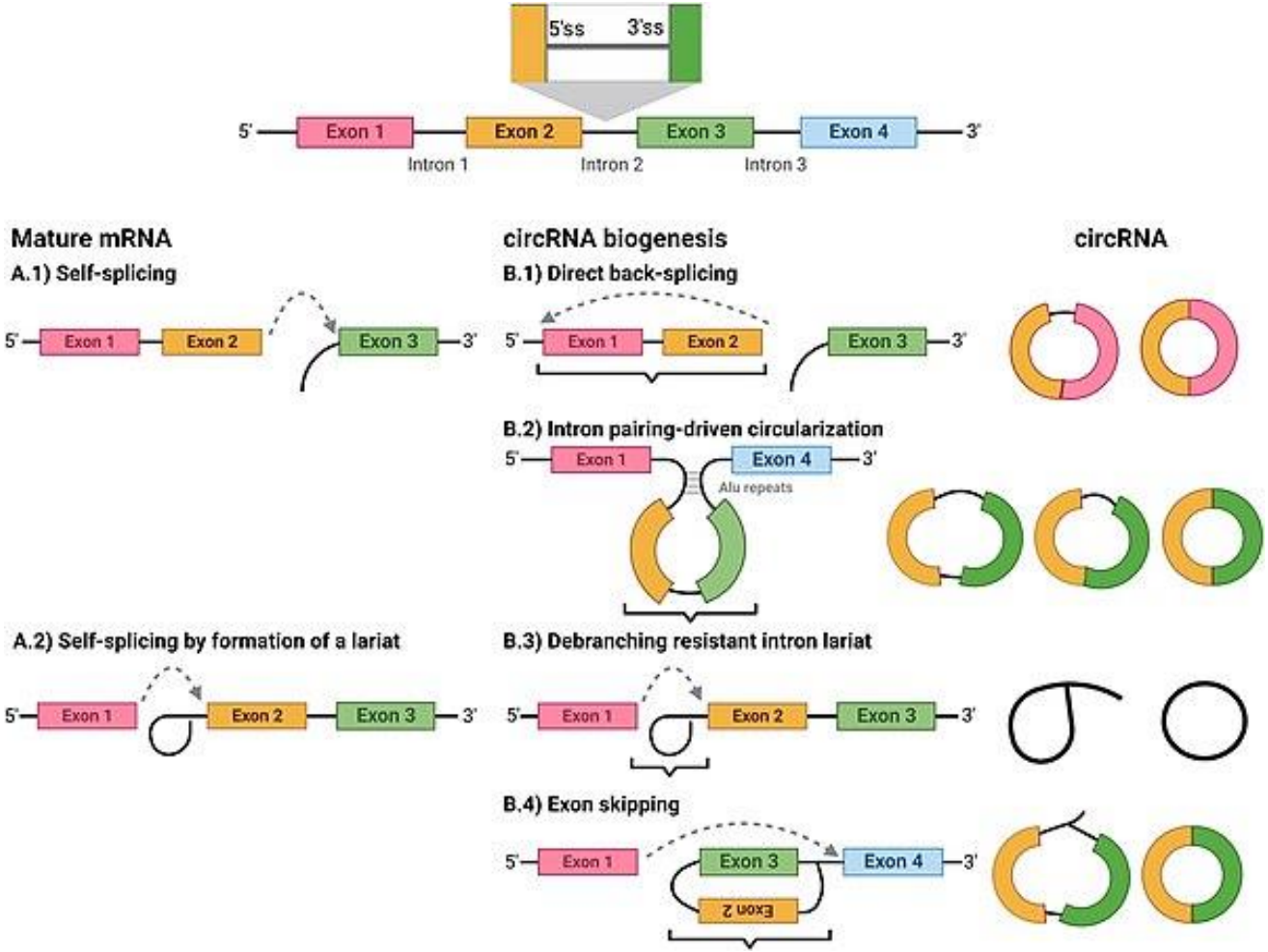

Circular lncRNA

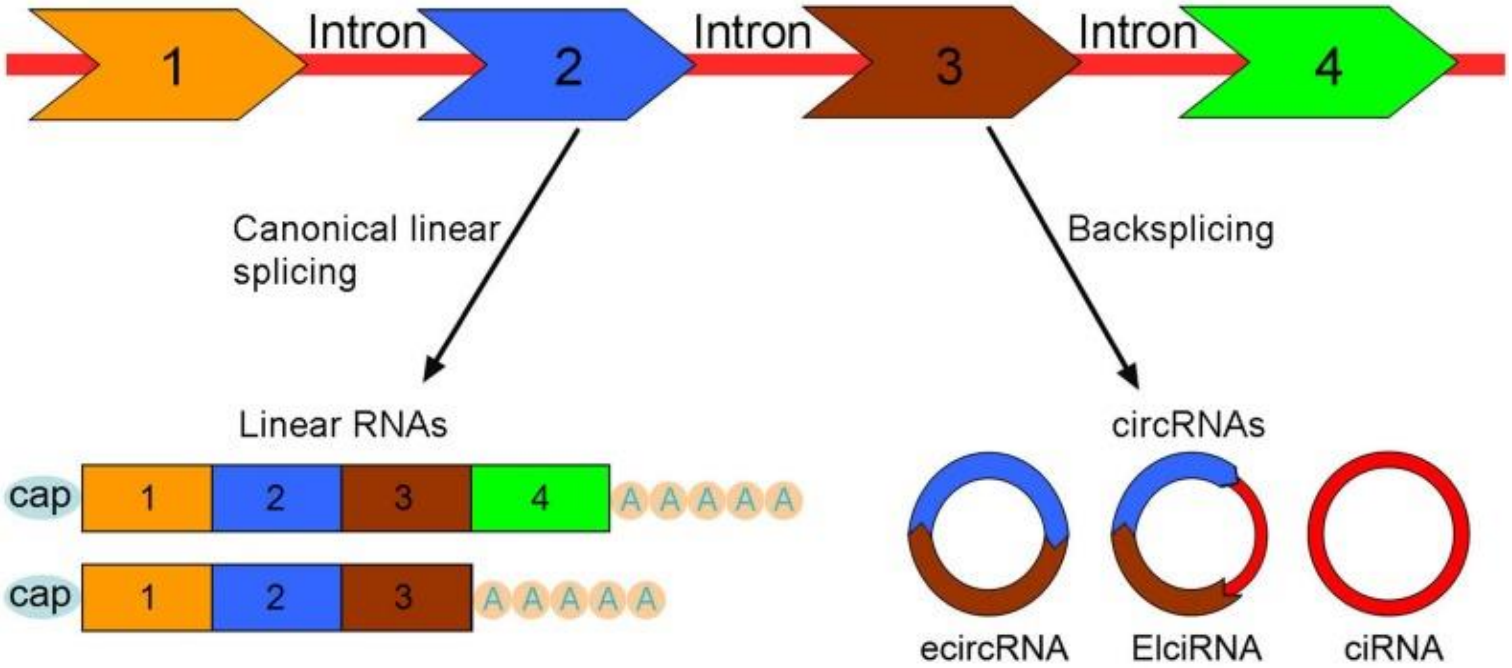

Exonic circular RNA

Intronic CircRNA (ciRNA)

Exon-intron CircRNA

10.7150/ijbs.22531

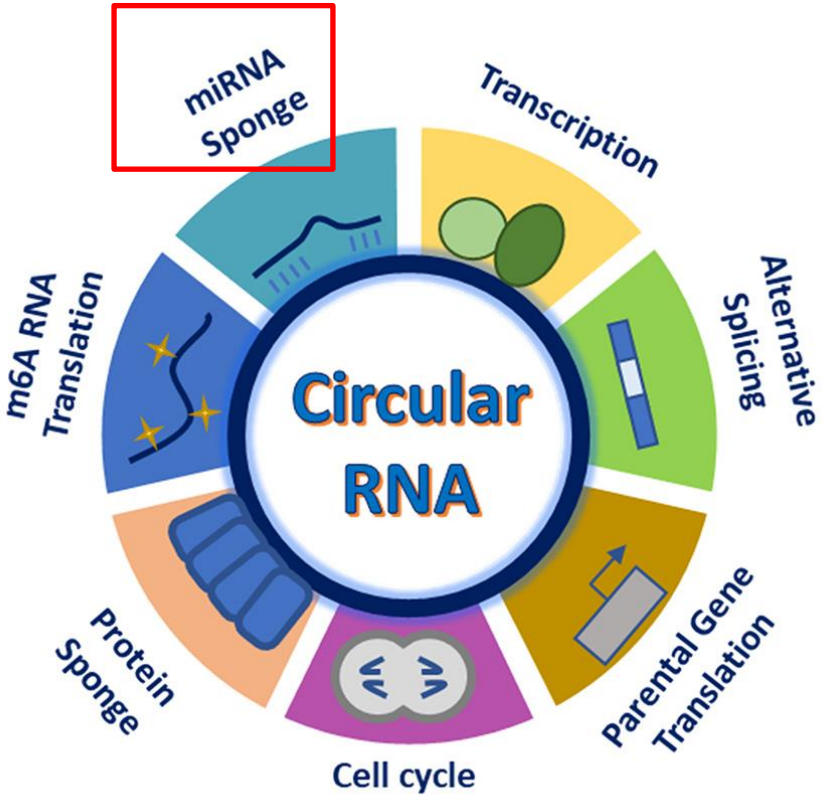
miRNA Sponge
Transcription
Alternative Splicing
Parental Gene Translation
Cell cycle
Protein Sponge
m6A RNA Translation
Circular RNA

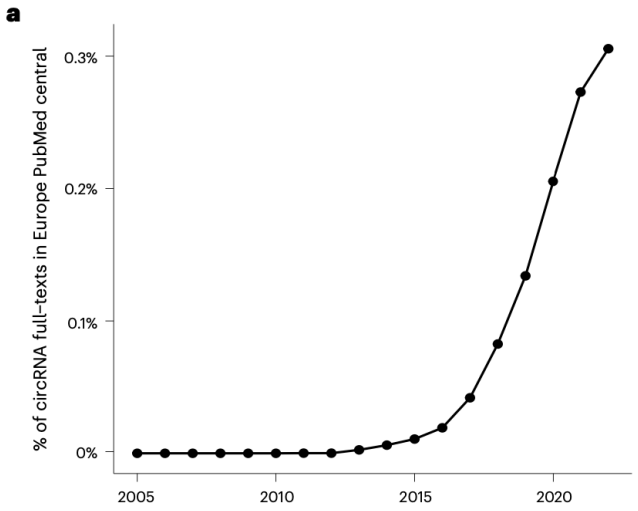
a
% of circRNA full-texts in Europe PubMed central
0.3%
0.2%
0.1%
0%
2005
2010
2015
2020

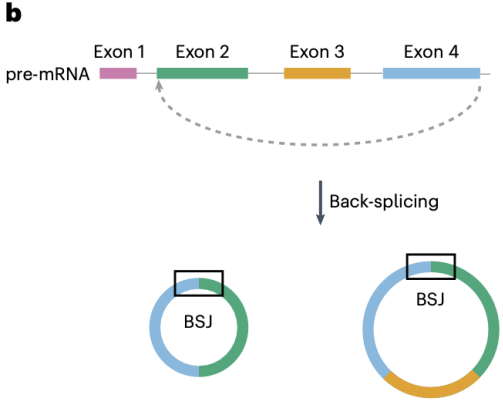
b
Exon 1
Exon 2
Exon 3
Exon 4
pre-mRNA
Back-splicing
BSJ
BSJ

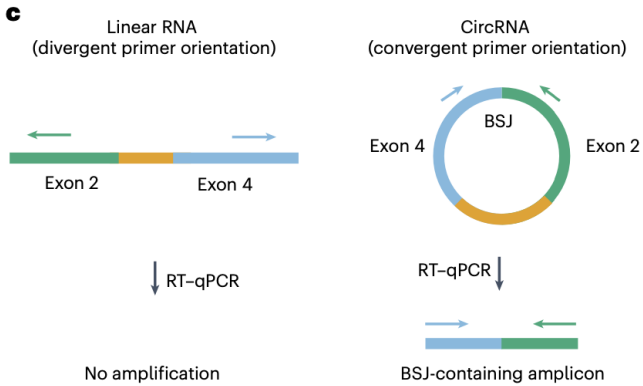
c
Linear RNA
(divergent primer orientation)
Exon 2
Exon 4
RT–qPCR
No amplification
CircRNA
(convergent primer orientation)
BSJ
Exon 4
Exon 2
RT–qPCR
BSJ-containing amplicon


d
BSJ-spanning read
Exon 4
Exon 2
Exon 2
Exon 4

Эпигенетика и мутации/повреждения ДНК
Роль в онкологических заболеваниях

Спонтанное деаминирование

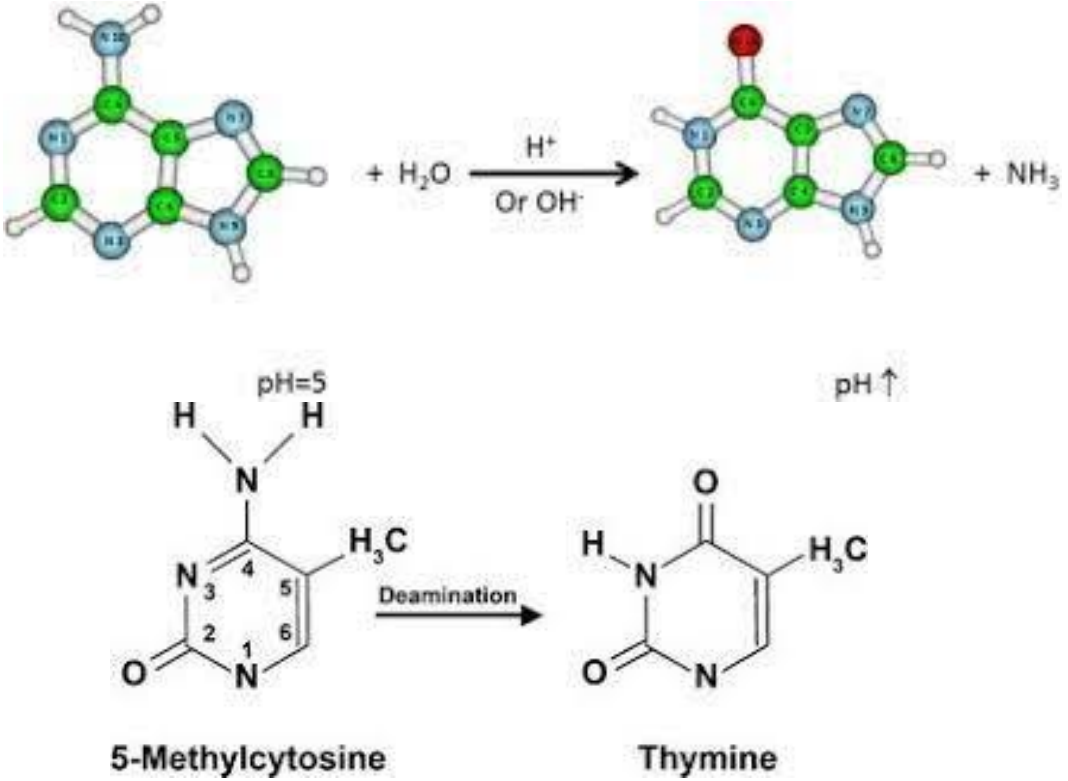

Механизмы мутаций

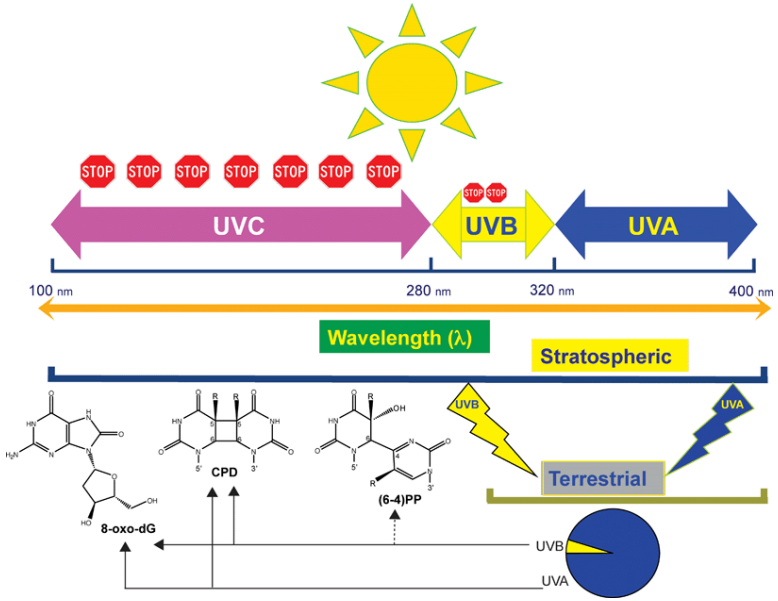

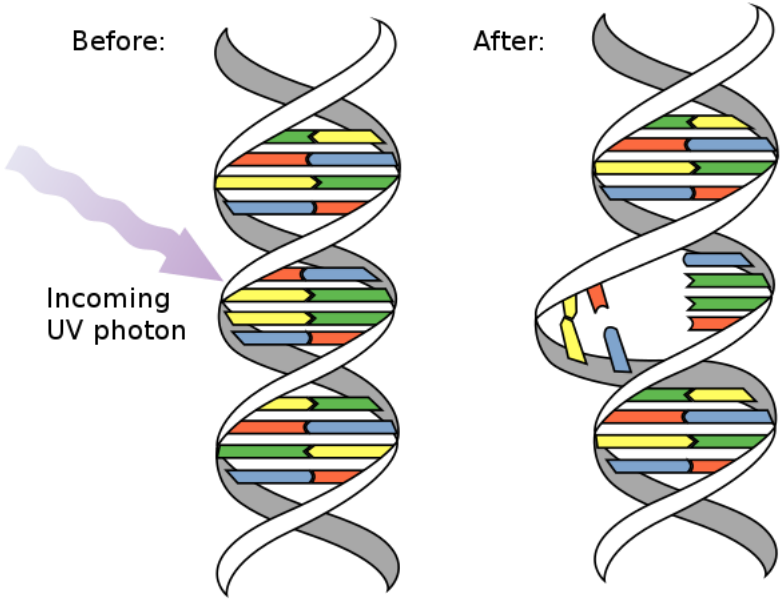

Механизмы мутаций

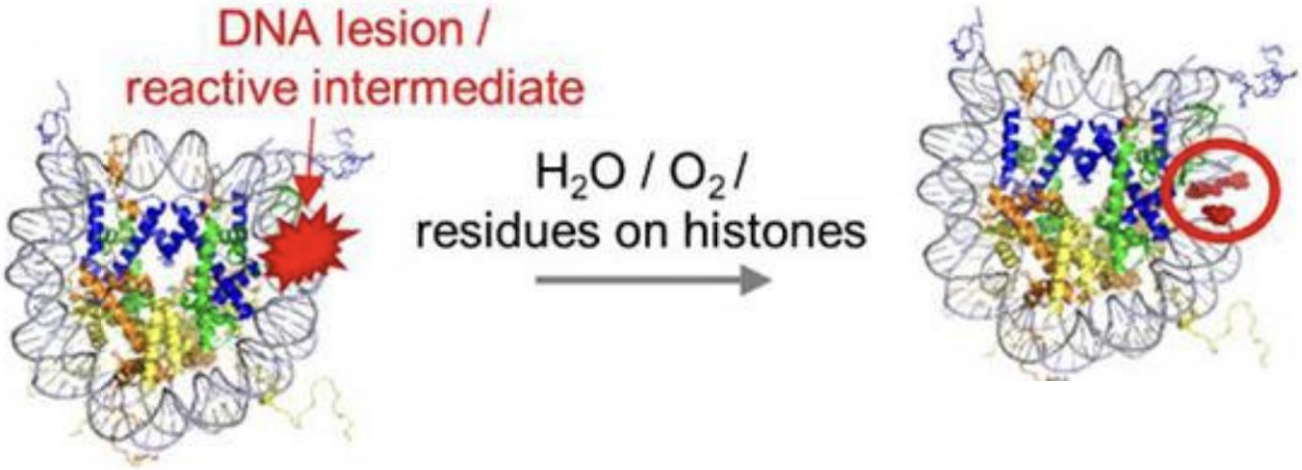

benzo[a]pyrene diol epoxide-DNA adducts

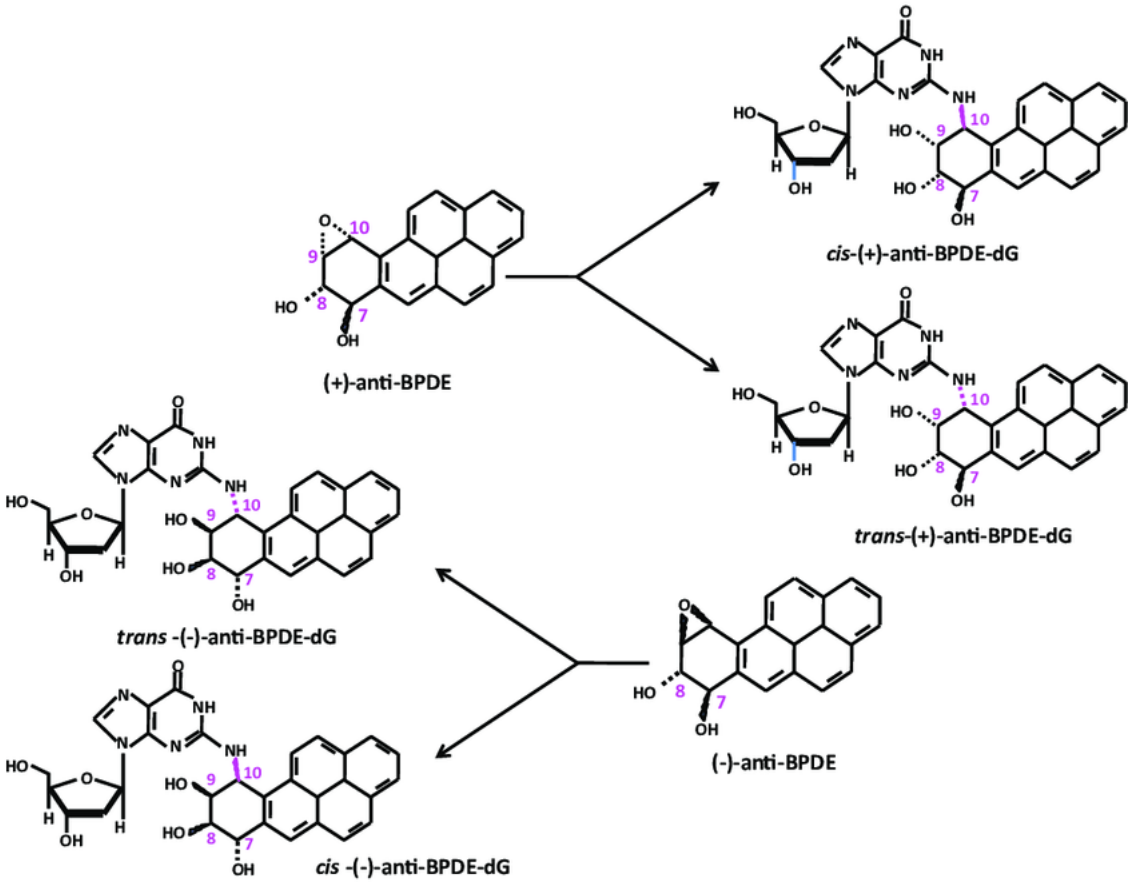

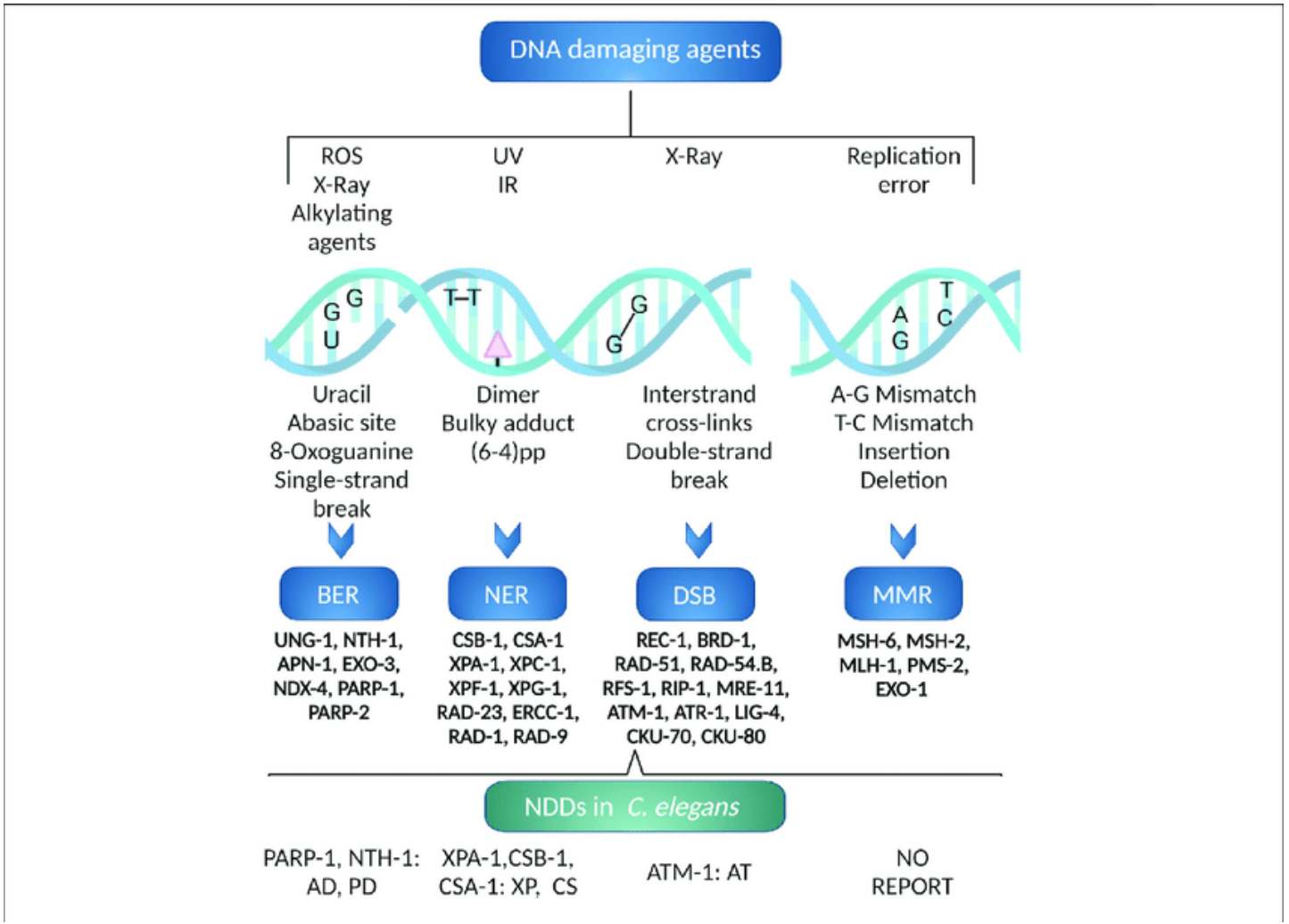
DNA damaging agents
ROS
X-Ray
Alkylating agents
UV
IR
X-Ray
Replication error
G
G
U
T–T
G
G
A
G
T
C
Uracil
Abasic site
8-Oxoguanine
Single-strand break
Dimer
Bulky adduct
(6-4)pp
Interstrand cross-links
Double-strand break
A-G Mismatch
T-C Mismatch
Insertion
Deletion
BER
NER
DSB
MMR
UNG-1, NTH-1, APN-1, EXO-3, NDX-4, PARP-1, PARP-2
CSB-1, CSA-1 XPA-1, XPC-1, XPF-1, XPG-1, RAD-23, ERCC-1, RAD-1, RAD-9
REC-1, BRD-1, RAD-51, RAD-54.B, RFS-1, RIP-1, MRE-11, ATM-1, ATR-1, LIG-4, CKU-70, CKU-80
MSH-6, MSH-2, MLH-1, PMS-2, EXO-1
NDDs in C. elegans
PARP-1, NTH-1: AD, PD
XPA-1,CSB-1, CSA-1: XP, CS
ATM-1: AT
NO REPORT

Nucleosomes and DNA mutations

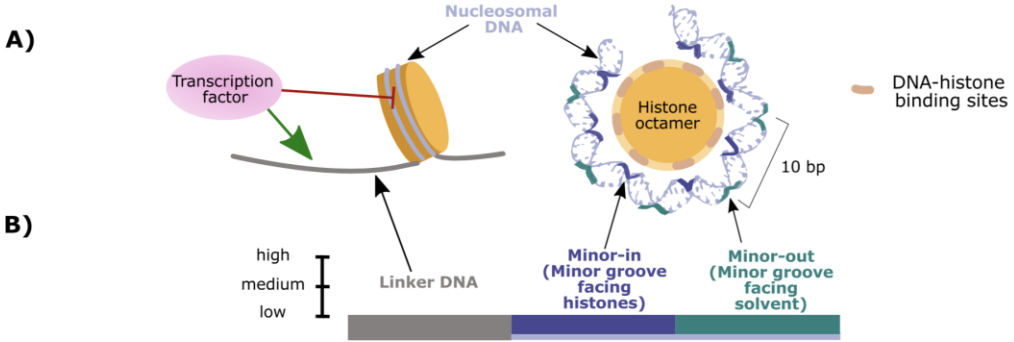

	UV-light (CPD, 6-4PP)	Smoking (BPDE-dG)	ROS (8-oxo-G)	Spontaneous deamination 5meC
Mutation type	C>T	C>A	T>C|G	C>T
DNA damage rate			?	
DNA repair rate	NER	NER	BER	MMR ? ?
Mutation rate			?	

Espiritu,D., Gribkova,A.K., Gupta,S., Shaytan,A.K. and Panchenko,A.R. (2021) Molecular Mechanisms of Oncogenesis through the Lens of Nucleosomes and Histones. *J. Phys. Chem. B*, 10.1021/acs.jpcb.1c00694.

APOBEC3 deaminases drive the acquisition of clustered mutations in human cancer cells

APOBEC — белки-дезаминазы (C>T). Известны как редакторы РНК, но они могут быть нацелены и на ДНК, например, для защиты от вирусов с ДНК-геномами.

Мутационные сигнатуры, связанные с APOBEC3 — замены C>T и C>G и/или C>A в тринуклеотидах TCN, где N — любой нуклеотид.
В классификации мутационных сигнатур они обозначены как SBS2 и SBS13.
Сигнатуры, характерные для APOBEC3, обнаружены в 70% типов рака и в 50% всех раковых геномов.

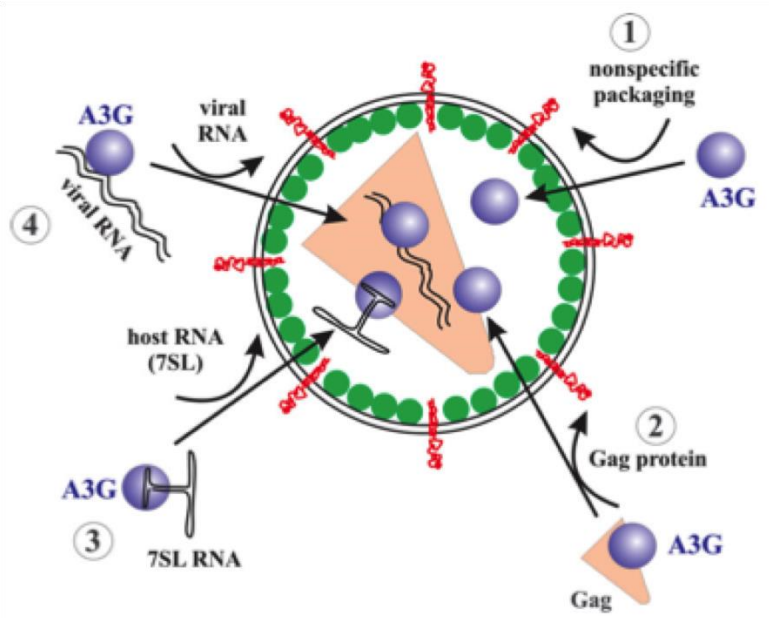

Petljak, M., Dananberg, A., Chu, K. *et al.* Mechanisms of APOBEC3 mutagenesis in human cancer cells. *Nature* 607, 799–807 (2022). https://doi.org/10.1038/s41586-022-04972-y, https://pcr.news/novosti/belki-apobec3-generiruyut-mutatsii-v-rakovykh-kletkakh/

Kataegis

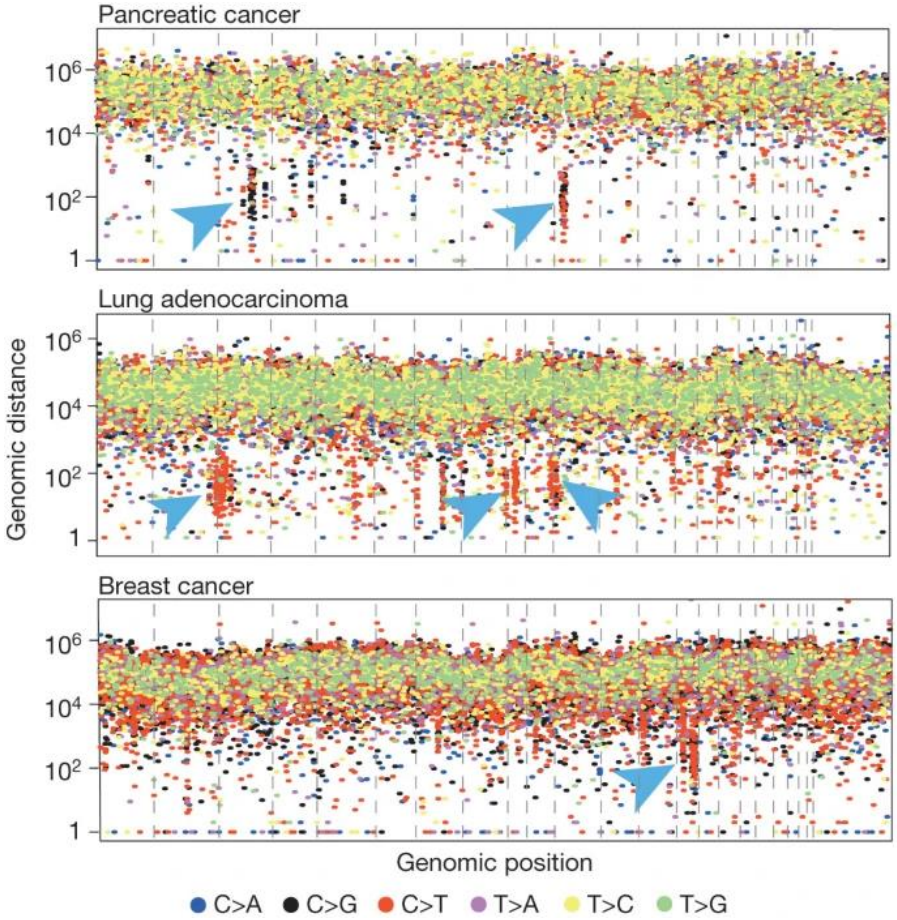

- Kataegis (after the Greek for thunderstorm) - hypermutation localized to small genomic regions
- Kataegis is characterized by clusters of C>T and/or C>G mutations which are substantially enriched at TpCpN trinucleotides and on the same DNA strand. Foci of kataegis include from a few to several thousand mutations and are often found in the vicinity of genomic rearrangements.

Alexandrov, L., Nik-Zainal, S., Wedge, D. *et al.* Signatures of mutational processes in human cancer. *Nature* 500, 415–421 (2013). https://doi.org/10.1038/nature12477

Онкогистоны

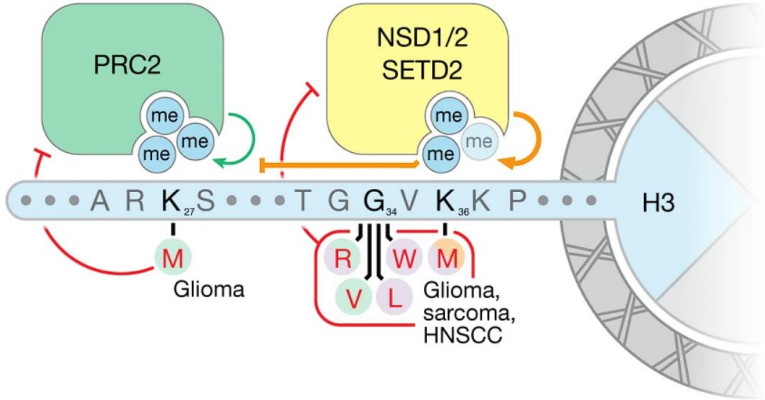

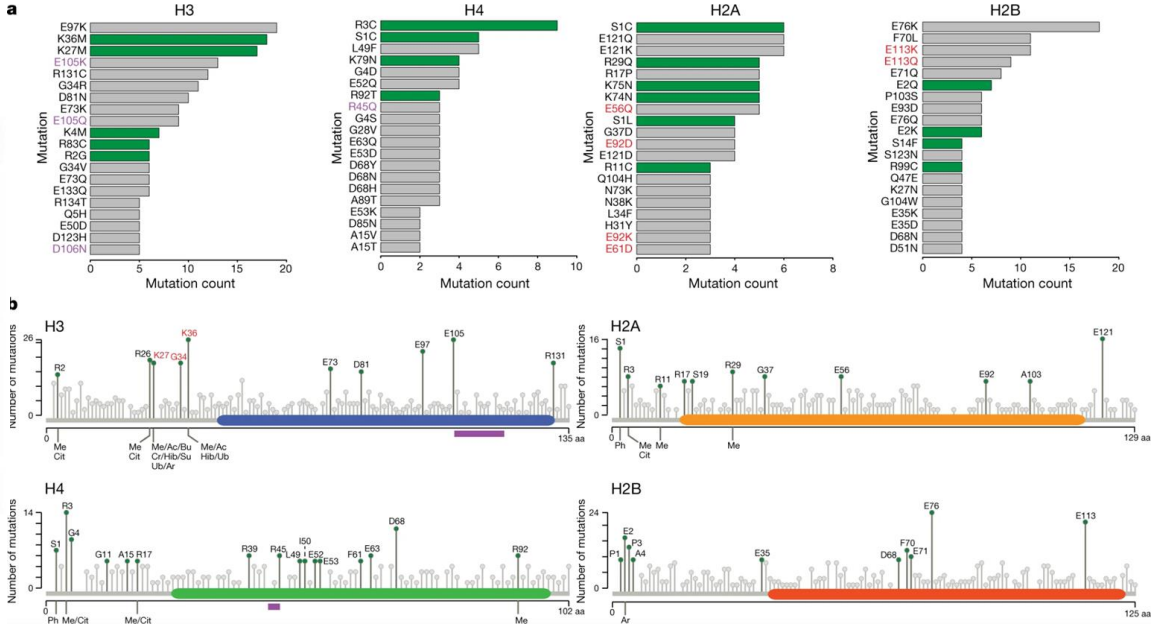

Nacev, B.A., Feng, L., Bagert, J.D. *et al.* The expanding landscape of ‘oncohistone’ mutations in human cancers. *Nature* 567, 473–478 (2019). https://doi.org/10.1038/s41586-019-1038-1

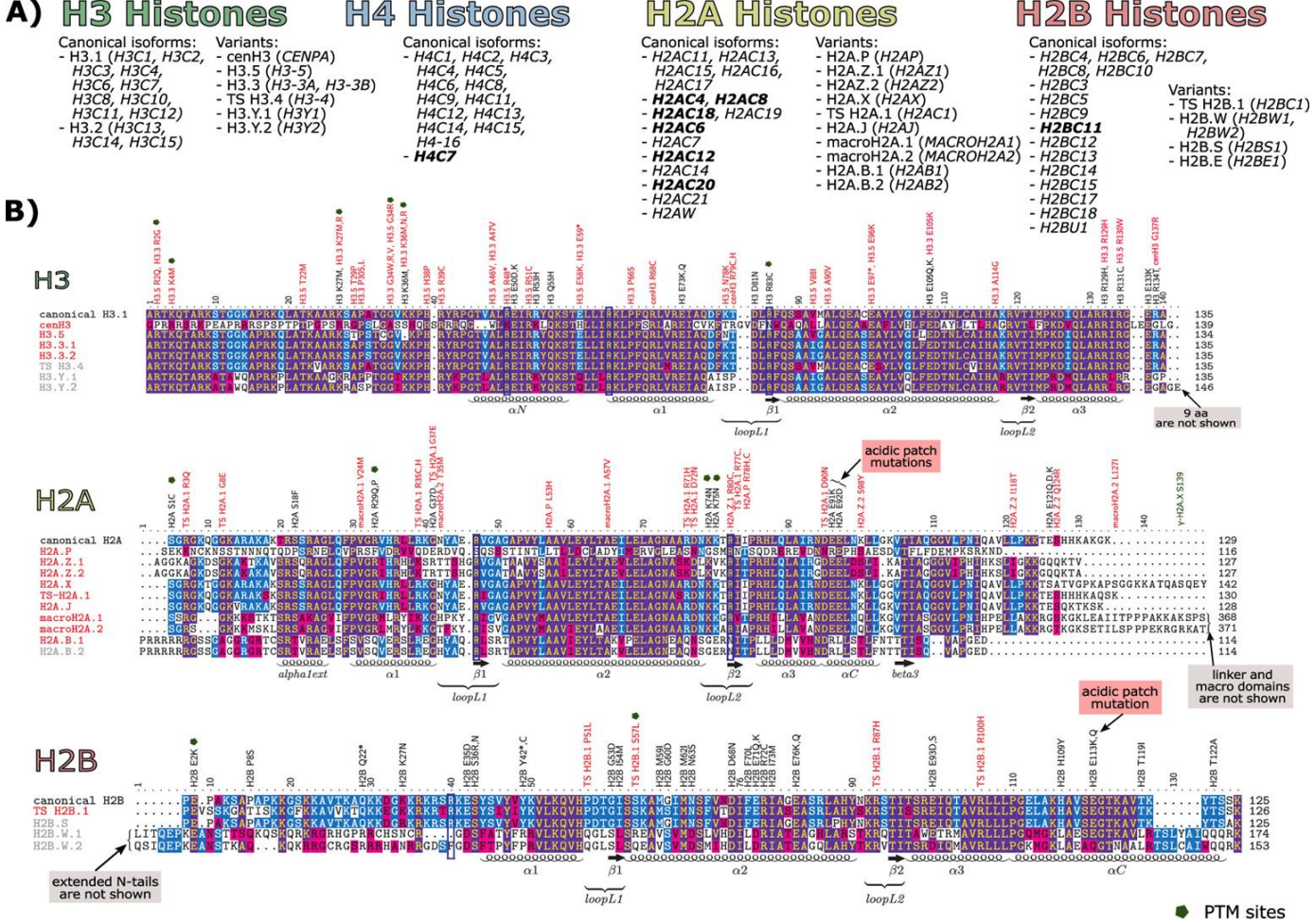

Espiritu, D.; **Gribkova, A. K.**; Gupta, S.; **Shaytan, A. K.**; Panchenko, A. R. Molecular Mechanisms of Oncogenesis through the Lens of Nucleosomes and Histones. *J. Phys. Chem. B* **2021**. https://doi.org/10.1021/acs.jpcb.1c00694.

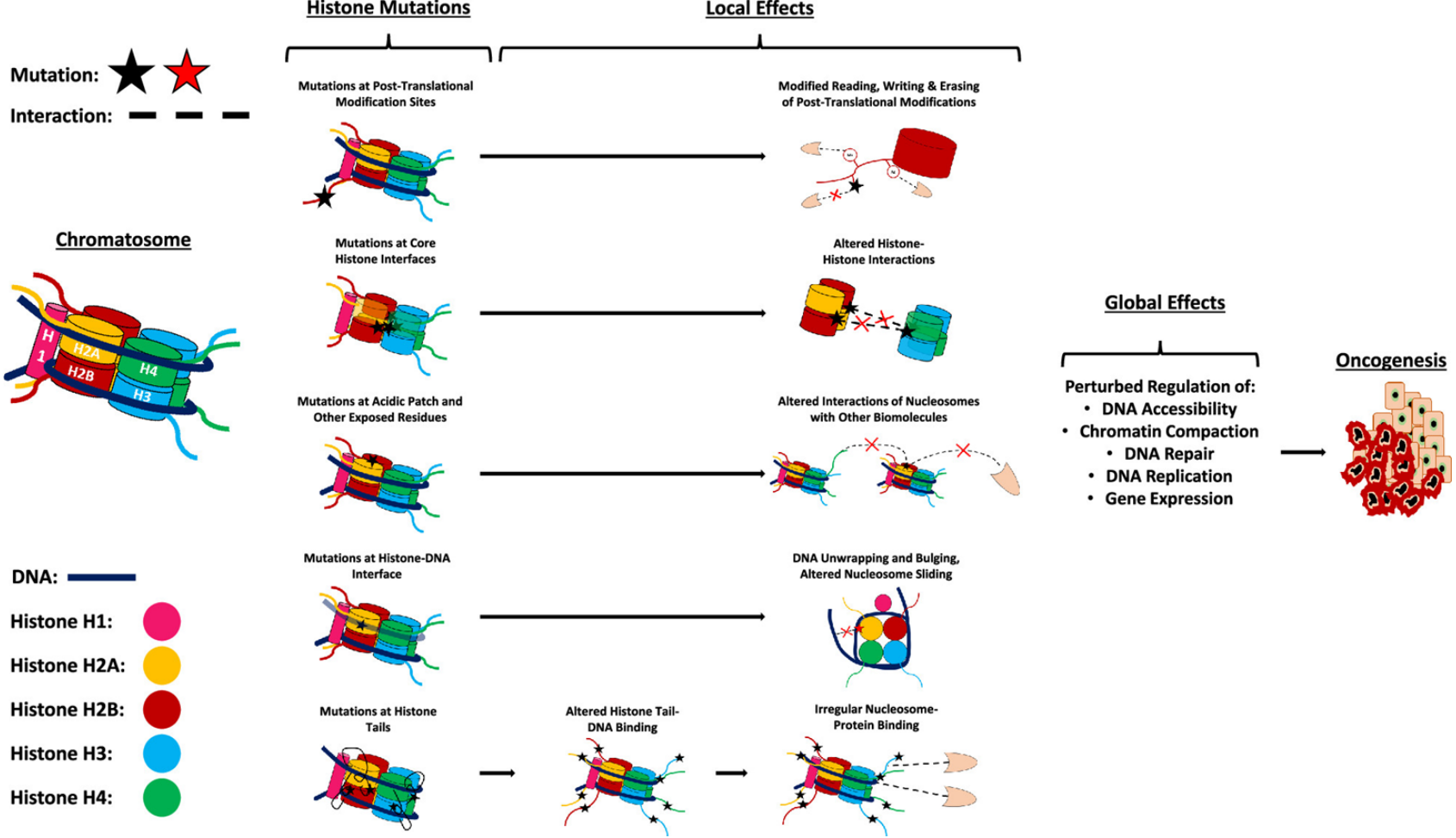

Espiritu, D.; **Gribkova, A. K.**; Gupta, S.; **Shaytan, A. K.**; Panchenko, A. R. Molecular Mechanisms of Oncogenesis through the Lens of Nucleosomes and Histones. *J. Phys. Chem. B* **2021**. https://doi.org/10.1021/acs.jpcb.1c00694.

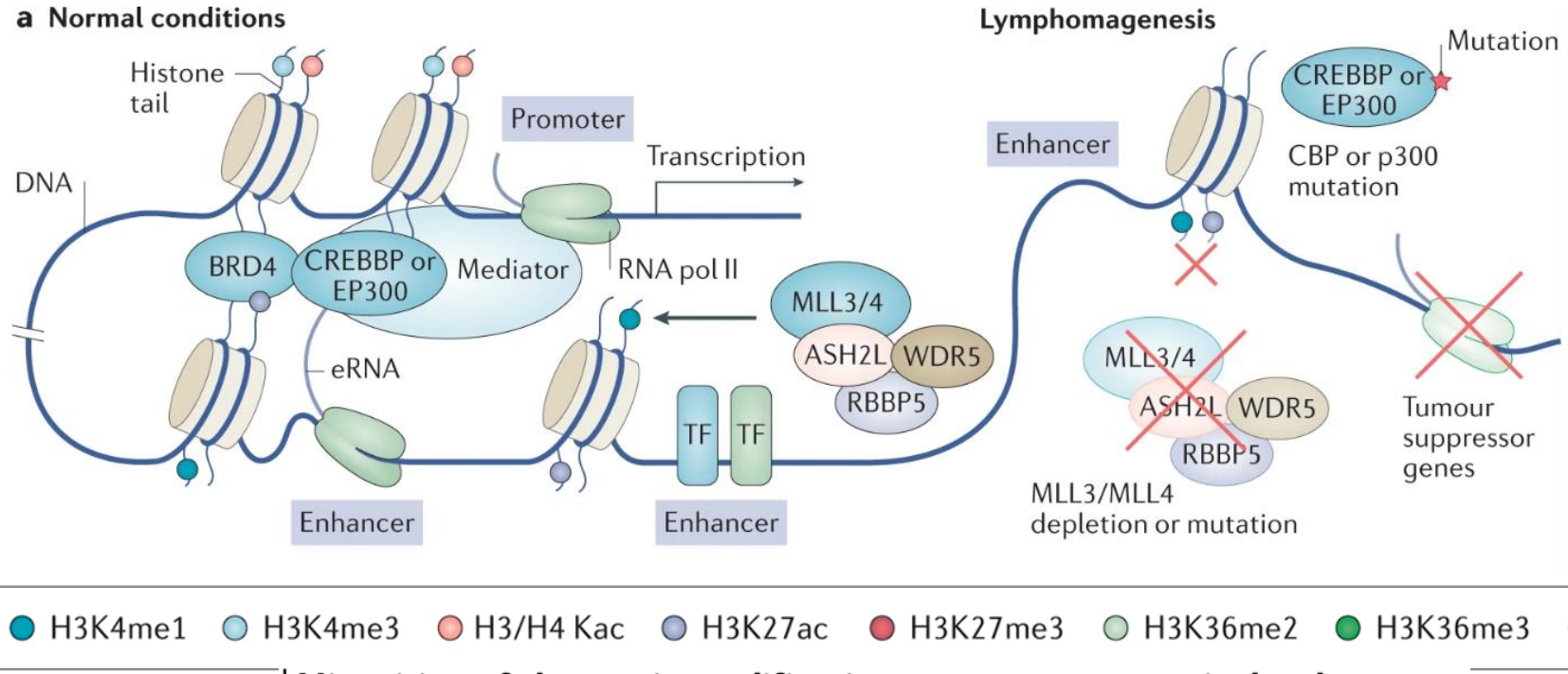

| Miswriting of chromatin modification promotes oncogenic development.

a | An active enhancer is marked by H3K4me1 and H3K27ac, which are generated by mixed lineage leukaemia 3 (MLL3) and MLL4, and histone acetyltransferases such as CREB-binding protein (CREBBP) and EP300. Enhancers are bound by transcription factors (TFs), mediators and transcription coactivators such as BRD4, which activate RNA polymerase II (RNA pol II) for mediating productive transcription from promoters and generating enhancer RNA (eRNA) to facilitate gene activation. Enhancer–promoter looping underlies activation of gene transcription. **Loss or inactivation mutation of *CREBBP* or *EP300* and/or *MLL3* or *MLL4* is characteristic of cancers such as B cell lymphoma, resulting in decreased H3K27ac and/or H3K4me1 at enhancers and reduced expression of genes related to tumour suppression, cell differentiation and/or antitumour immunity**.

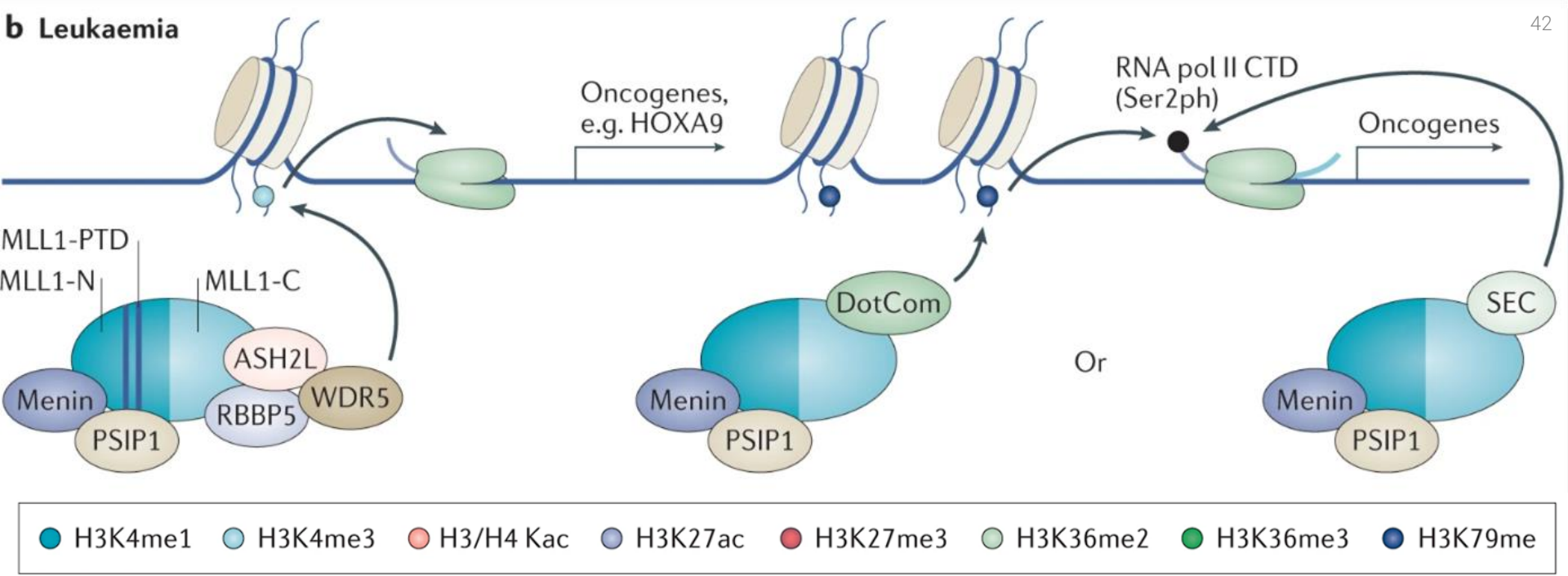

b | Wild-type MLL1 uses an N-terminal region for interacting with chromatin-binding cofactors, menin and PC4 and SFRS1-interacting protein (PSIP1). **MLL1 or its partial tandem duplication (PTD) results in elevated H3K4me3 at oncogenes such as HOX, promoting acute leukaemogenesis.** An MLL1 fusion oncoprotein gains a C-terminal segment from its fusion partner, such as AF9, ENL or AF4, which recruits DOT1L complex (DotCom) for catalysing H3K79 methylation and/or the super elongation complex (SEC) for catalysing serine 2 phosphorylation (Ser2ph) of the C-terminal domain (CTD) of RNA pol II. H3K79me and RNA pol II CTD Ser2ph, possibly with other activators such as PAF1, promote expression of oncogenes such as those of the HOX family.

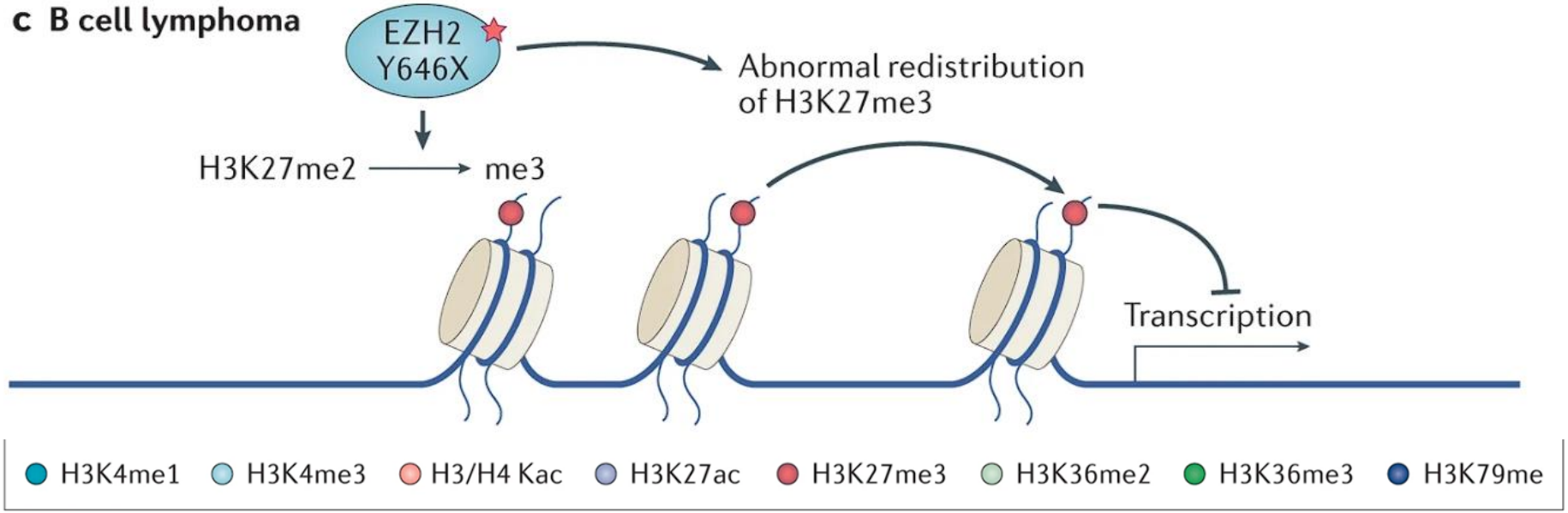

c | A collective action of wild-type EZH2 and its gain-of-function mutation, Y646X (X = F, C, H, S or N), causes abnormal elevation of H3K27me3 in lymphoma, leading to downregulation of transcripts related to cell cycle control and B cell differentiation.

Zhao, S., Allis, C.D. & Wang, G.G. The language of chromatin modification in human cancers. *Nat Rev Cancer* 21, 413–430 (2021). https://doi.org/10.1038/s41568-021-00357-x

DOT1-like histone H3K79 methyltransferase

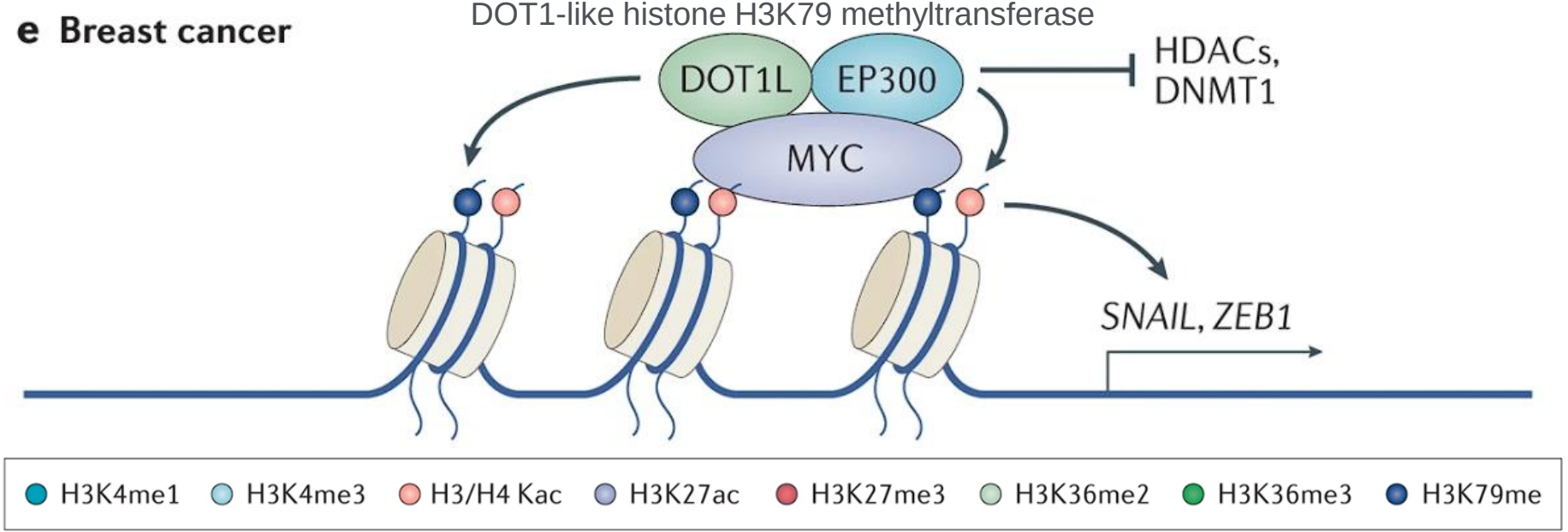

e | In breast cancer, overexpressed DOT1L interacts with MYC and EP300 to antagonize histone deacetylases (HDACs) and DNMT1, leading to the elevated H3K79me and H3Kac levels at epithelial–mesenchymal transition (EMT)-promoting oncogenes such as SNAIL and ZEB1.

Zhao, S., Allis, C.D. & Wang, G.G. The language of chromatin modification in human cancers. *Nat Rev Cancer* 21, 413–430 (2021). https://doi.org/10.1038/s41568-021-00357-x

Cell free nucleosomes

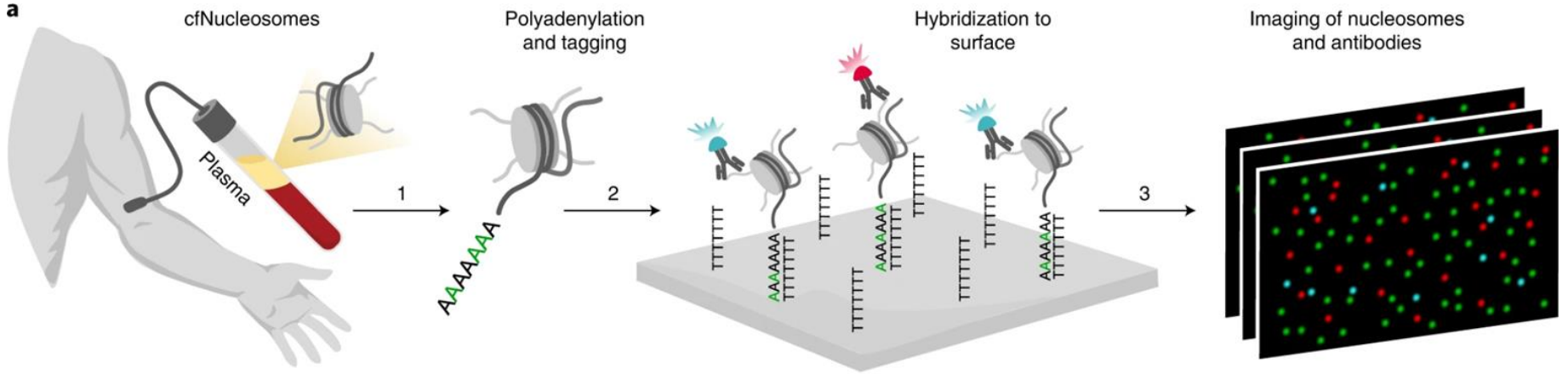

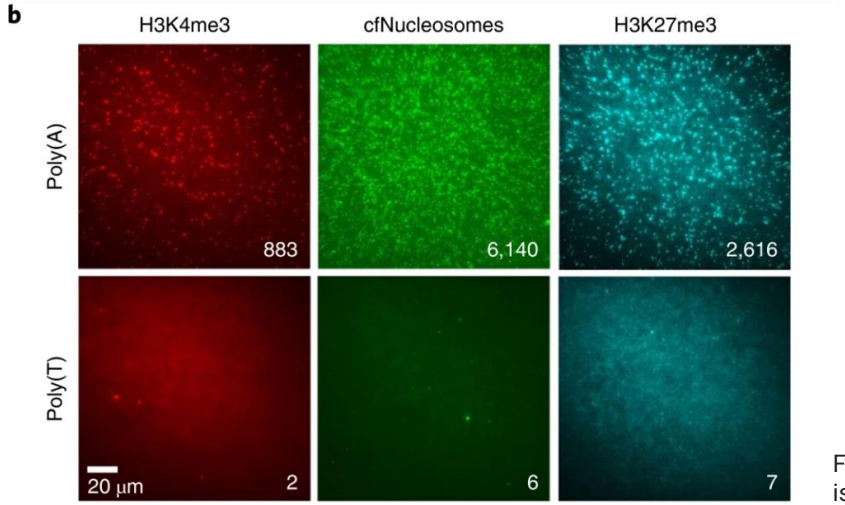

We developed a single-molecule multiparametric assay to comprehensively profile the epigenetics of plasma-isolated nucleosomes (EPINUC), DNA methylation and cancer-specific protein biomarkers. Our system allows for high-resolution detection of six active and repressive histone modifications and their ratios and combinatorial patterns on millions of individual nucleosomes by single-molecule imaging.

EPINUC analysis of a cohort of 63 colorectal cancer, 10 pancreatic cancer and 33 healthy plasma samples detected cancer with high accuracy and sensitivity, even at early stages.

Fedyuk, V., Erez, N., Furth, N. et al. Multiplexed, single-molecule, epigenetic analysis of plasma-isolated nucleosomes for cancer diagnostics. Nat Biotechnol 41, 212–221 (2023). https://doi.org/10.1038/s41587-022-01447-3

Эпигенетическое репрограммирование и импринтинг

Epigenetic genome wide reprogramming

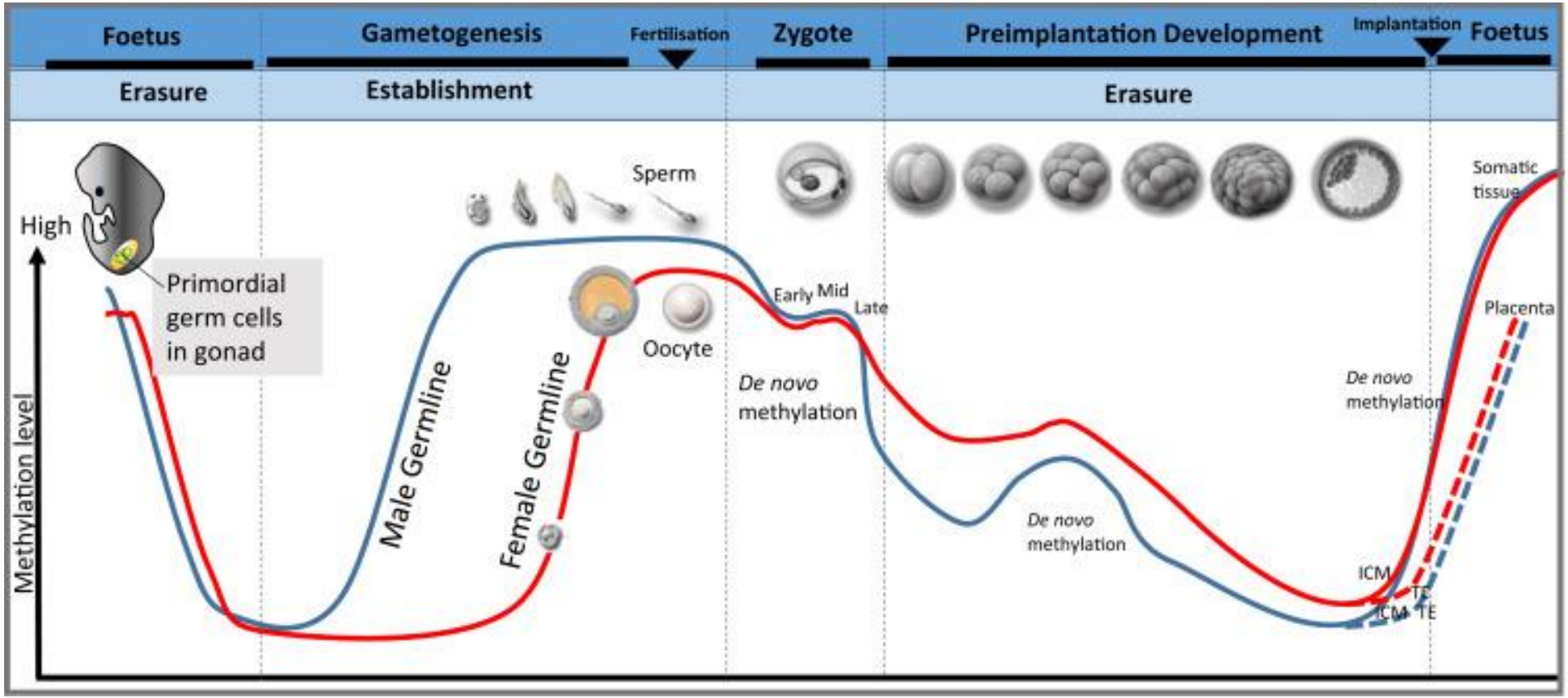

Epigenetic genome wide reprogramming

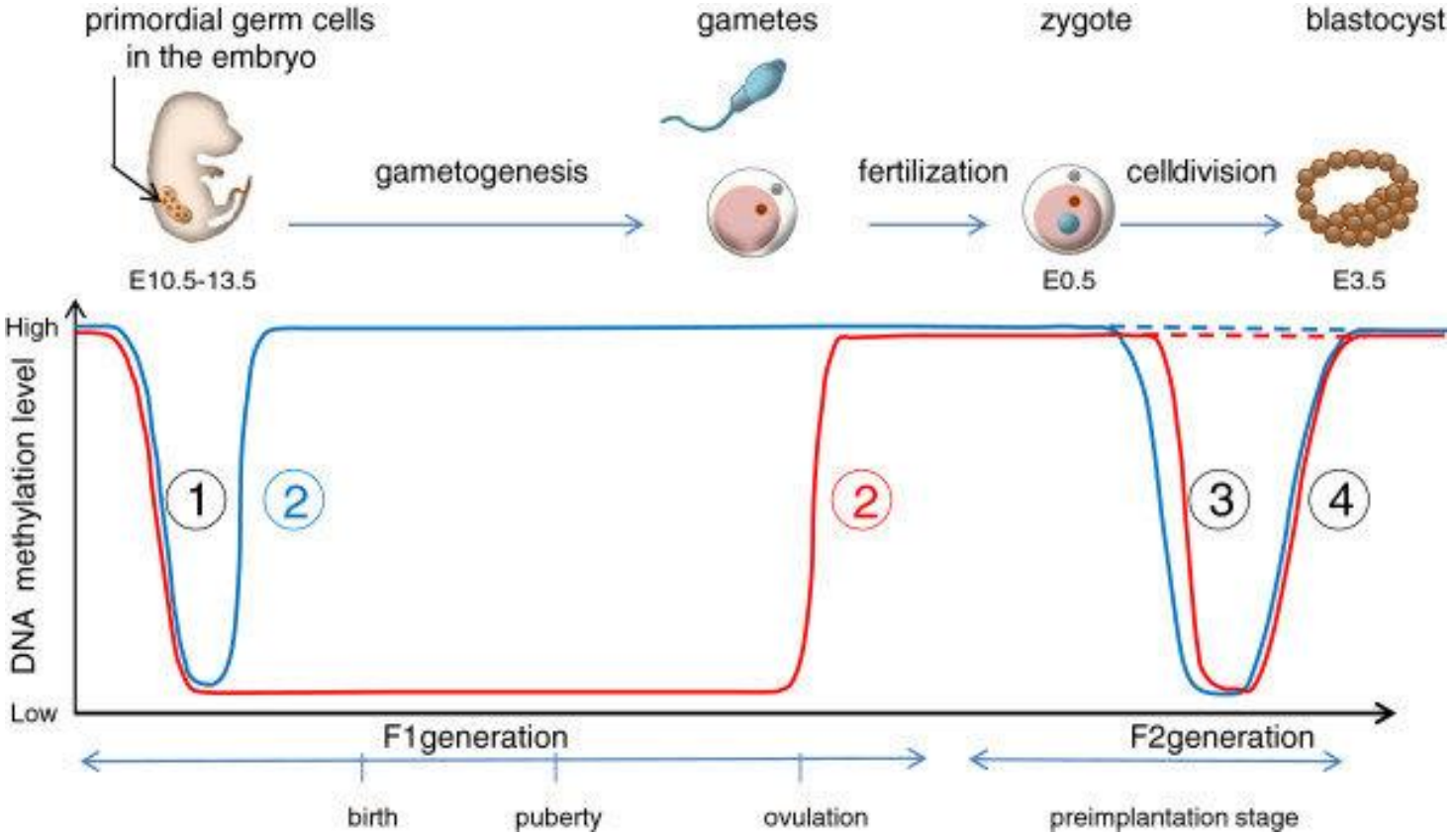

Импринтинг

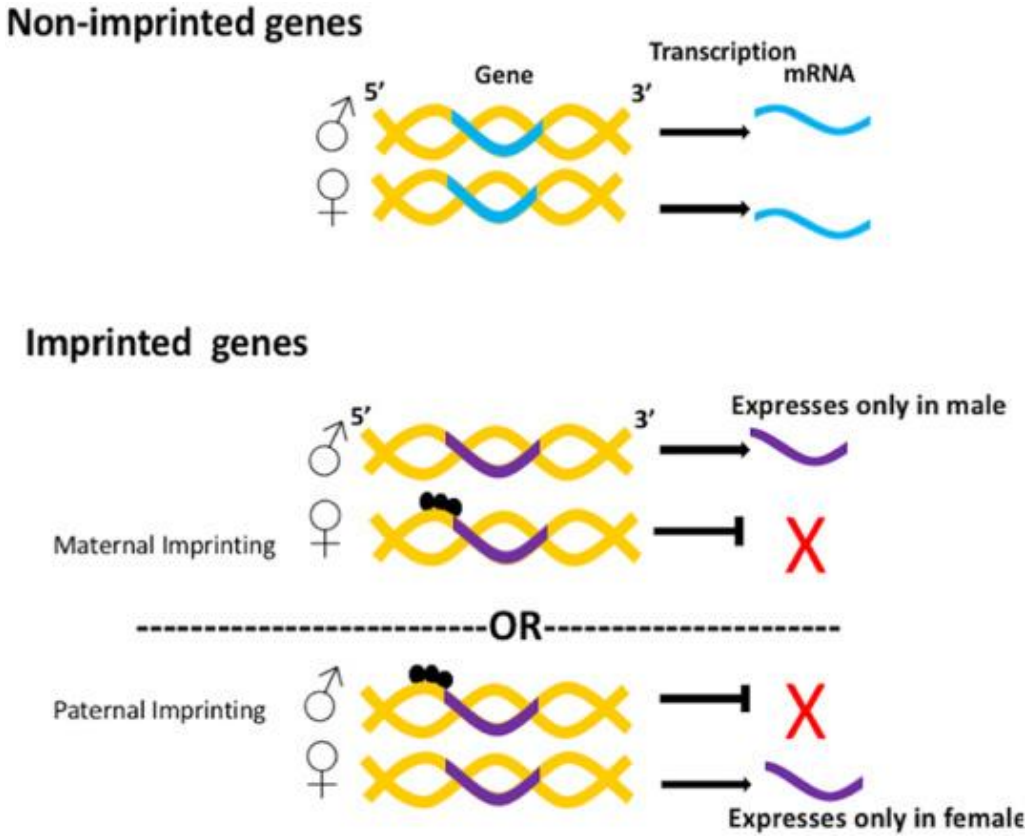
Non-imprinted genes
Transcription
Gene
mRNA
5′
3′
Imprinted genes
5′
3′
Expresses only in male
Maternal Imprinting
X
----------OR----------
Paternal Imprinting
X
Expresses only in female

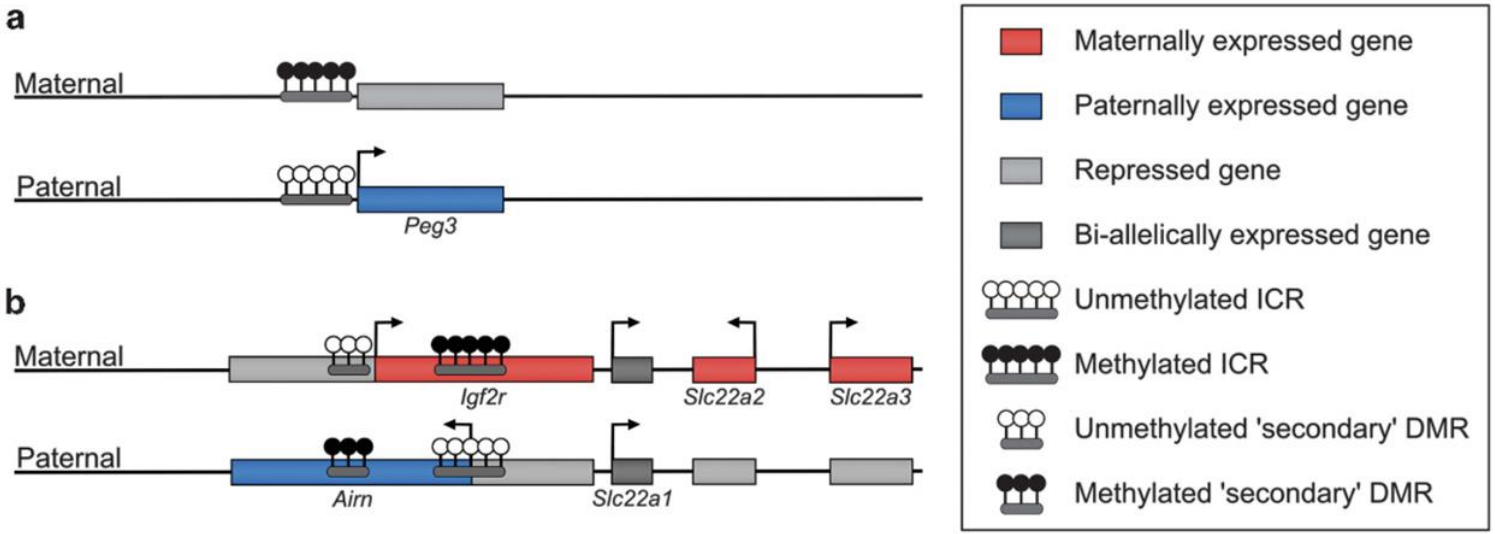

Figure 1 Examples of directly and indirectly regulated imprinted regions. Schematic representation of the (**a**) *Peg3* imprinted gene on chromosome 7 and (**b**) the *Igf2r* imprinted cluster on chromosome 17. The expression status of the genes on the maternal and paternal alleles is illustrated; active promoters are represented by horizontal arrows. (**a**) The differentially methylated ICR established during germ cell development is located at the promoter of the *Peg3* gene and directly regulates the monoallelic transcription of this gene. (**b**) The maternally methylated ICR indirectly regulates the monoallelic expression of the adjacent genes at this locus, partially mediated by the monoallelic methylation acquired at the nearby secondary DMR at the *Igf2r* promoter.

As of 2019, 260 imprinted genes have been reported in mice and 228 in humans

10.1038/hdy.2014.54

AN EXAMPLE OF IMPRINTING

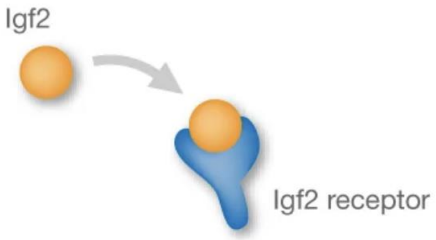

1 In mammals, the growth factor Igf2 interacts with the Igf2 receptor.

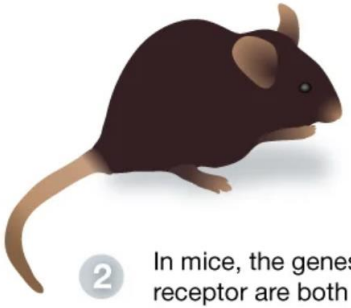

Genes from mom:
Igf2 receptor - ON
Igf2 - OFF

Genes from dad:
Igf2 receptor - OFF
Igf2 - ON

2 In mice, the genes for Igf2 and the Igf2 receptor are both imprinted.

Deleting the mother's Igf2 receptor gene produces overly large offspring.

Deleting the father's Igf2 gene produces dwarf offspring.

Deleting the mother's Igf2 receptor gene AND the father's Igf2 gene produces normally sized offspring.

3 The imprints on the Igf2 and Igf2 receptor genes normally cancel each other out. Changing the imprint on one copy of the gene has a dramatic effect on the size of the offspring. This result supports the genetic conflict hypothesis

- In germline cells the imprint is erased and then re-established according to the sex of the individual, i.e. in the developing sperm (during spermatogenesis), a paternal imprint is established, whereas in developing oocytes (oogenesis), a maternal imprint is established. This process of erasure and reprogramming is necessary such that the germ cell imprinting status is relevant to the sex of the individual.

Эпигенетическая разметка мешает клонированию

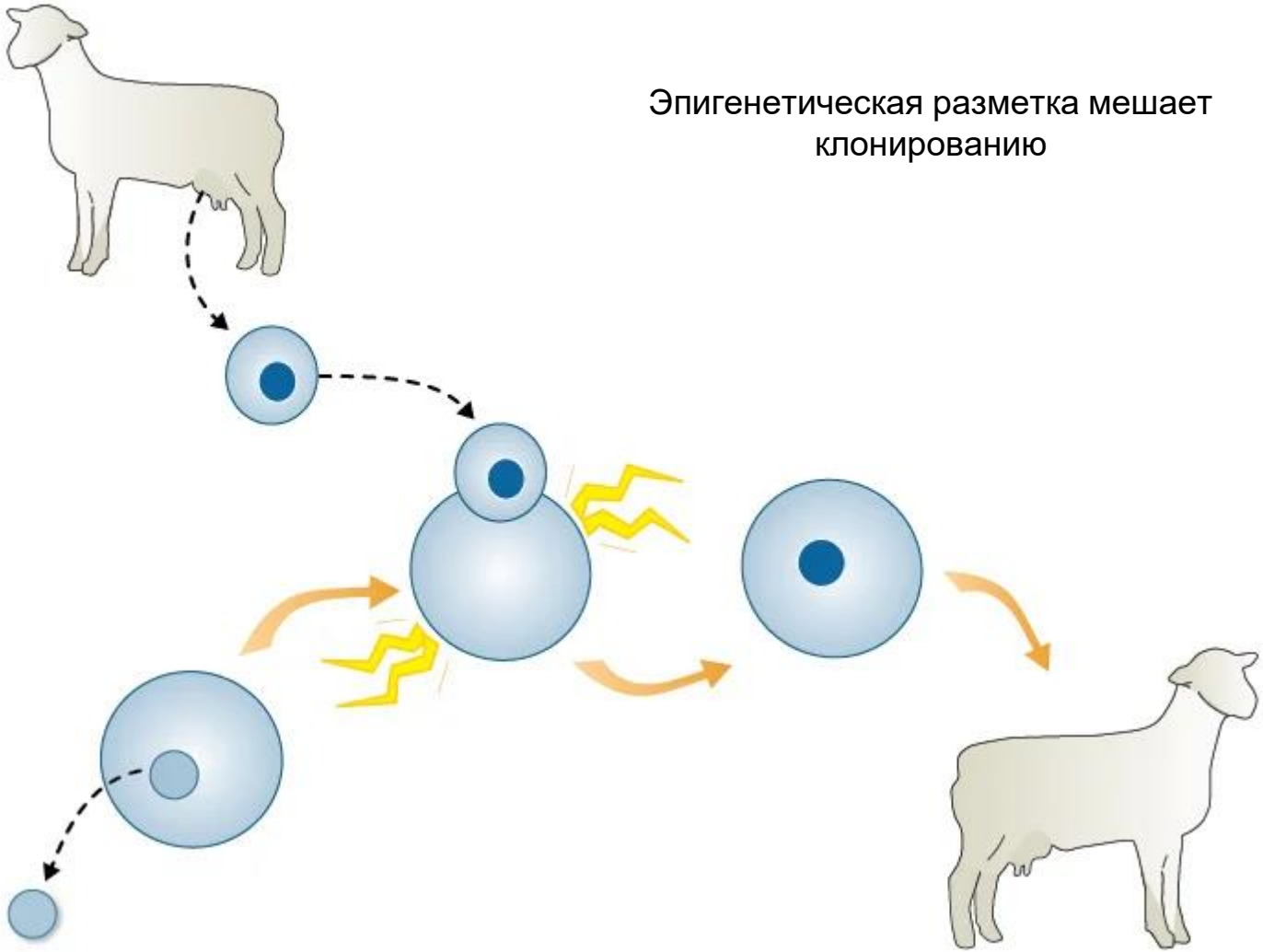

News in focus

CIOBANILC ADRIAN EUGEN/ALAMY

Only a few of the embryos derived from all-male cells developed into healthy mouse pups.

THE MICE WITH TWO DADS: SCIENTISTS CREATE EGGS FROM MALE CELLS

Proof-of-concept mouse experiment will have a long road before use in humans is possible.

Актуальные вопросы эпигенетики

Часы Хорвата

Genome Biol. 2013; 14(10): R115.
Published online 2013 Oct 21. doi: 10.1186/gb-2013-14-10-r115

DNA methylation age of human tissues and cell types

Steve Horvath[1,2,3]

I developed a multi-tissue predictor of age that allows one to estimate the DNA methylation age of most tissues and cell types. The predictor, which is freely available, was developed using 8,000 samples from 82 Illumina DNA methylation array datasets, encompassing 51 healthy tissues and cell types. I found that

the same set of 353 CpGs and the same prediction algorithm is used irrespective of the DNA source within the organism

The median error of estimated age is 3.6 years across a wide spectrum of tissues and cell types

Steve Horvath

Horvath spent over 4 years collecting publicly available Illumina DNA methylation data and identifying suitable statistical methods

the epigenetic clock captures an emergent property of the epigenome

Schematics of DNA methylation patterns in early life and ageing

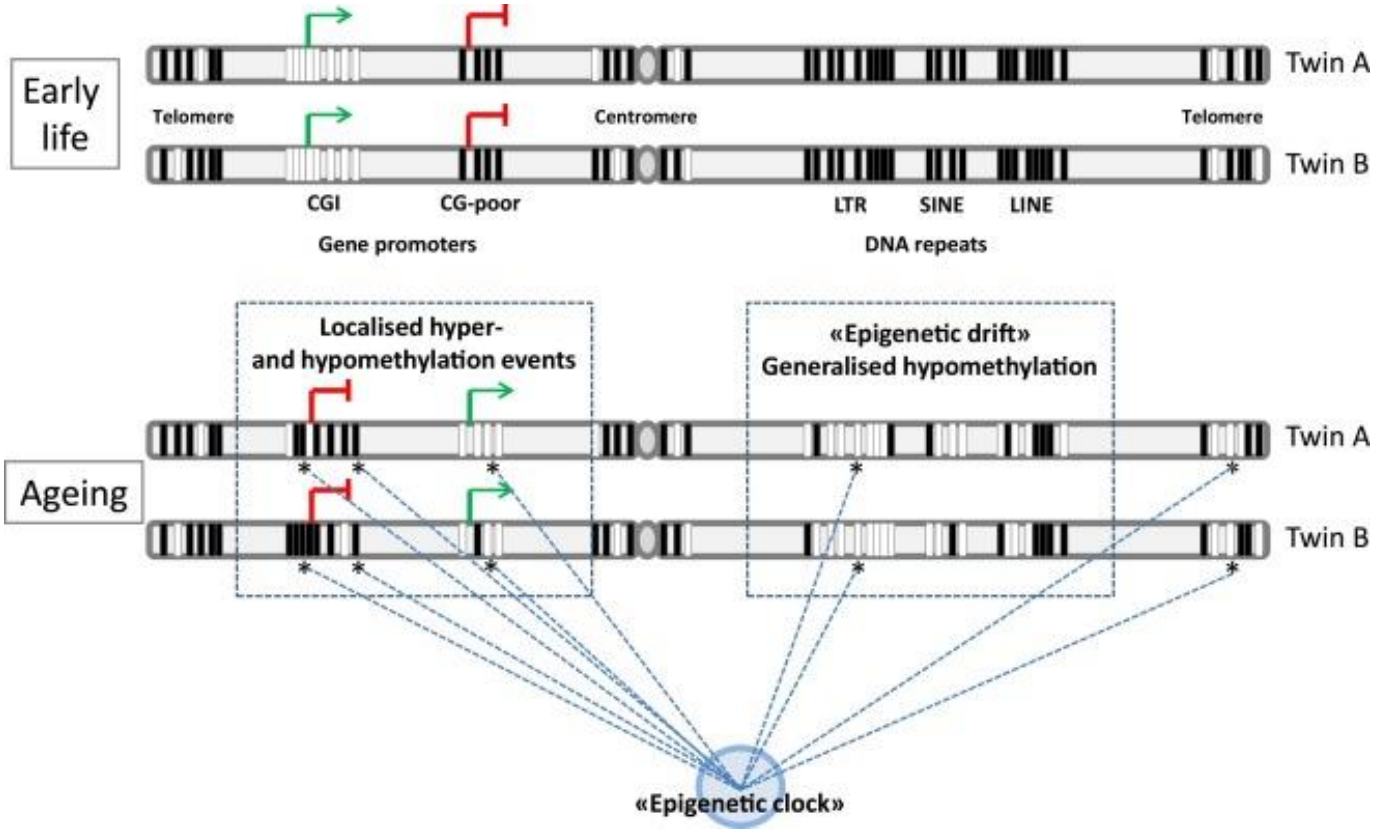

Ciccarone F, Tagliatesta S, Caiafa P, Zampieri M. DNA methylation dynamics in aging: how far are we from understanding the mechanisms? Mech Ageing Dev. 2018 Sep;174:3-17. doi: 10.1016/j.mad.2017.12.002.

Часы Хорвата

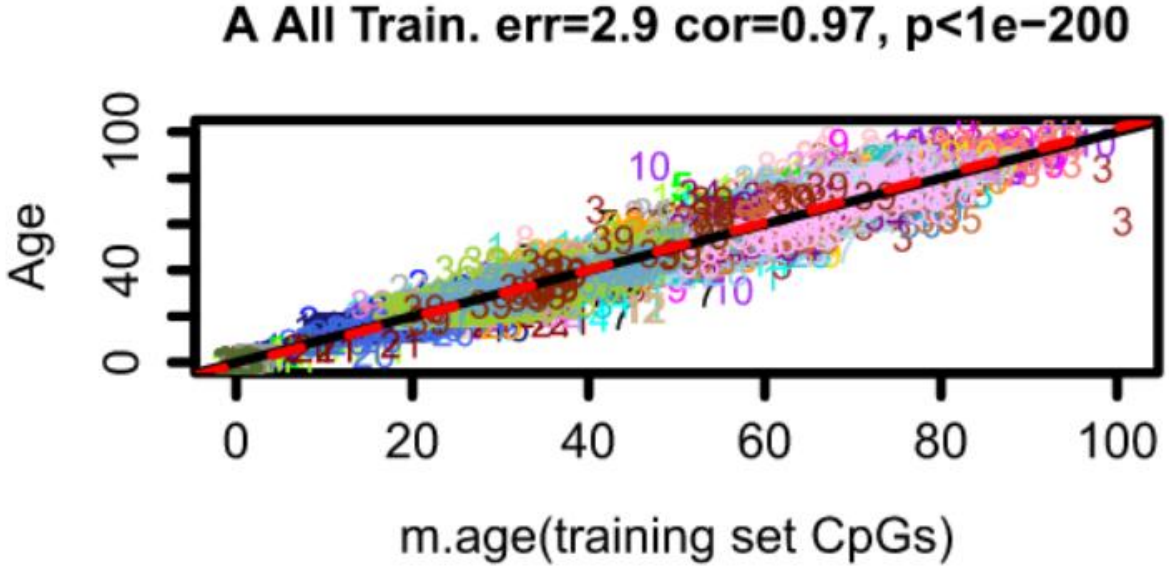

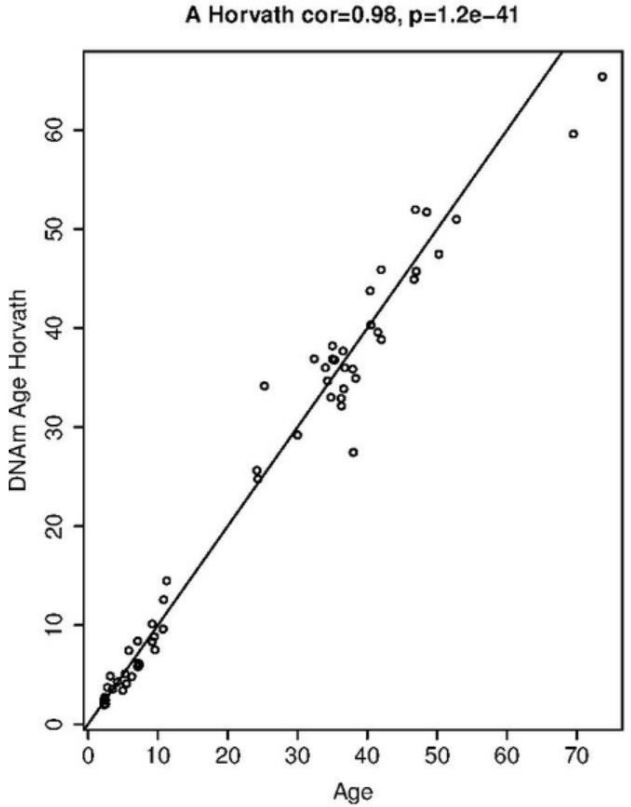

iPSC - механизмы

Induced pluripotent stem cell

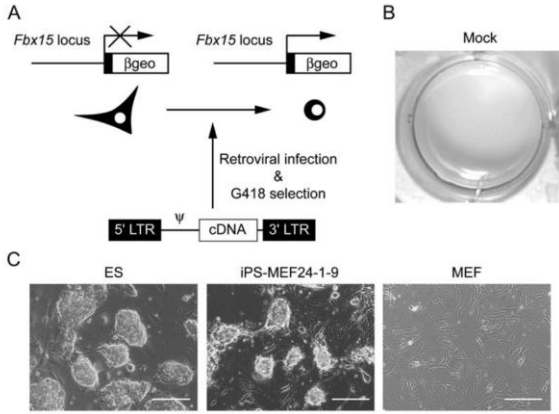

Induction of Pluripotent Stem Cells from Mouse Embryonic and Adult Fibroblast Cultures by Defined Factors

Kazutoshi Takahashi[1] and Shinya Yamanaka[1,2,*]
[1] Department of Stem Cell Biology, Institute for Frontier Medical Sciences, Kyoto University, Kyoto 606-8507, Japan
[2] CREST, Japan Science and Technology Agency, Kawaguchi 332-0012, Japan
*Contact: yamanaka@frontier.kyoto-u.ac.jp
DOI 10.1016/j.cell.2006.07.024

Cell *126*, 663–676, August 25, 2006

Differentiated cells can be reprogrammed to an embryonic-like state by transfer of nuclear contents into oocytes or by fusion with embryonic stem (ES) cells. Little is known about factors that induce this reprogramming. Here, we demonstrate induction of pluripotent stem cells from mouse embryonic or adult fibroblasts by introducing four factors, Oct3/4, Sox2, c-Myc, and Klf4, under ES cell culture conditions.

Shinya Yamanaka

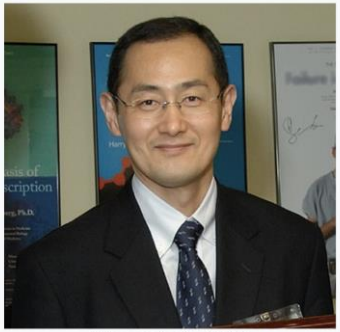

Yamanaka in 2010

September 4, 1962 (age 60)

Nobel Prize in Physiology or Medicine (2012)

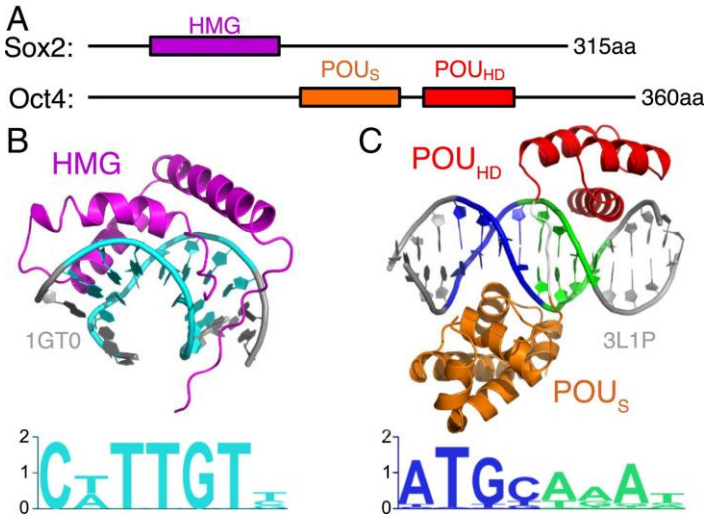

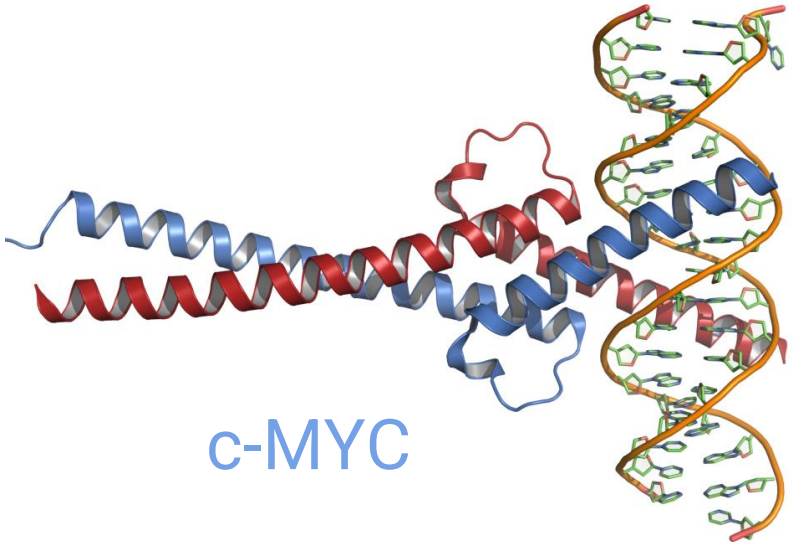

60

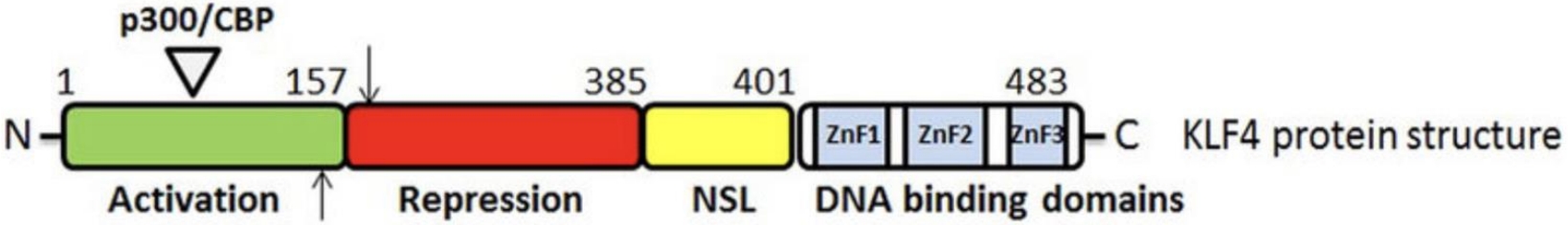

Krüppel-like factor 4

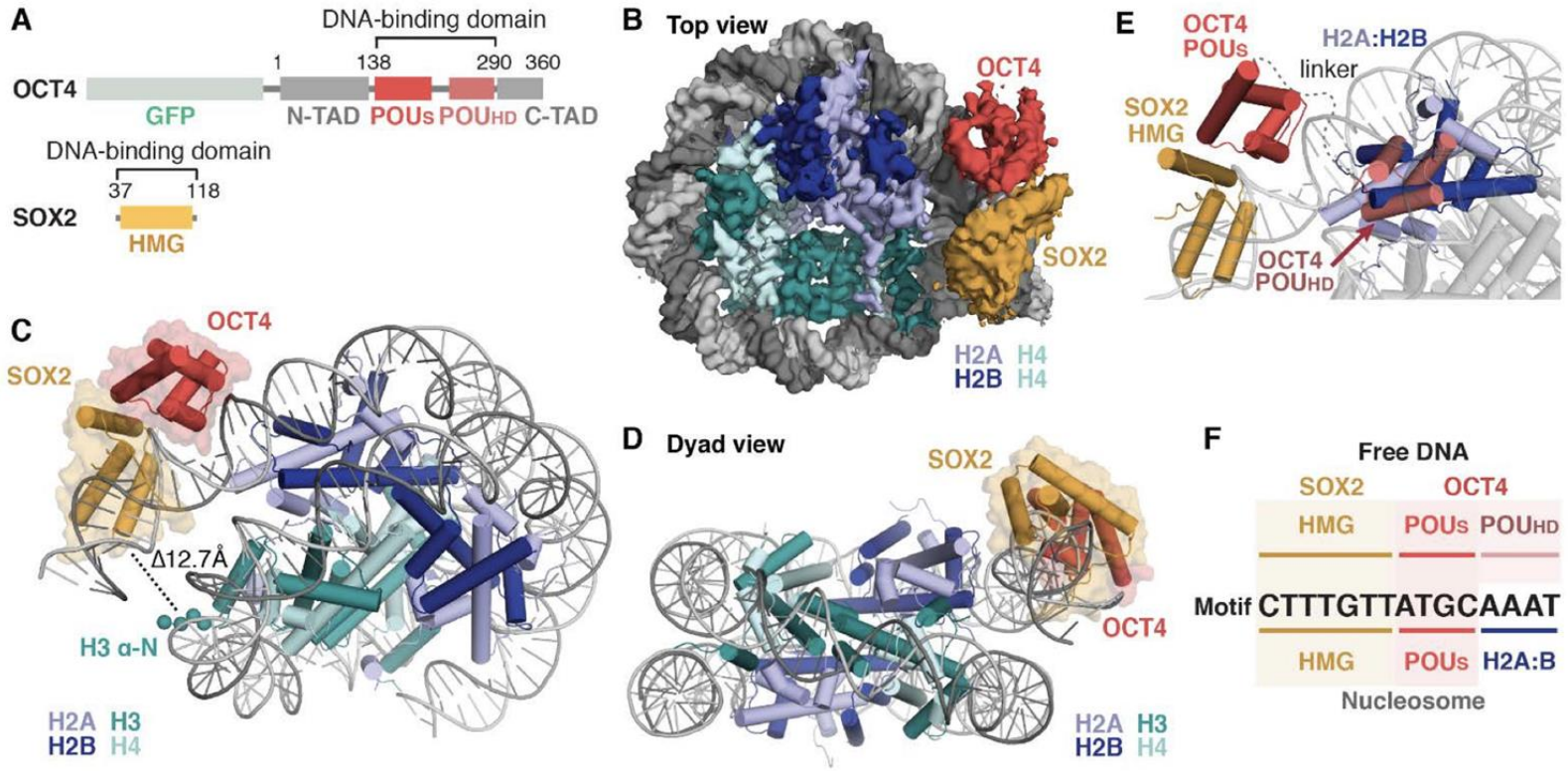

10.1126/science.abb007

Управление эпигеномом

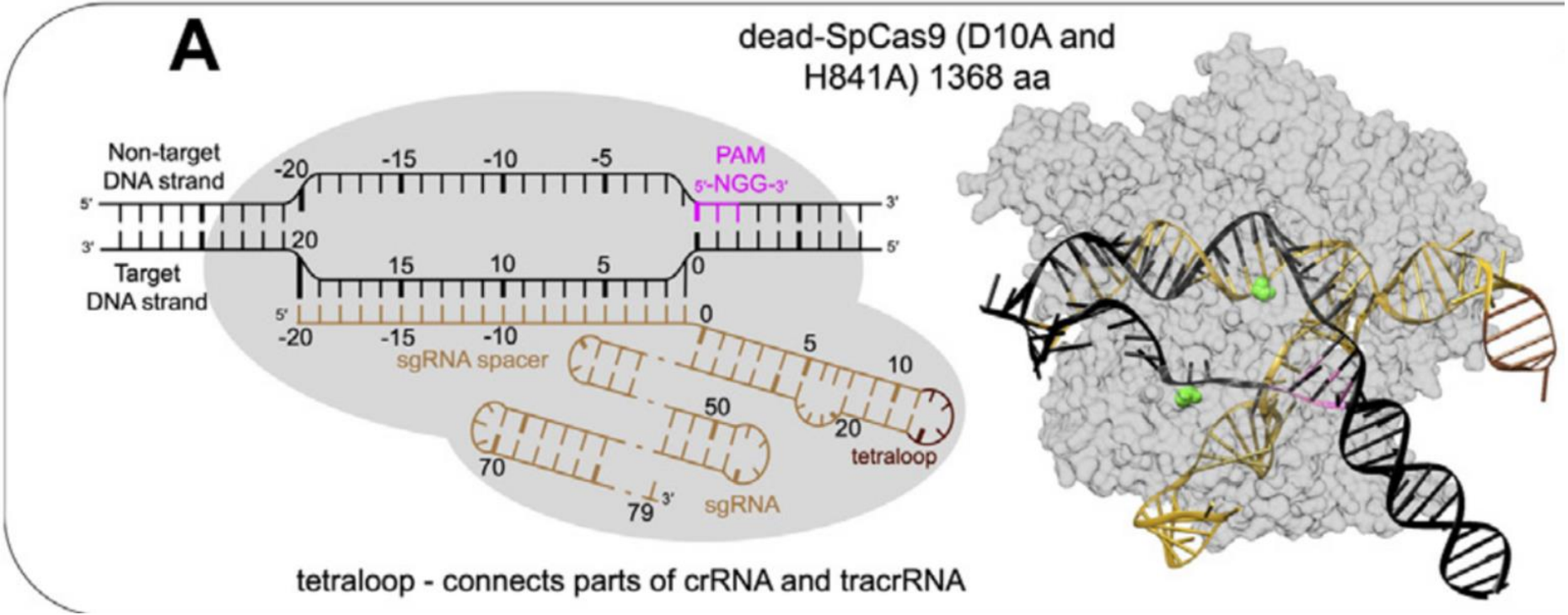

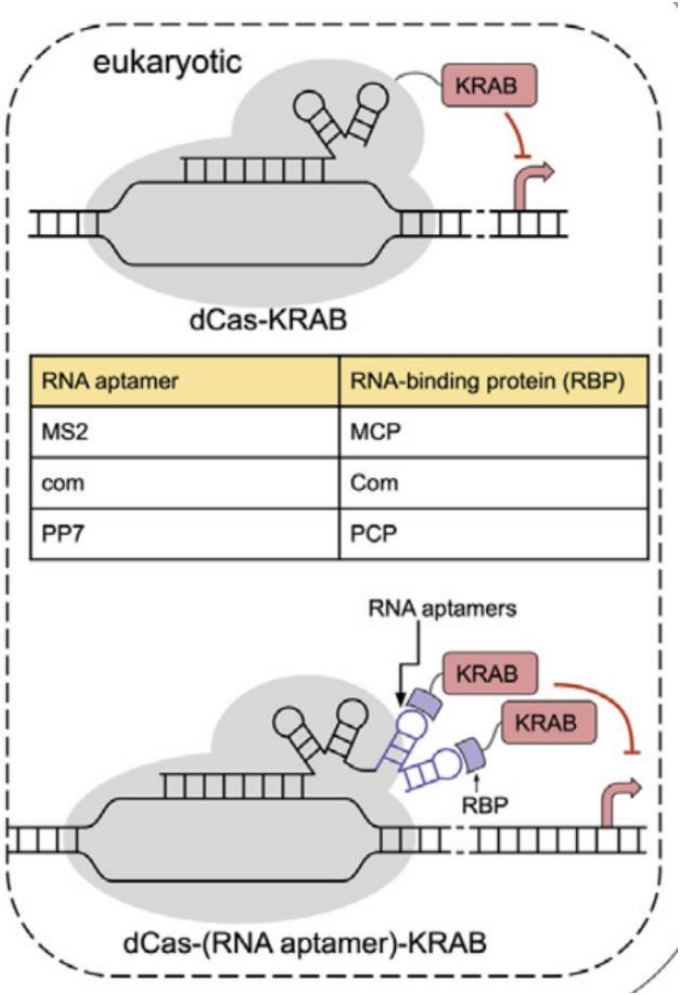

RNA aptamer	RNA-binding protein (RBP)
MS2	MCP
com	Com
PP7	PCP

Krüppel Associated Box

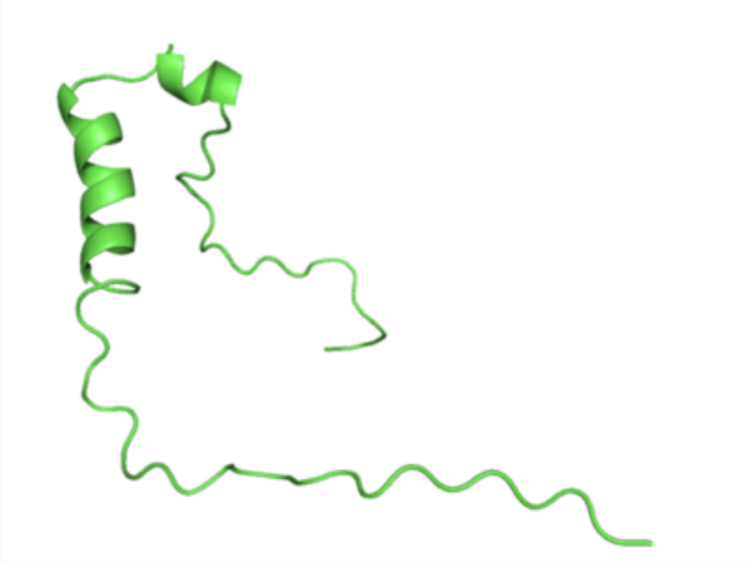

KRAB domain

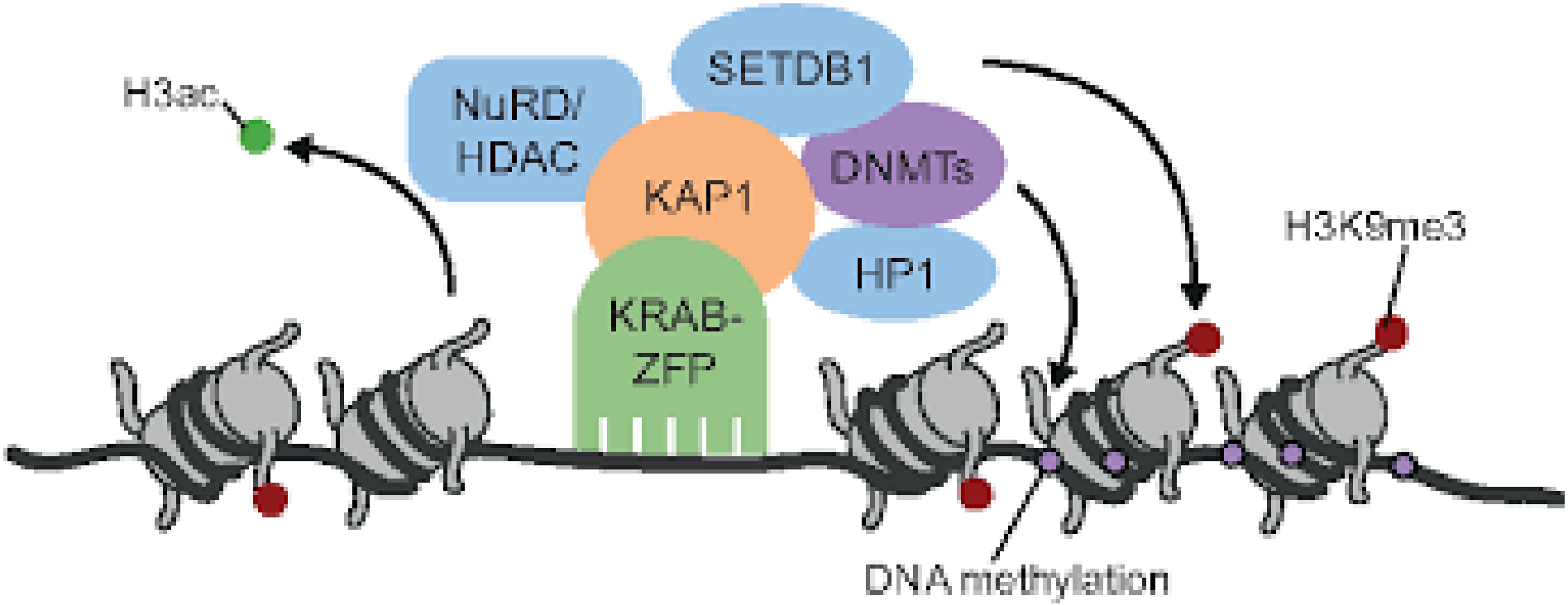
H3ac
NuRD/
HDAC
SETDB1
KAP1
DNMTs
HP1
KRAB-
ZFP
H3K9me3
DNA methylation

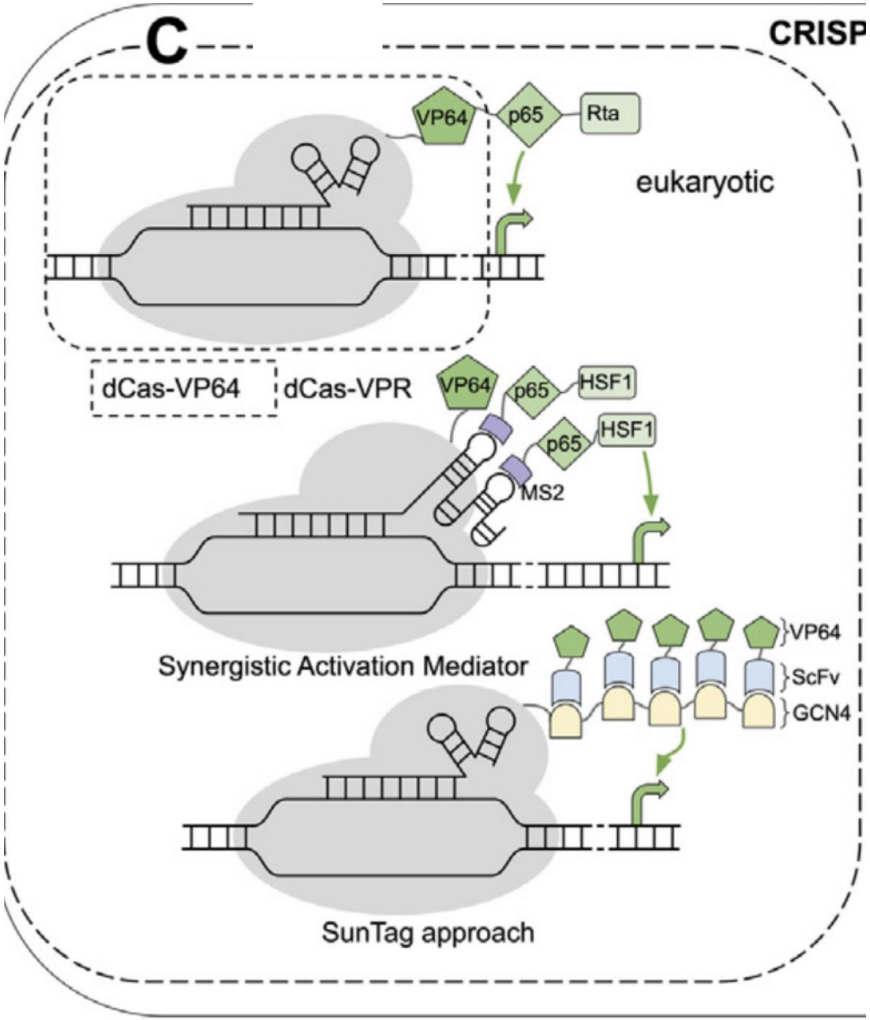
C
CRISP
VP64
p65
Rta
eukaryotic
dCas-VP64
dCas-VPR
VP64
p65
HSF1
p65
HSF1
MS2
Synergistic Activation Mediator
VP64
ScFv
GCN4
SunTag approach

Vmw65, also known as VP16 or α-TIF (Trans Inducing Factor) is a trans-acting protein that forms a complex with the host transcription factors Oct-1 and HCF to induce immediate early gene transcription in the herpes simplex viruses.

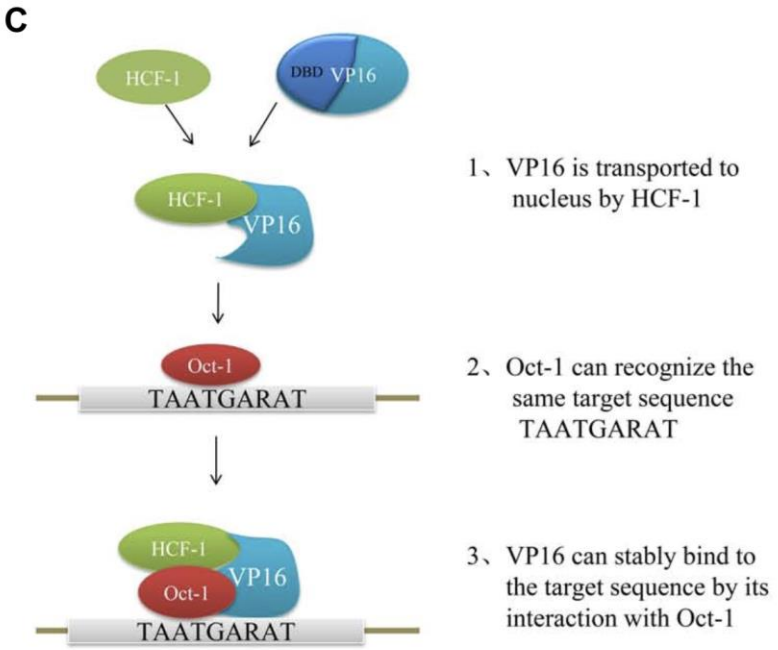

Stage 1. VP16 through its core domain (DBD) with two cell factors--HCF-1 and Oct-1, to bind to the promoter of IE genes stably

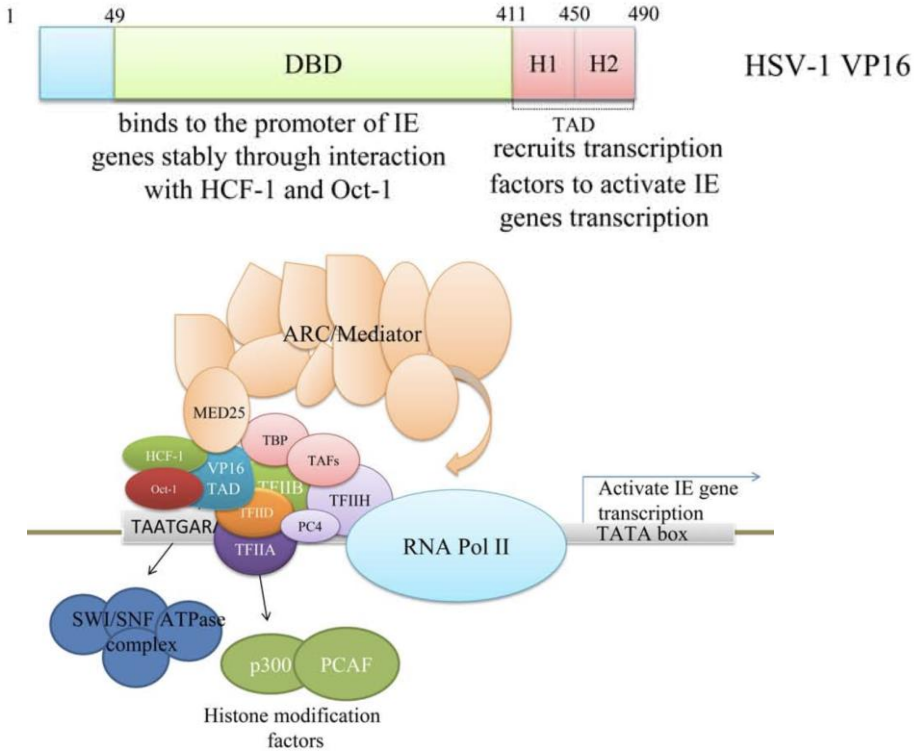

Stage 2. Once VP 16 is firmly bound to the promoter of IE genes, it will recruit various of transcriptional factors through the transcriptional activation domain (TAD), thus activating the transcription of target IE genes.

DOI: 10.1038/s41467-018-05067-x OPEN

Human pluripotent reprogramming with CRISPR activators

Jere Weltner[1], Diego Balboa[1], Shintaro Katayama[2], Maxim Bespalov[1], Kaarel Krjutškov[2,3], Eeva-Mari Jouhilahti[1], Ras Trokovic[1], Juha Kere[1,2,4,5] & Timo Otonkoski[1,6]

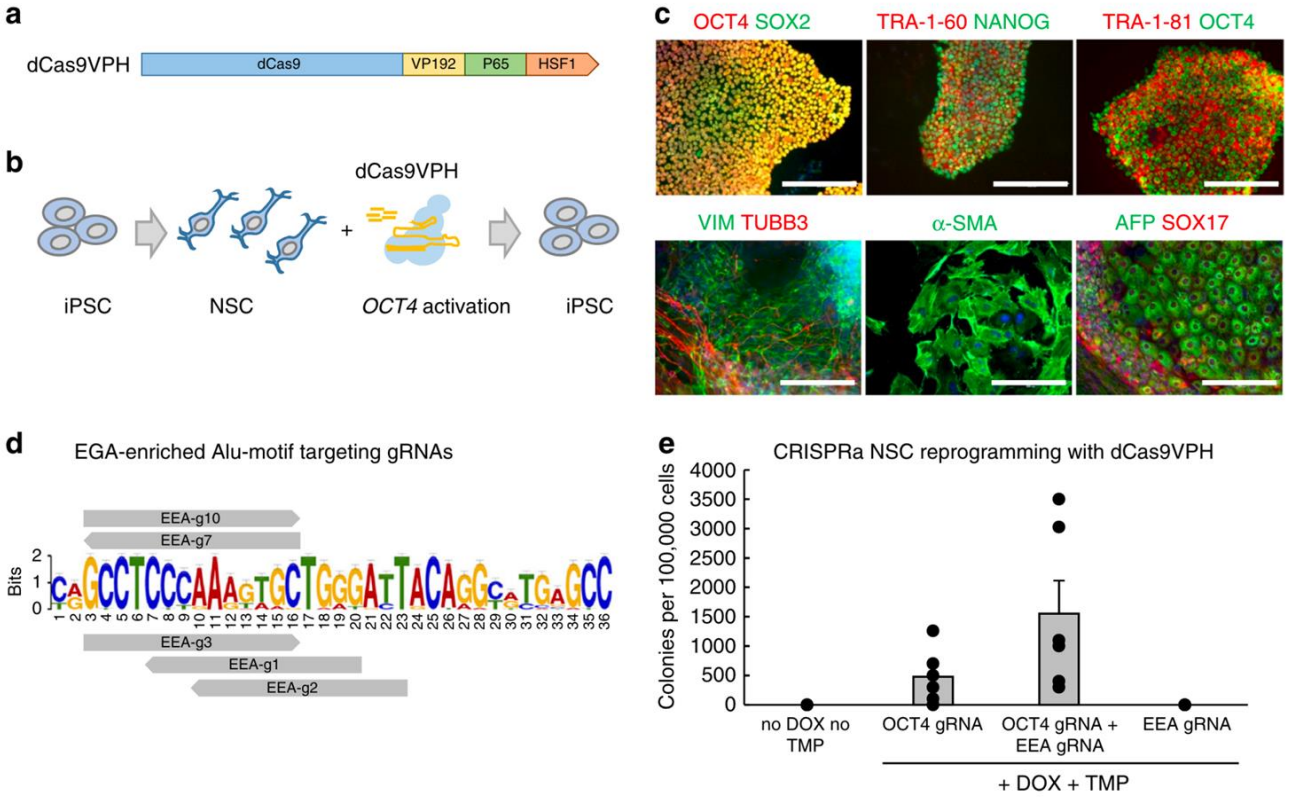

Genome-scale transcriptional activation by an engineered CRISPR-Cas9 complex

Silvana Konermann[1,2,3,4]*, Mark D. Brigham[1,2,3,4]*, Alexandro E. Trevino[1,2,3,4], Julia Joung[1,4], Omar O. Abudayyeh[1,2,3,4], Clea Barcena[1,2,3,4], Patrick D. Hsu[1,2,3,4], Naomi Habib[1], Jonathan S. Gootenberg[1,2,3,4,5], Hiroshi Nishimasu[6,7], Osamu Nureki[6] & Feng Zhang[1,2,3,4]

29 JANUARY 2015 | VOL 517 | NATURE |

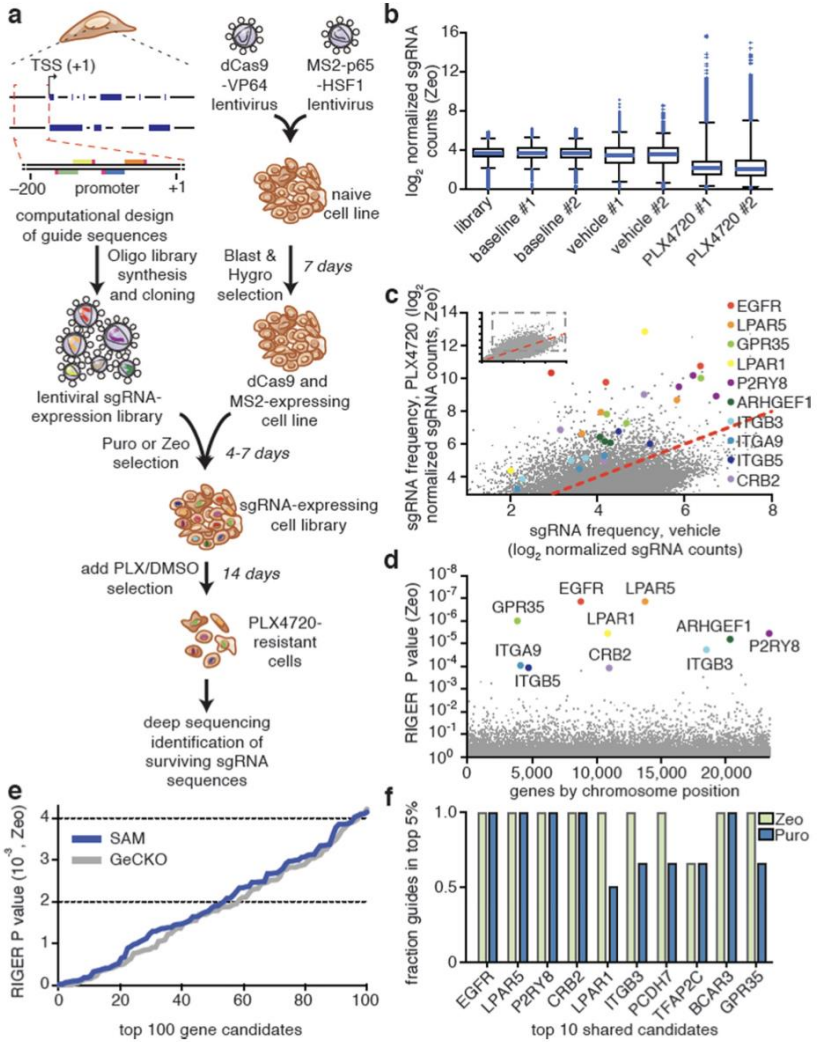

Z-ДНК

REVIEW ARTICLE

https://doi.org/10.1038/s42003-018-0237-x OPEN

Z-DNA and Z-RNA in human disease

Alan Herbert[1]

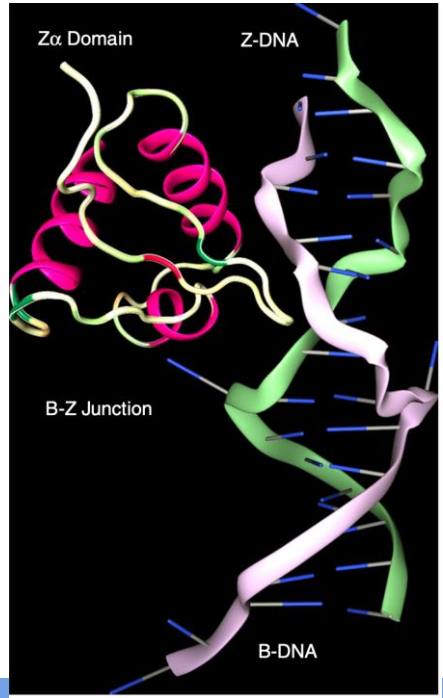

Left-handed Z-DNA/Z-RNA is bound with high affinity by the Zα domain protein family that includes ADAR (a double-stranded RNA editing enzyme), ZBP1 and viral orthologs regulating innate immunity.

Z-ДНК связывающие домены у человека есть в генах ADAR и ZBP1 – они связаны с внутриклеточным иммунным ответом.

Adenosine deaminases acting on RNA (ADARs) catalyze adenosine to inosine editing within double-stranded RNA (dsRNA) substrates

Aicardi–Goutières syndrome (**AGS**), which is completely distinct from the similarly named Aicardi syndrome, is a rare, usually early onset childhood, inflammatory disorder most typically affecting the brain and the skin (neurodevelopmental disorder)

In humans, the P193A mutation in the Zα domain is causal for Aicardi–Goutières syndrome

RNA. 2023 Mar; 29(3): 273–281.
doi: 10.1261/rna.079429.122

Z-RNA biology: a central role in the innate immune response?

Parker J. Nichols,[1] Jeffrey B. Krall,[1] Morkos A. Henen,[1,2] Beat Vögeli,[1,3] and Quentin Vicens[1,3]

If Z-RNA could be adopted by some RNAs in the cell—even transiently—its recognition by Zα-containing proteins like ADAR1 (adenosine deaminase acting on RNA 1) and ZBP1 (Z/D-RNA binding protein 1) would explain how it could be stabilized in vivo.

Flipons

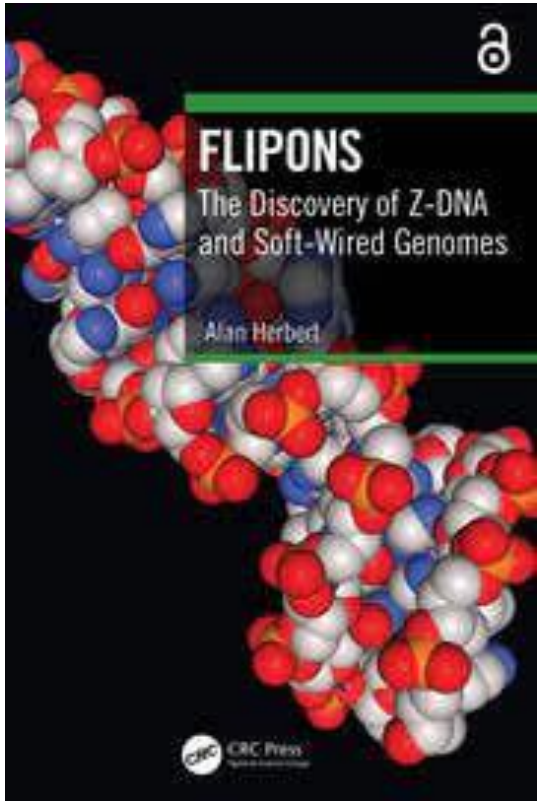
FLIPONS
The Discovery of Z-DNA and Soft-Wired Genomes
Alan Herbert
CRC Press

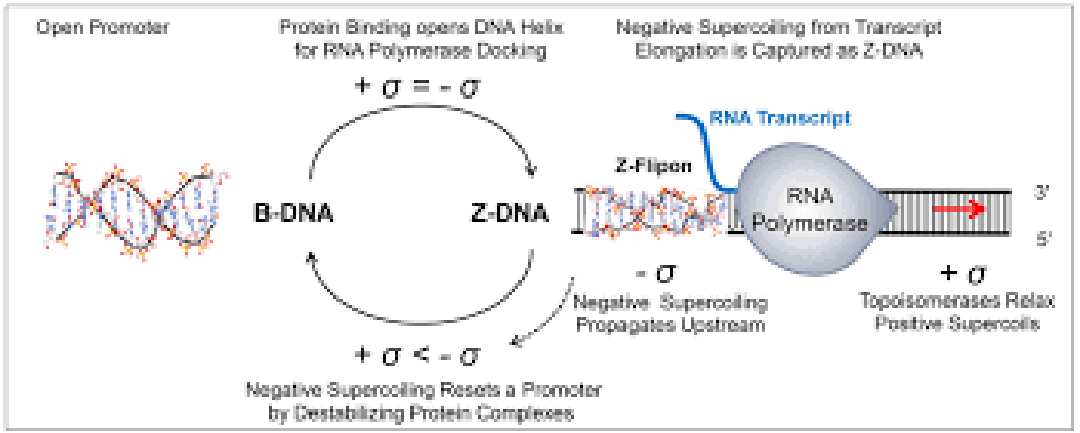
Open Promoter
Protein Binding opens DNA Helix for RNA Polymerase Docking
Negative Supercoiling from Transcript Elongation is Captured as Z-DNA
+ σ = - σ
B-DNA
Z-DNA
RNA Transcript
Z-Flipon
RNA Polymerase
3'
5'
- σ
+ σ
Negative Supercoiling Propagates Upstream
Topoisomerases Relax Positive Supercoils
+ σ < - σ
Negative Supercoiling Resets a Promoter by Destabilizing Protein Complexes

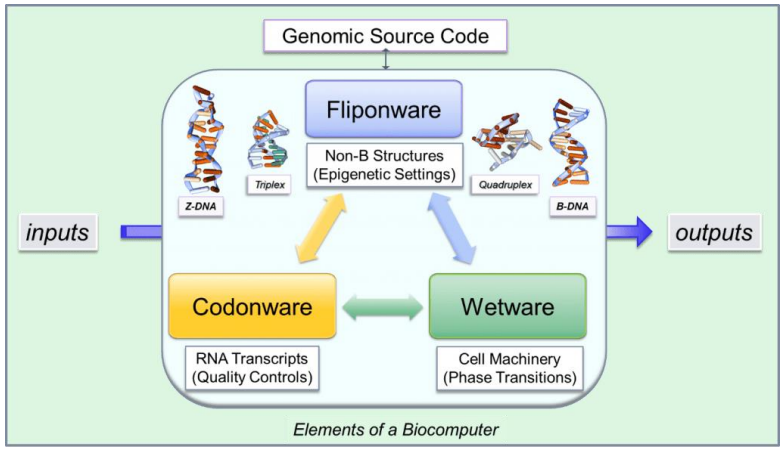
Genomic Source Code
Fliponware
Non-B Structures (Epigenetic Settings)
Z-DNA
Triplex
Quadruplex
B-DNA
inputs
outputs
Codonware
Wetware
RNA Transcripts (Quality Controls)
Cell Machinery (Phase Transitions)
Elements of a Biocomputer

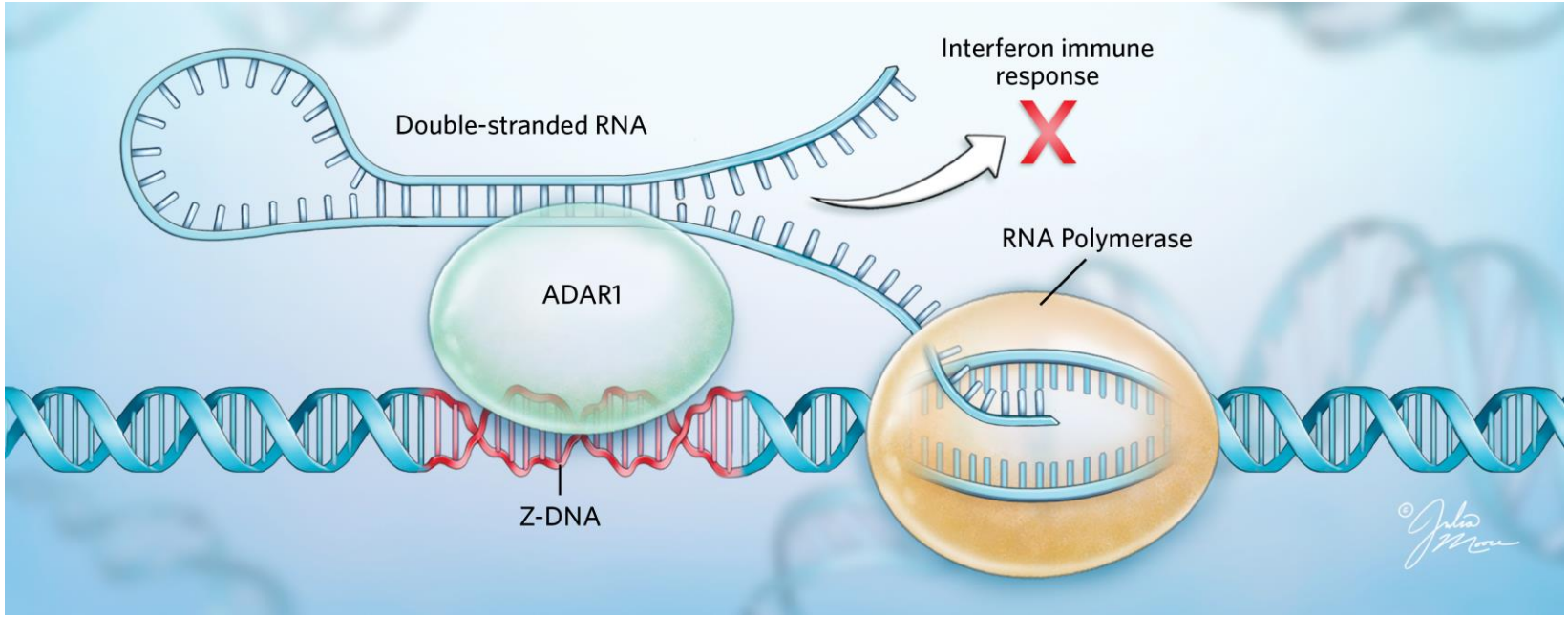
Interferon immune response
Double-stranded RNA
RNA Polymerase
ADAR1
Z-DNA

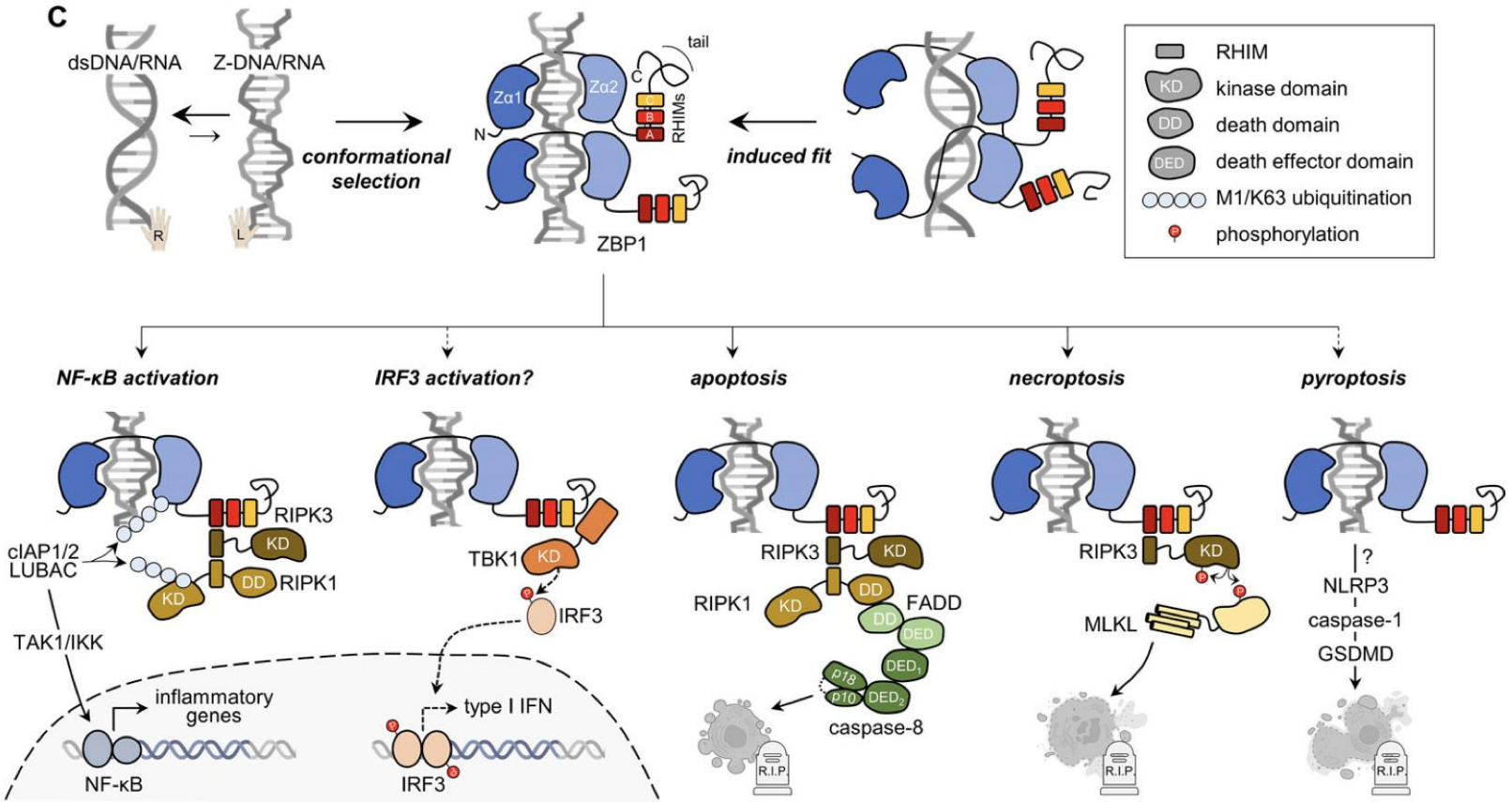

10.1084/jem.20221156

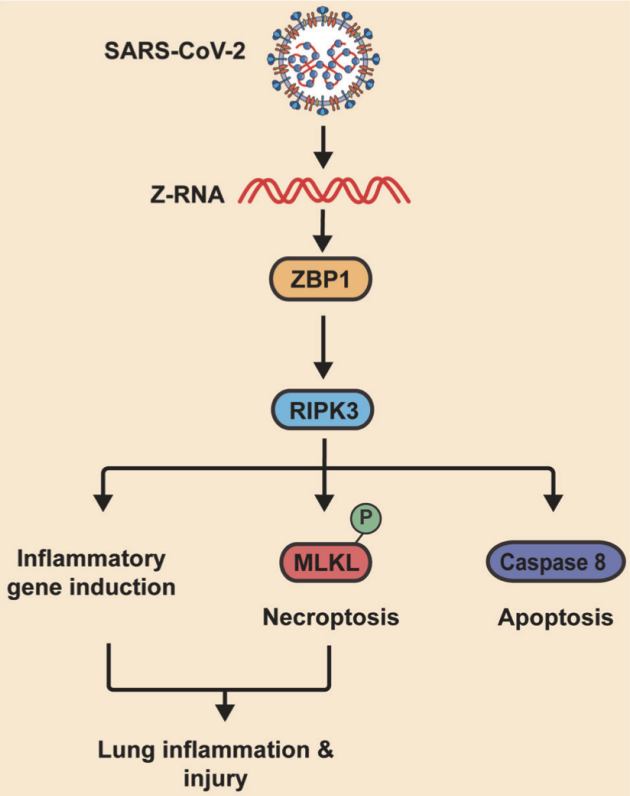

Fig. 1 SARS-CoV-2-initiated pathways of ZBP1-dependent lung inflammation. SARS-CoV-2 infection produces Z-RNAs, which are sensed by the host protein ZBP1. ZBP1 activates RIPK3, which induces cell death via parallel pathways of necroptosis driven by MLKL, and apoptosis mediated by caspase 8. RIPK3 can also induce expression of inflammatory genes in a necroptosis-independent manner. ZBP1/RIPK3-driven necroptosis and inflammatory gene expression may contribute to lung inflammation and injury in COVID-19.

The innate immune sensor Z-form nucleic acid binding protein 1 (ZBP1) detects Z-RNAs and induces Receptor Interacting Protein Kinase 3 (RIPK3)-driven pathways of cell death and inflammation during acute virus infections. In a recent paper published in *Cell Research*, Li et al. report that SARS-CoV-2 infections generate Z-RNAs and activate ZBP1/RIPK3-mediated necroptosis and inflammation, leading to lung injury in a mouse model.

10.1038/s41422-023-00784-5

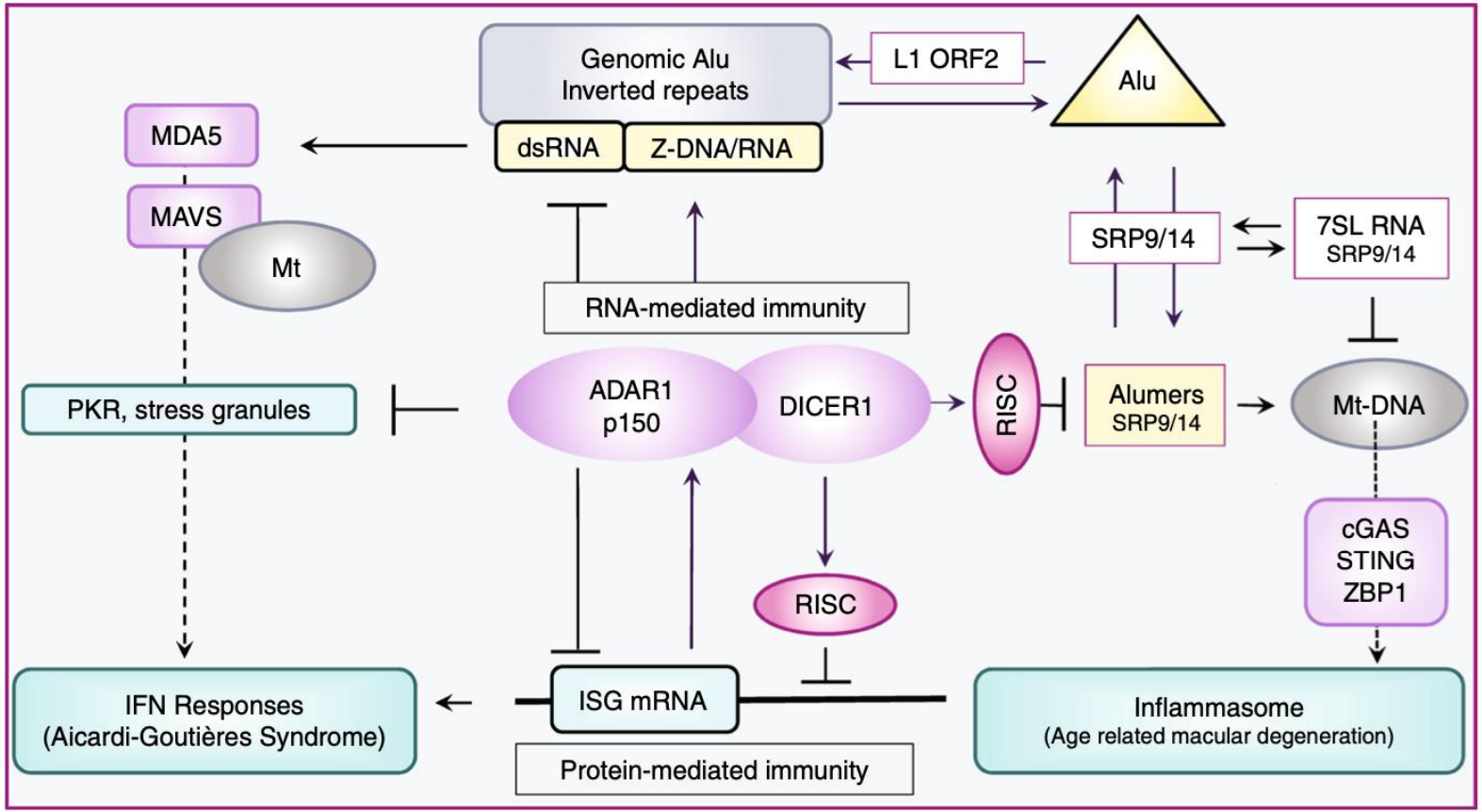
Genomic Alu
Inverted repeats
L1 ORF2
Alu
MDA5
dsRNA
Z-DNA/RNA
MAVS
Mt
RNA-mediated immunity
SRP9/14
7SL RNA
SRP9/14
PKR, stress granules
ADAR1
p150
DICER1
RISC
Alumers
SRP9/14
Mt-DNA
cGAS
STING
ZBP1
RISC
IFN Responses
(Aicardi-Goutières Syndrome)
ISG mRNA
Protein-mediated immunity
Inflammasome
(Age related macular degeneration)

Z-DNA enhances immunotherapy by triggering death of inflammatory cancer-associated fibroblasts

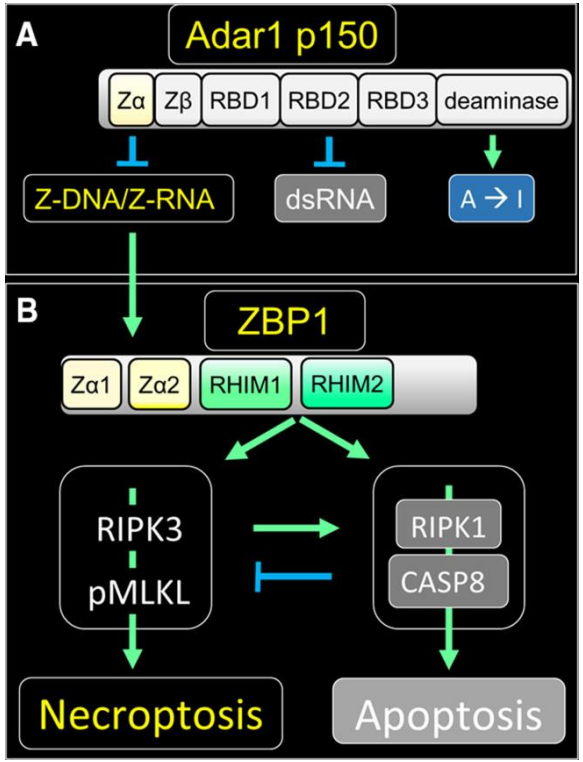

ZBP1-initiated cell death signaling and its repression by ADAR1.

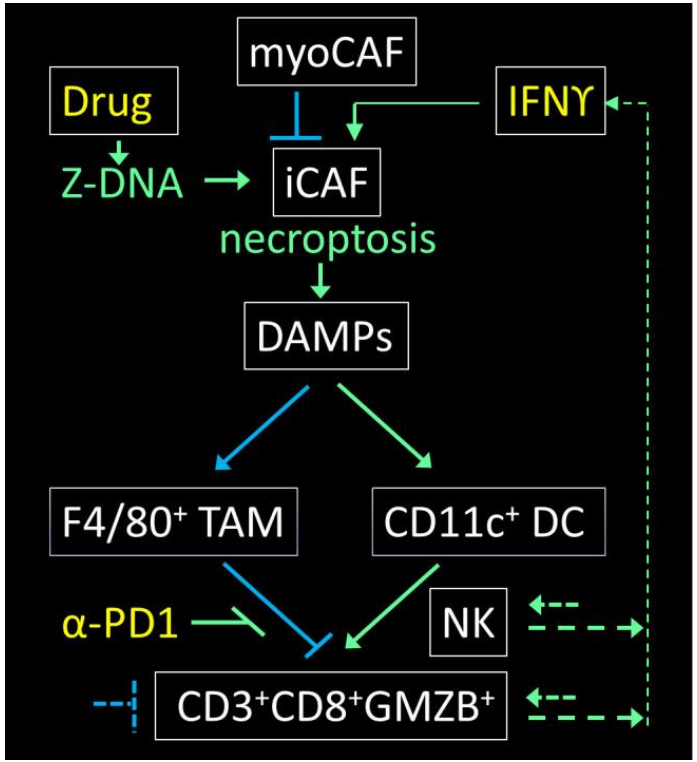

ZNA induced by a small molecule bypasses the need for ADAR1 inhibition and directly activates ZBP1 to induce necroptosis in iCAFs.

Herbert A, Balachandran S. Z-DNA enhances immunotherapy by triggering death of inflammatory cancer-associated fibroblasts. J Immunother Cancer. 2022 Nov;10(11):e005704. doi: 10.1136/jitc-2022-005704.

Интер/Трансгенарационное эпигенетическое наследование: есть или нет?

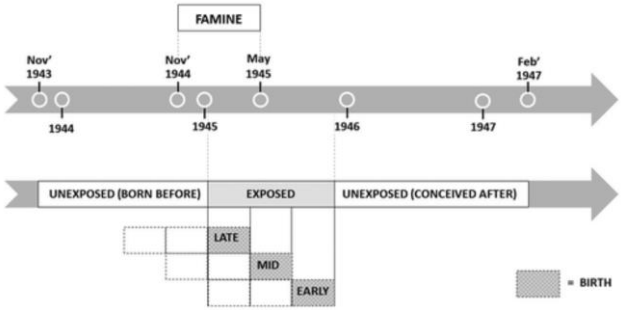

The Dutch Famine Birth Cohort

Table 1. Phenotypic differences and famine exposure.

	Controls	Famine exposure
N	463	348
Age (years) [SD]+	58.0 [5.4]	58.9 [0.5]***
Male (%)	43.0	46.0
BMI[1] [SD]	27.0 [4.2]	28.5 [5.0]***
LDL-C[2] [SD]	3.42 [0.96]	3.45 [0.97]
Triglycerides[2] [SD]	1.48 [0.86]	1.68 [1.30]**
Glucose baseline[3] [SD]	5.32 [0.93]	5.52 [1.19]*

Nominal *P* value either $*P < 0.05$, $**P < 0.01$ or $***P < 0.001$ from a linear mixed-effects model with the denoted variable as the dependent variable and family identifier as random effect. +Model included an additional random effect for exposure status to control for the difference in variance in age between groups. [1]Model-applied correction for age and gender. [2]Model-applied correction for age, gender, and statin used, and individuals who were nonfasting at examination were excluded (excluding two controls and five famine-exposed individuals). [3]Model-applied correction for age and gender. Individuals who were nonfasting and had prediagnosed diabetes (thus receiving treatment) before the clinical examination were excluded (excluding 19 controls and 32 famine-exposed individuals).

Here we show that individuals who were prenatally exposed to famine during the Dutch Hunger Winter in 1944–45 had, 6 decades later, less DNA methylation of the imprinted *IGF2* gene compared with their unexposed, same-sex siblings. The association was specific for periconceptional exposure, reinforcing that very early mammalian development is a crucial period for establishing and maintaining epigenetic marks. These data are the first to contribute empirical support for the hypothesis that early-life environmental conditions can cause epigenetic changes in humans that persist throughout life.

10.1126/sciadv.aao4364

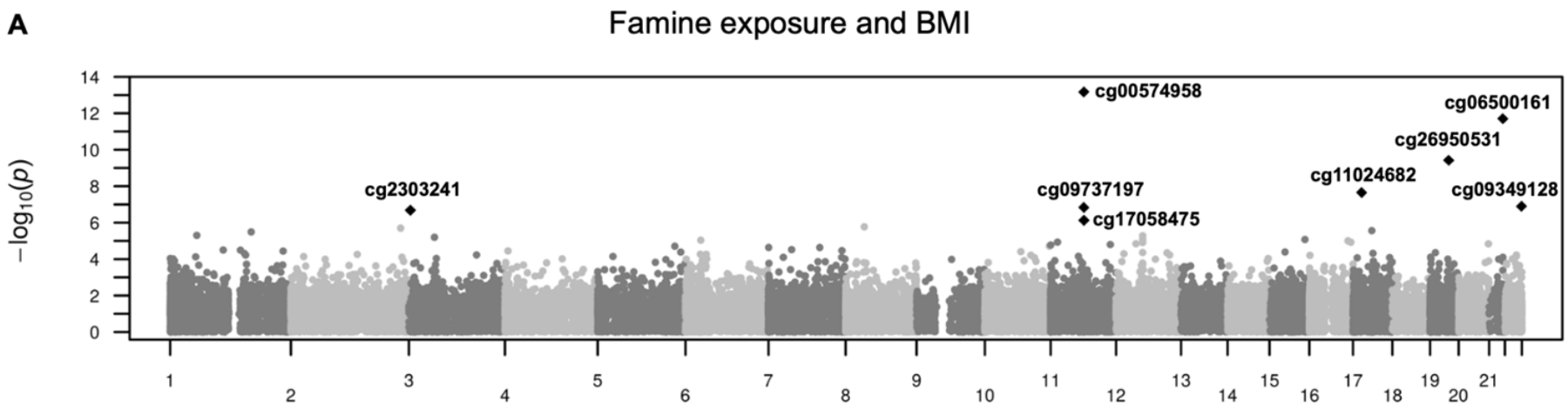

Manhattan plots: Outcome genome-wide screens for potential mediators.

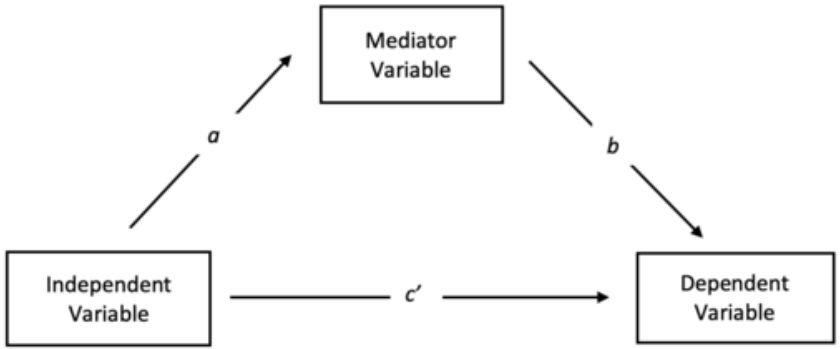

В статистике модель медиации стремится идентифицировать и объяснить механизм, лежащий в основе наблюдаемой связи между независимой переменной и зависимой переменной, путем включения третьей гипотетической переменной, известной как переменная-медиатор, или промежуточная переменная.

Table 2. Genome-wide screen for potential mediators: famine exposure and BMI.

CpG characteristics				Mediation EWAS			Associations with either famine exposure or BMI*				
CpG	Location (hg19)	Nearest gene (expression)†	Methylation (SD)‡	Rank	EWAS P§	EWAS P_{FDR}	β_{famine}	P_{famine}	β_{BMI}	P_{BMI}	Previous EWAS
cg00574958	chr11:68607622	*CPT1A*	13.6 (2.6)	1	6.7×10^{-14}	2.3×10^{-8}	−0.2	0.19	−4.0	1.7×10^{-16}	(*33*, *56*, *72*, *73*)
cg06500161	chr21:43656587	*ABCG1*	65.9 (3.0)	2	2.0×10^{-12}	3.3×10^{-7}	−0.1	0.75	4.3	2.5×10^{-13}	(*33*, *43*, *56*, *73*)
cg26950531	chr19:38704515	*DPF1*	32.5 (6.1)	3	2.2×10^{-10}	4.3×10^{-5}	0.3	0.50	−8.9	1.3×10^{-11}	(*56*)
cg11024682	chr17:17730094	*SREBF1*	53.2 (3.2)	4	2.2×10^{-8}	1.9×10^{-3}	−0.1	0.70	3.3	1.2×10^{-9}	(*33*, *43*, *56*)
cg09349128	chr22:50327986	*CRELD2*	39.0 (3.8)	5	1.3×10^{-7}	8.3×10^{-3}	−0.7	1.5×10^{-3}	−3.5	6.5×10^{-8}	(*33–36*, *56*)
cg09737197	chr11:68607675	*CPT1A*	20.4 (4.6)	6	1.5×10^{-7}	8.3×10^{-3}	−0.4	0.093	−4.4	3.2×10^{-9}	(*33*, *73*)
cg23032421	chr3:3152038	*IL5RA*	73.9 (4.1)	7	2.1×10^{-7}	0.01	−0.3	0.18	−3.4	5.8×10^{-9}	(*33*)
cg17058475	chr11:68607737	*CPT1A*	16.1 (4.1)	8	7.4×10^{-7}	0.032	−0.1	0.66	−4.2	2.3×10^{-8}	(*30*, *56*, *72–74*)
cg15659713¶	chr8:38586183	*TACC1*	24.6 (3.9)	9	1.7×10^{-7}	0.064	1.3	1.7×10^{-7}	−0.4	0.63	(*28*)
cg26199857¶	chr12:54764265	*ZNF385A*	68.9 (5.7)	14	5.2×10^{-7}	0.13	2.0	3.1×10^{-7}	1.3	0.28	(*28*)

*The estimate and (nominal) P value belonging to the EWAS for famine exposure (β = exposed − unexposed) or BMI (β/log(BMI)). †Nearest gene within 100 kb. ‡The Illumina 450k array β value (ranging from 0 to 1) multiplied by 100 for easy interpretation. This is done throughout the presented work. §The P value belonging to an analysis of variance (ANOVA) test (χ^2, df = 2) between a generalized estimating equations (GEE) model with and without both famine exposure and BMI. ¶The two CpGs identified in a previous EWAS on famine exposure (*28*).

Интер/Трансгенарационное эпигенетическое наследование: есть или нет?

fetal programming

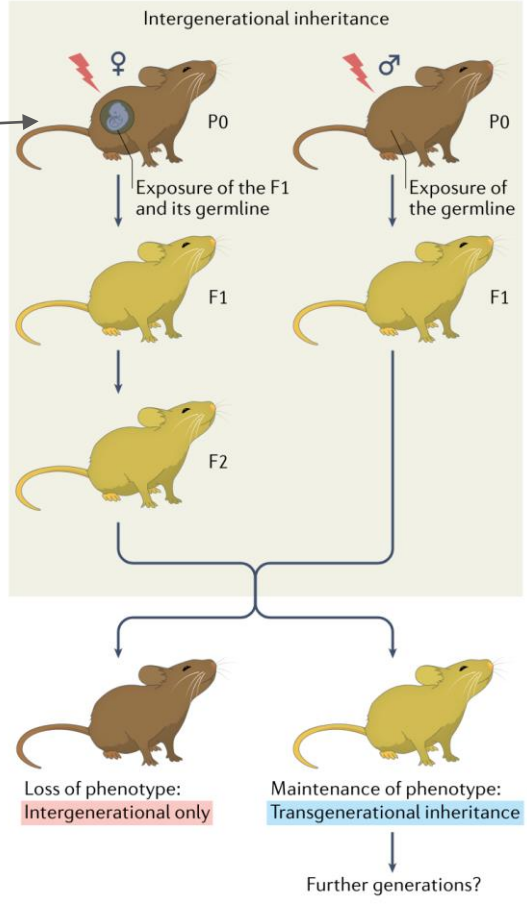

Трансгенарационное наследование: есть или нет?

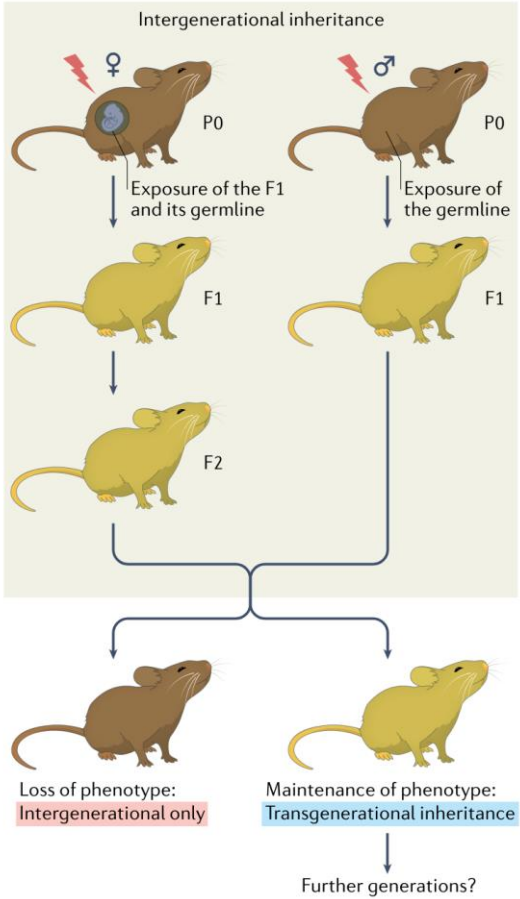

Table 1 | **Example cases of TEI with molecular mechanisms**

Organism	Observed phenotype	Generations inherited	Epigenetic signals	Refs
Plants				
A. thaliana	Pathogen resistance	9	DNA methylation	29
A. thaliana	Gene expression changes	8	DNA methylation	148
A. thaliana	Flowering time	Naturally occurring	DNA methylation	26
S. lycopersicum	Fruit ripening	Naturally occurring	DNA methylation	25
L. vulgaris	Floral symmetry	Naturally occurring	DNA methylation	24
H. foetidus	Plant size and fecundity	Naturally occurring	DNA methylation	149
Fungi				
S. pombe	Caffeine resistance	Many (mitotic)	H3K9me	35
S. pombe	Metabolic gene silencing	32 (mitotic) 5 (meiotic)	siRNA H3K9me	36
M. circinelloides	Anti-fungal resistance	>3	ncRNA	46,47
Vertebrates				
R. norvegicus	Obesity and testis disease	3	DNA methylation, ncRNA	17,150
M. musculus	Traumatic stress behaviour	3	ncRNA	80
M. musculus	Developmental defects	3	H3K4me3	40,41
M. musculus	Testis and kidney disease	3	DNA methylation	147
M. musculus	Obesity	6	DNA methylation	132
D. rerio	Sex ratio	3	DNA methylation	16
C. japonica	Egg-laying, social behaviour	3	DNA methylation	15
Insects				
D. melanogaster	Eye colour	>50	H3K27me3	32
D. melanogaster	Eye colour	5	H3K9me3	37
Nematodes				
C. elegans	Longevity	3	H3K4me3	151
C. elegans	Pathogen avoidance	4	siRNA, piRNA	71
C. elegans	*daf-21* gene expression	14	H3K9me3	38
C. elegans	Chemotaxis	3	siRNA	72
C. elegans	Longevity	3	siRNA	69
C. elegans	Gene expression changes	4	siRNA	70
C. elegans	Gene expression changes	4	siRNA, H3K23me3	62

NATURE REVIEWS | GENETICS

10.1038/ s41576-021-00438-5

Article

Transgenerational inheritance of acquired epigenetic signatures at CpG islands in mice

Yuta Takahashi,[1,2] Mariana Morales Valencia,[1,2] Yang Yu,[1,3,4] Yasuo Ouchi,[1,2,5] Kazuki Takahashi,[1,2] Maxim Nikolaievich Shokhirev,[6] Kathryn Lande,[6] April E. Williams,[6] Chiara Fresia,[1] Masakazu Kurita,[1,7] Tomoaki Hishida,[1,8] Kensaku Shojima,[1] Fumiyuki Hatanaka,[1,2] Estrella Nuñez-Delicado,[9] Concepcion Rodriguez Esteban,[1,2] and Juan Carlos Izpisua Belmonte[1,2,10,*]

previously established approach, in which integration of CpG-free DNA can induce stable de novo DNA methylation of the entire targeted CGIs

For this study, as target loci, we selected two CGIs associated with metabolism-related gene promoters, the Ankyrin repeat domain 26 (Ankrd26) and low-density lipoprotein receptor (Ldlr). These genes were of particular interest, as knockout of Ankrd26 or Ldlr results in obesity or hypercholesterolemia, respectively, but does not affect mouse viability and fertility

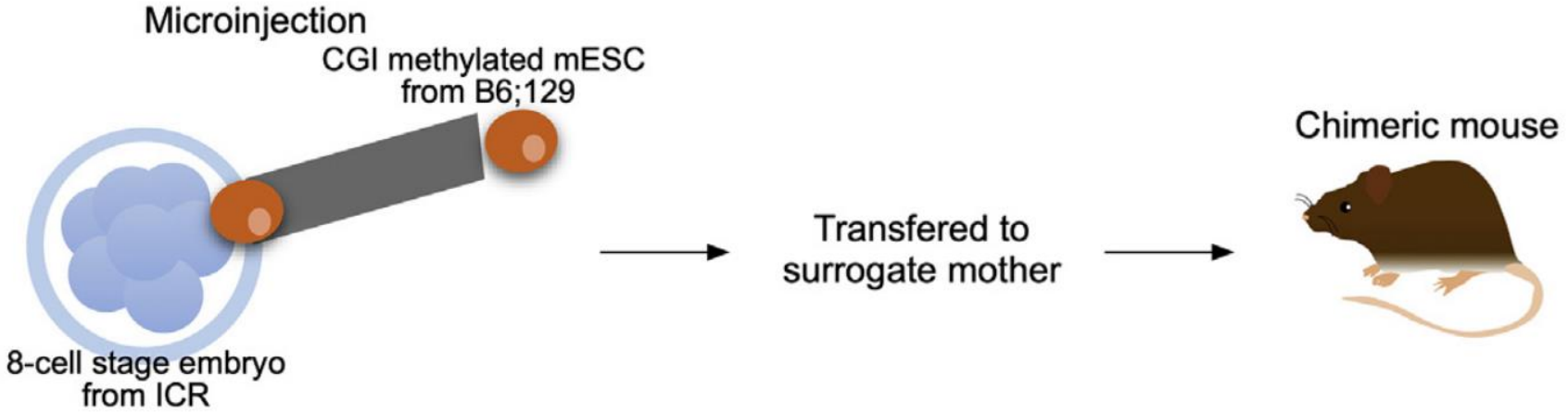
Microinjection
CGI methylated mESC
from B6;129
8-cell stage embryo
from ICR
Transfered to
surrogate mother
Chimeric mouse

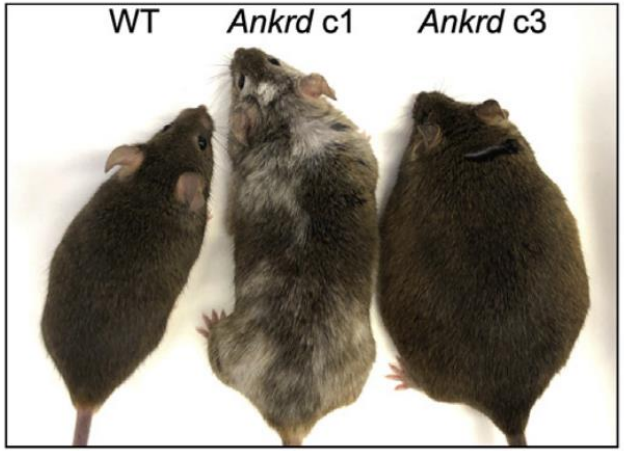
WT
Ankrd c1
Ankrd c3

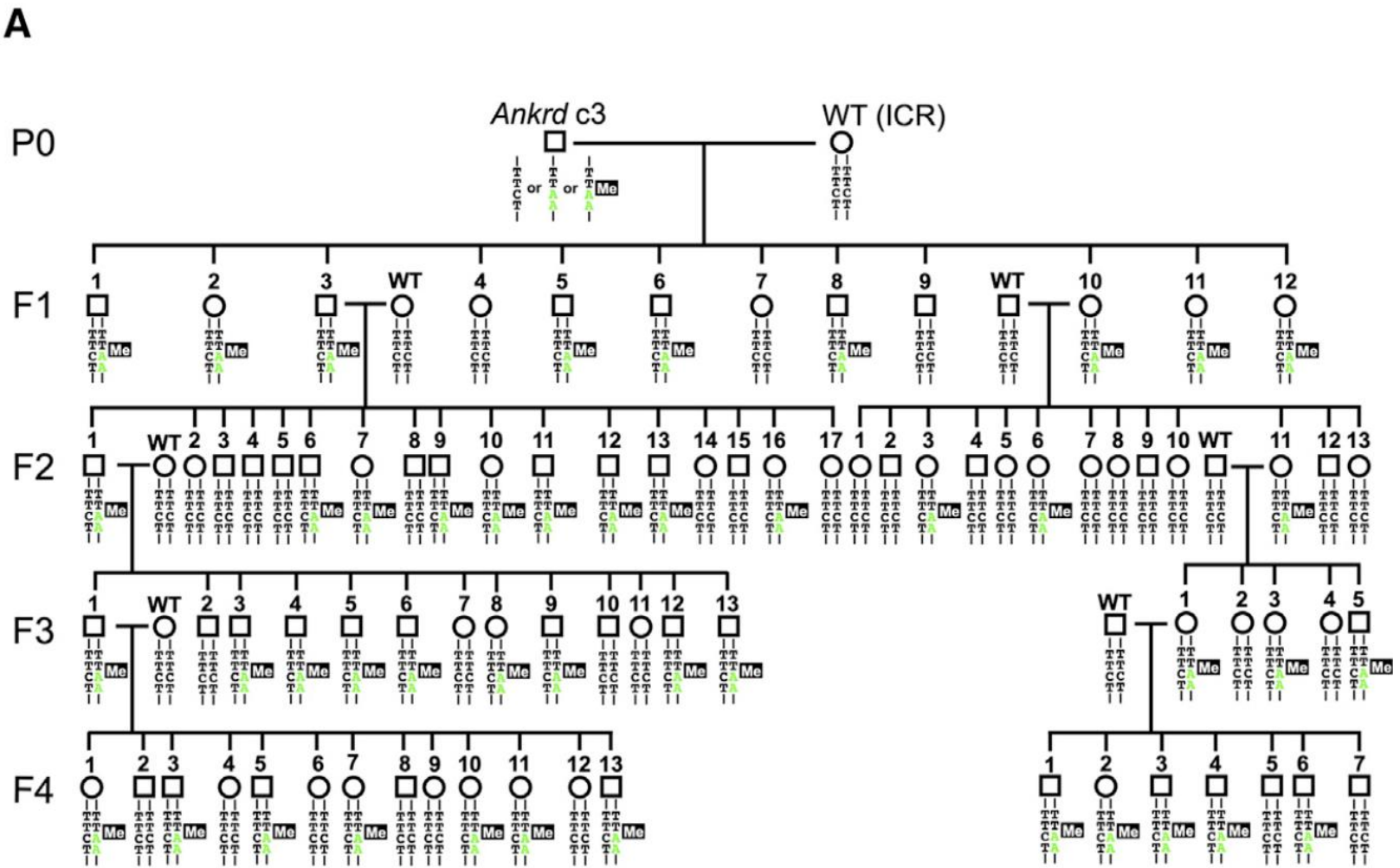
A
P0
Ankrd c3
WT (ICR)
or
or
Me
F1
1 2 3 WT 4 5 6 7 8 9 WT 10 11 12
F2
1 WT 2 3 4 5 6 7 8 9 10 11 12 13 14 15 16 17
1 2 3 4 5 6 7 8 9 10 WT 11 12 13
F3
1 WT 2 3 4 5 6 7 8 9 10 11 12 13
WT 1 2 3 4 5
F4
1 2 3 4 5 6 7 8 9 10 11 12 13
1 2 3 4 5 6 7

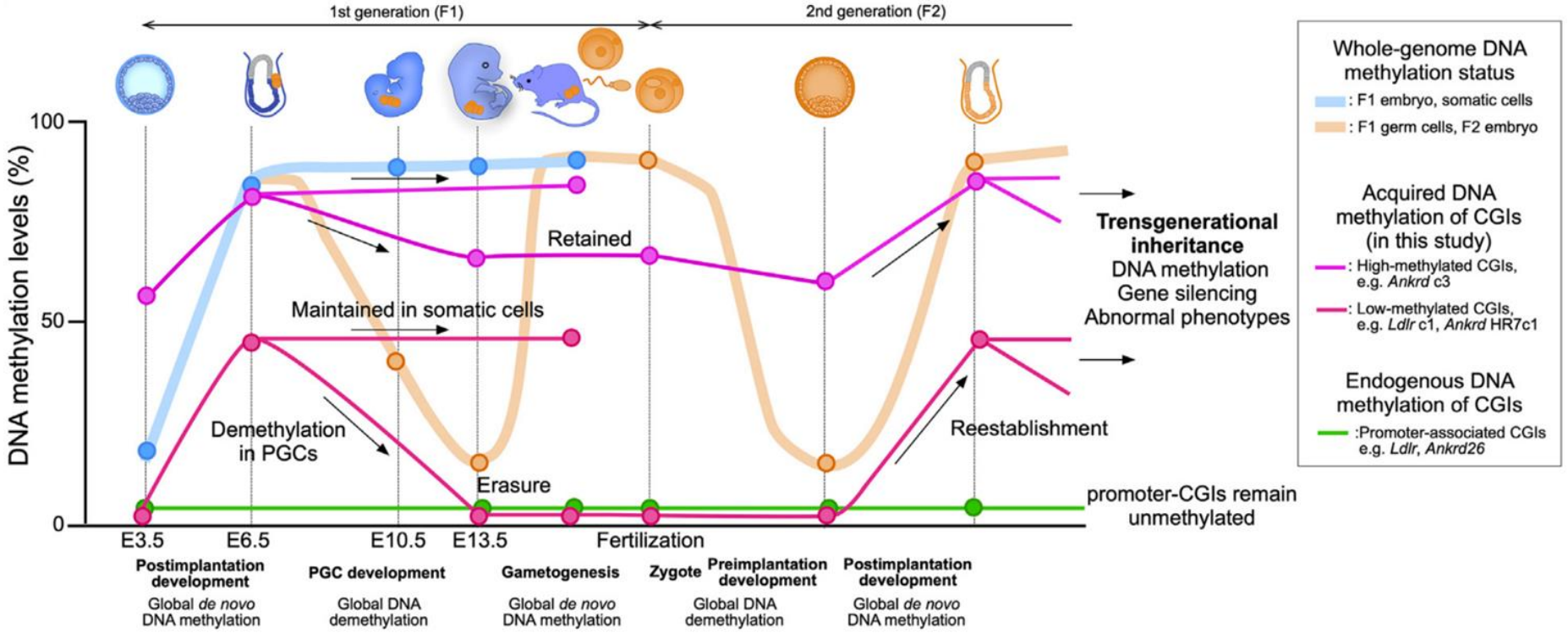
1st generation (F1)
2nd generation (F2)
DNA methylation levels (%)
100
50
0
Retained
Maintained in somatic cells
Demethylation in PGCs
Erasure
Reestablishment
promoter-CGIs remain unmethylated
Trensgenerational inheritance
DNA methylation
Gene silencing
Abnormal phenotypes
E3.5
E6.5
E10.5
E13.5
Fertilization
Postimplantation development
Global de novo DNA methylation
PGC development
Global DNA demethylation
Gametogenesis
Global de novo DNA methylation
Zygote
Preimplantation development
Global DNA demethylation
Postimplantation development
Global de novo DNA methylation
Whole-genome DNA methylation status
: F1 embryo, somatic cells
: F1 germ cells, F2 embryo
Acquired DNA methylation of CGIs (in this study)
: High-methylated CGIs, e.g. Ankrd c3
: Low-methylated CGIs, e.g. Ldlr c1, Ankrd HR7c1
Endogenous DNA methylation of CGIs
:Promoter-associated CGIs e.g. Ldlr, Ankrd26

Эпигенетическое наследование у людей? (пример)

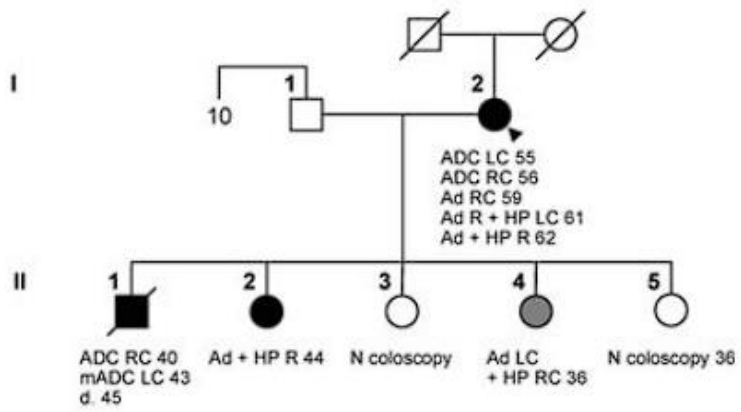

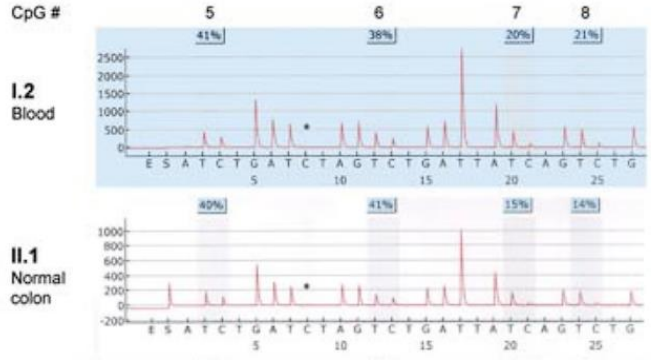

У женщины заметилирован ген для починки ДНК MLH1, что приводит к раку кишечника. Эпигенетическое наследование проявляется и у потомков.

ADC, adenocarcinoma; LC, left colon

Methylation analysis of the MLH1 promoter by pyrosequencing in blood or normal tissue from the different family members. The CpG sites and percentages of methylation are indicated at the top of each panel.

Crépin M. et al. Evidence of constitutional MLH1 epimutation associated to transgenerational inheritance of cancer susceptibility //Human mutation. – 2012. – Т. 33. – №. 1. – С. 180-188.

Вирусы и эпигенетика

NS1 protein of influenza A H3N2 subtype

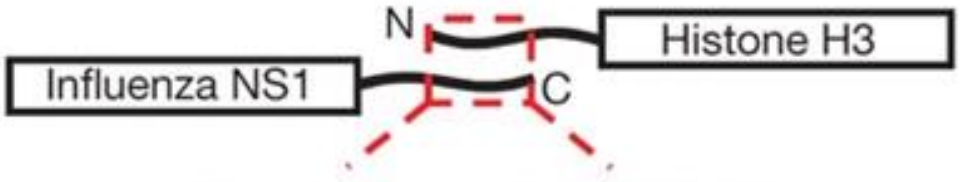

Histone H3 1 ARTKQTARKS 10
NS1 221 KMARTARSKV 230

Strain	Year of appearance	NS1 C-terminal
H3N2	1968-2011	216 PKQKRKMARTARSKV 230
H1N1	1933-2011	216 PKQKRKMARTIRSEV 230
H5N1	2003	216 PNQKRKMARTIESEV 230
H1N1	1918*	216 PKQKRKMARTIKSEV 230
H1N1	2009*	216 PKQK---------- 219

*Influenza A pandemic strains

We show that the NS1 protein of influenza A H3N2 subtype possesses a histone-like sequence (histone mimic) that is used by the virus to target the human PAF1 transcription elongation complex (hPAF1C). We demonstrate that binding of NS1 to hPAF1C depends on the NS1 histone mimic and results in suppression of hPAF1C-mediated transcriptional elongation.

Similar to the NS1 histone mimic, the acetylated histone H3 tail did not bind to either hPAF1C components.

Marazzi, I., Ho, J., Kim, J. *et al.* Suppression of the antiviral response by an influenza histone mimic. *Nature* 483, 428–433 (2012). https://doi.org/10.1038/nature10892

Hepatitis Delta Virus histone mimicry drives the recruitment of chromatin remodelers for viral RNA replication

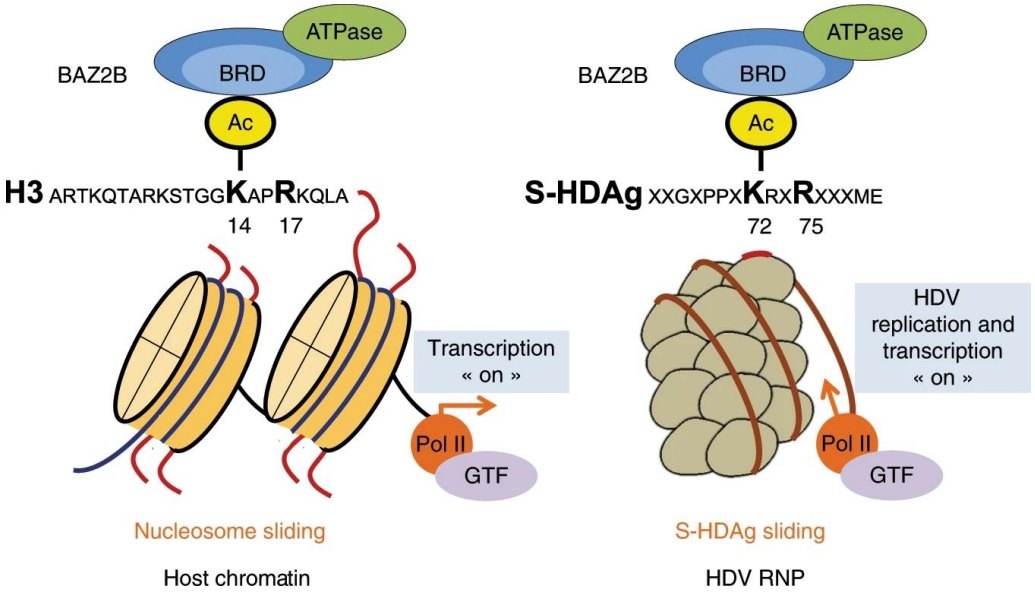

We show that BAZ2B BRD (regulatory subunit of the ISWI chromatin remodeling BRF complexes), which generally binds the K14acXXR motif in histone H3-tail, recognizes the same K72acXXR motif in S-HDAg.

Our results suggest that S-HDAg mimics histone [illegible] complex [illegible] RNP to sustain

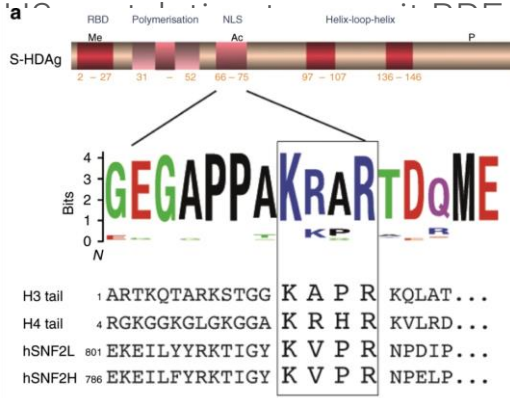

Natali Abeywickrama-Samarakoon et al., ‘Hepatitis Delta Virus Histone Mimicry Drives the Recruitment of Chromatin Remodelers for Viral RNA Replication’, *Nature Communications* 11, no. 1 (21 January 2020): 419, https://doi.org/10.1038/s41467-020-14299-9.

Спасибо за внимание!